Steroid conversions with the CYP106A subfamily from *Bacillus megaterium*

Kumulative Dissertation

zur Erlangung des Grades Doktor der
Naturwissenschaften (Dr. rer. nat.)
der Naturwissenschaftlich-Technischen Fakultät III
Chemie, Pharmazie, Bio- und Werkstoffwissenschaften
der Universität des Saarlandes

von

Dipl.-Ing. Flora Marta Kiss

Saarbrücken

2015

Tag des Kolloquiums: 23. 10. 2015	
Dekan:	Prof. Dr. Dirk Bähre
Berichterstatter:	Prof. Dr. Rita Bernhardt
	Prof. Dr. Gert-Wieland Kohring
Vorsitz:	Prof. Dr. Karin Römisch
Akad. Mitarbeiter:	Dr. Yutaka Suzuki

“Courage doesn’t always roar.

Sometimes courage is the quiet voice at the end of the day saying,

‘I will try again tomorrow’.”

Mary Anne Radmacher

Acknowledgements

I would like to thank Prof. Dr. Rita Bernhardt for her guidance during the past three years and providing me with the opportunity to take part in the Marie Curie ITN program. I'm grateful for such a great fellowship that allowed me to meet the crème de la crème of the P450 community, to make professional connections as well as good friends, and to travel around the world. Thanks to Dr. Frank Hannemann for the discussions, constructive suggestions and reassuring words especially at the beginning of my studies in the most critical times. Many thanks to Dr. Josef Zapp for the NMR measurement and data evaluation of the extensive amount of samples that I produced during these three years. His hard work allowed me to complete the three publications on which this thesis is based. I would like to express my special gratitude to Prof. Dr. John Woodley, from the Technical University of Denmark, who made my two-month exchange possible. I thank him for the stimulating discussions, his keen interest in the progress of my work, valuable comments and encouragement. I would also like to thank my Marie Curie fellow and friend Marie Lundemo, with who I worked side-by-side during my stay in Denmark. I'm grateful for her enthusiasm, hard work and sacrificed long working days while she was organizing her wedding. My sincere thanks go to our technicians Wolfgang Reinle and Birgit Heider-Lips for the excellent protein purifications, and their help in all technical matters. Many thanks to Adrian Gerber for letting me follow him everywhere in the lab at the very beginning of my work, when I had honestly no clue what I was supposed to be doing, for his help in HPLC matters and for his assistance in the administrative work, together with Jens Neunzig. Special thanks to Daniela Schmitz, to who I am particularly grateful for introducing me to cell culture handling, for the helpful discussions, advice and moral support throughout my work, especially during my first publication. I am also grateful to my Ausländer-office mates, Azzam Mosa and Yogan Khatri. Azzam was always willing to help, whether it was sharing experiences, cookies or tea, and was always very supportive from my first day in the lab. Yogan was an enormous help in the last year of my PhD work: thanks to him I was able to publish my third paper and learn new techniques in the lab. I would like to thank my friend, the chemist and hip-hop enthusiast Alexander "Sascha" Schifrin, who did not only provide me with a place to stay upon arrival in Saarbrücken, he introduced me to his friends, and made me feel welcome, which I really needed, living alone for the first time in a foreign country. I will always be grateful for the numerous favors he was willing to do, his guidance in the lab and around the university. Thanks to him, I had the chance to meet and become friends with Irina, Oriana, Mael and María, who were a tremendous help in starting to live a happy life in Saarbrücken. This includes Tanja Sagadin, my fellow vegetarian, special thanks for always being there when I needed help in the lab, teaching me the basics of protein purification and also for the great times in and outside of the lab. Thanks to Lina, Benni and Simone for the cheerful laughs coming to my office, which always made me smile and for the initiative and organization of extracurricular activities. Special acknowledgements go to all my colleagues from the Institute of Biochemistry for their scientific support, the great moments, the "company outflights" and the good atmosphere during the last

years. I would like to thank both my families (all the Kisses and the Souzas) and friends at home and around the world, who always believed in me more than I believed in myself. Despite being far away, we found our ways to keep in touch. I would like to thank my father, who taught me that being excellent in only one thing is not a must, nor the key to success and my mother, who encouraged me to take this fellowship and believes without a doubt that I will change the world. Thanks to my sister and my brother, who never stopped annoying me about being a nerd and an eternal student. Without them, I probably would have ended up pursuing my other dream as a dancer ☺.

I want to thank above all my husband, best friend and life-coach Nico, for his love, motivation, endless faith in me, his help and effort correcting my papers/presentations, proofreading the present work and keeping my head above water. Te lo dedico a ti, mi vida.

Thanks to the People Programme (Marie Curie Actions) of the European Union's 7th Framework Programme (FP7/2007-2013), P4FIFTY - FP7 PEOPLE ITN 2011-289217 for providing the financial support to complete this work.

Scientific contributions

This work is based on three original research papers reproduced in **Chapter 2**. The original manuscripts are printed with the kind permissions from Springer Science and Business Media, *Applied Microbiology and Biotechnology* (2.1 Kiss *et al.* (2015)), Elsevier, *FEBS letters* (2.2 Kiss *et al.* (2015)) and BioMed Central, *Microbial Cell Factories* (2.3 Kiss *et al.* (2015)).

2.1 Kiss *et al.* (2015)

The author performed all the laboratory work and data analysis involved in this study (*in vitro* and *in vivo* biotransformations, spectroscopic studies, HPLC analyses, product purification and data evaluation) and drafted the manuscript. The NMR measurements and structure determination was performed by Dr. Josef Zapp (Institute of Pharmaceutical Biology, Saarland University), the mass-determination of the compounds by HRMS was completed by Tobias K. F. Dier and Prof. Dr. Dietrich A. Volmer (Institute of Bioanalytical Chemistry, Saarland University). Dr. Daniela Schmitz and Prof Dr. Rita Bernhardt both participated in the design of the project and contributed to the manuscript drafting.

2.2 Kiss *et al.* (2015)

The author performed all the laboratory experiments, analyzed and interpreted the data and drafted the manuscript. Dr. Josef Zapp (Institute of Pharmaceutical Biology, Saarland University) performed the NMR measurements and the structure determination of the converted steroids. Dr. Yogan Khatri and Prof. Dr. Rita Bernhardt designed the project and assisted in interpreting the results and drafting the manuscript.

2.3 Kiss *et al.* (2015)

The author and Marie Therese Lundemo (CAPEC-PROCESS, Department of Chemical and Biochemical Engineering, Technical University of Denmark) contributed equally to the biochemical and biotechnological experiments, the data analysis and the drafting of the manuscript. The NMR measurement and the structure determination of the produced hydroxysteroid was performed by Dr. Josef Zapp (Institute of Pharmaceutical Biology, Saarland University). Prof. Dr. John M. Woodley (CAPEC-PROCESS, Department of Chemical and Biochemical Engineering, Technical University of Denmark) and Prof. Dr. Rita Bernhardt took part in the design of the project, the interpretation of the data and contributed to the manuscript drafting.

Table of contents

Abstract 1

Zusammenfassung 2

1. Introduction 3

1.1. Cytochromes P450 3

1.1.1. General aspects 3

1.1.2. Structural features 5

1.1.3. Catalytic cycle of cytochromes P450 6

1.1.4. Biotechnological application of cytochromes P450 7

1.2. Cytochromes P450 from *Bacillus megaterium* 9

1.2.1. CYP106A1 from *Bacillus megaterium* DSM 319 10

1.2.2. CYP106A2 from *Bacillus megaterium* ATCC 13368 10

1.3. Steroid hormones and steroidal drugs 12

1.4. Aim and outline of the work 13

2. Scientific articles 15

2.1. Kiss *et al.* (2015) 15

Comparison of CYP106A1 and CYP106A2 from *Bacillus megaterium* - identification of a novel 11-oxidase activity

2.2. Kiss *et al.* (2015) 44

Identification of new substrates for the CYP106A1-mediated 11-oxidation and investigation of the reaction mechanism

2.3. Kiss *et al.* (2015) 58

Process development for the production of 15β-hydroxycyproterone acetate using *Bacillus megaterium* expressing CYP106A2 as whole-cell biocatalyst

3. Discussion and outlook 75

4. List of abbreviations 83

5. Appendix 84

5.1. Investigating the applicability of a fluorescence assay for the analysis of cortisol-cortisone turnover by CYP106A1 84

5.2. XTT-based cell proliferation assay using the LNCaP cell line, cyproterone acetate and its 15β-hydroxy product 85

6. References 86

Abstract

Regio- and stereoselective hydroxylation represents a major challenge for synthetic chemistry. The cytochrome P450 subfamily CYP106A efficiently catalyzes such reactions in steroids, di-, and triterpenes. The well-studied CYP106A2, from *B. megaterium* ATCC 13368, is a promising candidate for the pharmaceutical industry. It shares 63% amino acid sequence identity with CYP106A1 from *B. megaterium* DSM 319 which was recently identified. The global objective of the work was the in depth characterization of the CYP106A subfamily concerning the bioconversion of steroids, to explore their potential application as industrial biocatalysts.

A focused steroid library was screened with the CYP106A subfamily. Binding studies, *in vitro* and *in vivo* reactions allowed the comparison of enzyme activity, product pattern and product structures. 13 new substrates were identified for CYP106A1 and 7 for CYP106A2. The hydroxylase activity was confirmed at positons 6β, 7β, 9α and 15β, in addition to an unprecedented 11-oxidase activity.

The 11-oxidase activity of CYP106A1 was further studied, identifying 3 11β-hydroxysteroids as novel substrates for 11-oxidation. The reaction mechanism was also investigated, resulting in a large inverse kinetic isotope effect (~0.44) suggesting the ferric peroxoanion as the reactive intermediate.

The CYP106A2 based *B. megaterium* whole-cell system has shown effective 15β-hydroxycyproterone acetate production. The conversion was scaled up from shake flask to bench-top bioreactor, the reaction-bottlenecks were identified and addressed, demonstrating a successful process development with a product formation of 0.43 g/L, approaching industrial process requirements and a future large-scale application.

Zusammenfassung

Regio- und stereoselektive Hydroxylierung stellt für die synthetische Chemie eine ernste Herausforderung dar. Die CYP106A-Subfamilie der Cytochrome P450 katalysiert diesen Reaktionstyp auf effiziente Weise für Steroide, Di- und Triterpene. Das intensiv untersuchte CYP106A2 aus *B. megaterium* ATCC 13368 teilt 63% Sequenzidentität mit CYP106A1 aus *B. megaterium* DSM 319, das erst kürzlich identifiziert wurde. Das Ziel der Arbeit war, beide Enzyme in Bezug auf den Umsatz von Steroiden zu charakterisieren und ihre potenzielle Anwendung als industrielle Biokatalysatoren zu erkunden.

Ein Steroidbibliothek-Screening wurde mit den CYP106A-Enzymen vorgenommen. Bindungsstudien, *in vitro*- und *in vivo*-Reaktionen ermöglichen den Vergleich der Enzymaktivität, der Produktmuster und der Produktstrukturen. 13 neue Substrate wurden für CYP106A1 und 7 für CYP106A2 identifiziert. Die Hydroxylaseaktivität wurde für die Positonen 6β, 7β, 9α und 15β, zusätzlich zu einer 11-Oxidaseaktivität bestätigt.

Die 11-Oxidaseaktivität von CYP106A1 wurde untersucht und 3 11β-Hydroxysteroide als neue Substrate für die 11-Oxidation identifiziert. Der in mechanistischen Studien große inverse kinetische Isotopeneffekt (~ 0,44) deutet auf ein Eisen(III)-peroxoanion als reaktives Zwischenprodukt hin.

Das CYP106A2-*B. megaterium*-Ganzzellsystem hat sich als effizienter Katalysator für die Herstellung von 15β-Hydroxycyproteronacetat erwiesen. Die Reaktion wurde von Schüttelkolben auf einen Tischbioreaktor hochskaliert, die Hauptengpässe der Reaktion beseitigt und somit ein Prozess erfolgreich etabliert. Die Produktausbeute von 0.43 g/L, bietet eine Basis für eine zukünftige Anwendung im industriellen Maßstab.

1. Introduction

1.1. Cytochromes P450

1.1.1. General aspects

Cytochrome P450 enzymes (P450s) are heme-containing monooxygenases, constituting one of the largest and oldest enzyme families, found in almost every life form, from prokaryotes to eukaryotes [1]. They are involved in various biological processes such as carbon-source degradation, secondary metabolite formation in prokaryotes, lower eukaryotes and plants, as well as in steroid hormone biosynthesis and xenobiotic metabolism in humans [2-4]. Their first experimental evidence dates to 1955, when the oxidation of xenobiotic compounds was detected in rabbit liver microsomes [5, 6]. This was followed by the independent discovery of a carbon monoxide binding pigment in rat and pig livers by Klingenberg and Garfinkel in 1958, respectively, showing an absorption maximum at 450 nm [7, 8]. In 1962, this microsomal carbon monoxide binding pigment was named **cytochrome P450** by Omura and Sato [9], who demonstrated the presence of iron-bound protoporphyrin IX in the enzyme. The **cytochrome** denotes the hemoprotein nature, while **P** stands for "pigment" and **450** refers to the characteristic absorption maximum observed at 450 nm during complex formation with CO (Soret peak). This characteristic absorption is induced by the thiolate group of a conserved cysteine, forming the fifth ligand of the heme iron [10], thus assigning these enzymes as heme thiolate proteins [11]. Their unusual spectral property is still in use for the quantitative determination of the P450 content of a protein probe [4].

Today the P450 database (http://drnelson.uthsc.edu/CytochromeP450.html) lists more than 21000 representatives. The amount of P450 genes varies enormously in different species. For instance, 7446 P450 genes are found in plants, 6313 in animals, 1254 in bacteria, 27 in archaea and only 2 are discovered in viruses. They are classified according to the guidelines of a systematic nomenclature, introduced by Nebert *et al.* in 1989 [12]. The enzymes are divided into families based on their amino acid sequence identity (> 40 %) and are given the CYP designation for **Cy**tochrome **P**450 followed by a number (**Figure 1**). The letter behind the family number represents the subfamily, which requires a similarity of more than 55 % in their amino acid sequences. The last number is unique for each P450, indicating the individual isoenzyme.

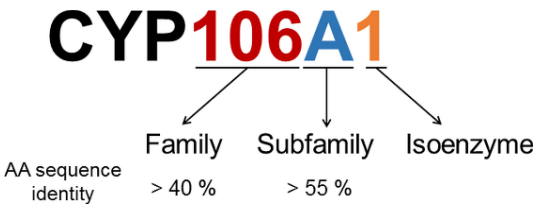

Figure 1 - Nomenclature of P450s exemplified by CYP106A1

Categorized as external monooxygenases, P450s are able to activate molecular oxygen with the support of one or more redox-partners, which transfer electrons from the cofactor, usually nicotinamide

adenine dinucleotide phosphate (NAD(P)H), to the P450 heme [4]. The general P450-catalyzed reaction is performed by inserting a single oxygen atom, delivered from molecular oxygen, into the aliphatic or aromatic substrate, while the remaining oxygen atom is reduced to water (**Figure 2**):

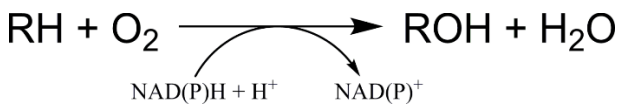

Figure 2 - General reaction mechanism catalyzed by P450s

Based on the electron transport system, and their cellular localization, P450s can be assigned to different classes. In 2007, their classification was elaborated by Hannemann *et al.* resulting in 10 classes [13]. Class I involves mostly bacterial P450 systems along with the mitochondrial ones from eukaryotes, in which the electrons are transferred from NAD(P)H via a flavin adenine dinucleotide (FAD)-containing reductase to a soluble iron-sulfur protein, which then eventually reduces the P450 system itself. In the bacterial system, all proteins are present in a soluble form, whereas in the mitochondrial system only the ferredoxin is soluble, the reductase is associated and the P450 is embedded in the inner membrane [4, 13-16]. The second category (class II) comprises the microsomal system, in which all the protein components are embedded in the membrane. Here, the electron is transferred from NAD(P)H via cytochrome P450 reductase (CPR), which contains the prosthetic groups FAD and a flavin mononucleotide (FMN). The FAD acts as an electron acceptor for NAD(P)H and the FMN domain transfers the electrons to the P450 [17] (**Figure 3**).

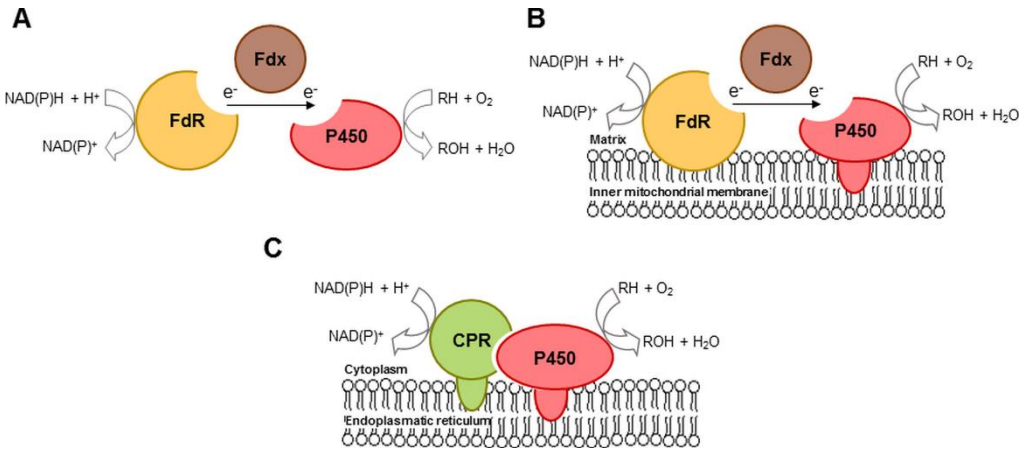

Figure 3 - Schematic organisation of the Class I, bacterial (A), mitochondrial (B) and the Class II, microsomal P450 systems. (Scheme adapted from Hannemann *et al.*, 2007 [13])

In addition to the main categories, there are many fascinating other systems, such as P450BM-3 (CYP102A1) from *Bacillus megaterium* from class VIII in which the P450 is fused to its eukaryotic-like diflavin reductase partner in a single polypeptide chain and is, therefore, catalytically self-sufficient [13].

1.1.2. Structural features

Although P450s from different gene families often demonstrate less than 20 % sequence identity, their structural organization shows similar folding and conserved topography (**Figure 4**), indicating a common mechanism of oxygen activation [18]. They consist of two domains, the first one being the α domain, rich in helices, including the highly conserved core formed by a four-helix bundle (D, L and I and the antiparallel E-helix) besides two other helices (J and K) [19]. The second one is the β domain with two beta-sheets (β_1 and β_2) in addition to another highly preserved structural motif, the meander loop at the C-terminal end of the K-helix, stabilized by the conserved sequence ExxR [20]. The heme is located between the distal I-helix and the proximal L-helix bound via a cysteine thiolate, including the signature heme-binding motive FxxGx(H/R)xCxG. The long I-helix forms a wall for the substrate-binding pocket and contains the conserved consensus sequence (A/G)GxS(E/D)T. The well preserved threonine in the active center is believed to be involved in the activation of molecular oxygen throughout the catalytic cycle [21].

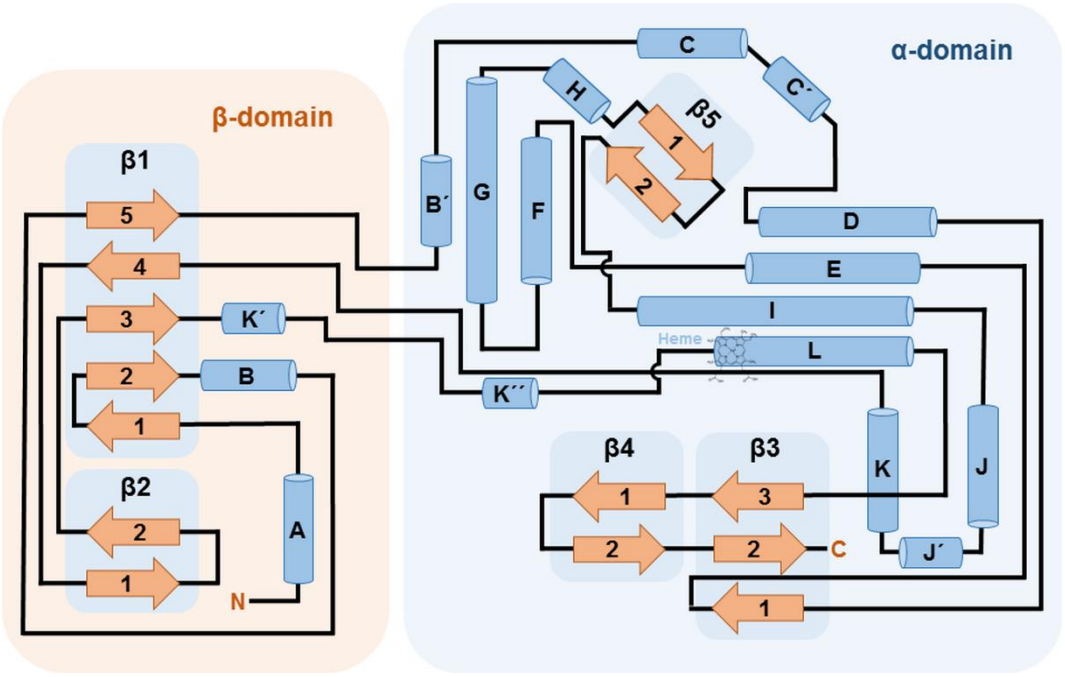

Figure 4 - Topographic map showing the secondary structural elements of cytochromes P450, exemplified by P450 BM3. The blue cylinders represent α-helices, the orange arrows the β-strands. The random coil structures are shown as black lines, linking the individual secondary structure elements. The elements are grouped in two domains, as first described by Poulos *et al.*, 1987 [22] (Figure modified after Peterson and Graham, 1998 [23]).

There are six regions identified by Gotoh named substrate recognition sites (SRS) having particular importance in the recognition and binding of substrates: the B'-helix region (SRS1), parts of helices F and G (SRS2 and SRS3), a portion of the I-helix (SRS4), the β4 hairpin structure (SRS5) and the area between K-helix and β2 (SRS6) [24]. The SRSs are considered to be the most variable regions,

showing structural rearrangement of the protein upon substrate binding in favor of the catalytic reaction, according to the proposed model of induced fit by Koshland [21, 25, 26].

1.1.3. Catalytic cycle of cytochromes P450

P450s were shown to catalyze a vast number of reactions with abundant substrate diversity. The ability to perform these different reactions using the same catalytic cycle lies in the changing oxidation states of the iron atom. Seven intermediates including three oxidation states form the complex catalytic reaction mechanism of P450s, identified for CYP101 [21]. An overview of the reaction cycle is shown in **Figure 5**.

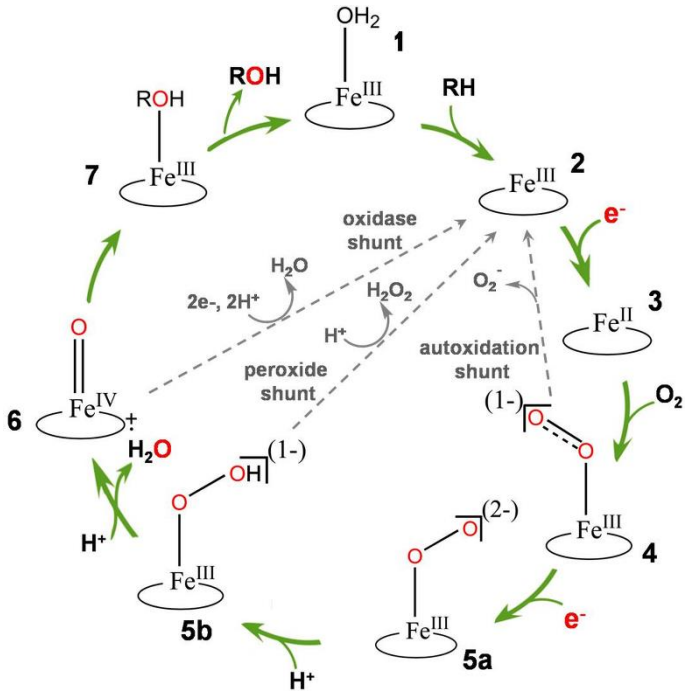

Figure 5 - Catalytic cycle of cytochrome P450 monooxygenases. The numbers (**1-7**) represent the actual state of the enzyme: **1** – Low-spin substrate-free state. **2** – High-spin enzyme-substrate complex. **3** - High-spin ferrous state. **4** – Oxy-ferrous state. **5a** - Ferric peroxo intermediate. **5b** – Ferric hydroperoxo intermediate/compound 0. **6** – High-valent iron-oxo state/compound I. **7** - Product oxidation and release. **RH** and **ROH** illustrate the substrate and the product, respectively. The three unproductive shunt-pathways are marked with dashed grey arrows and the reduced oxygen products are shown as outlets. (Figure adapted from Makris *et al*., 2002 [27] and Denisov *et al*., 2005 [21])

The cycle starts with the substrate-free, inactive ferric state (Fe (III)) of the heme iron, where the sixth coordination center is occupied by a water molecule (**1**). Upon substrate binding, the water at the distal site of the heme is partially or completely displaced, resulting in an increase of the redox potential (by 100-130 mV) and a transition from the low spin to the five-times coordinated high spin Fe (III) complex (**2**). This triggers the first electron transfer from NAD(P)H to the heme iron, producing a high spin ferrous iron (Fe II) (**3**). The subsequent binding of molecular oxygen, generates the oxy-ferrous intermediate, one of the key intermediates of the cycle (**4**). The following step is a second electron transfer, yielding the highly reactive peroxoanion state (**5a**), which is then protonated at the distal oxygen

atom to form the hydroperoxo intermediate, Compound 0 (Cpd 0) (**5b**). The next protonation step of the distal oxygen atom and the subsequent cleavage of the O-O bond leads to the release of a water molecule and the formation of the so-called Compound I (Cpd I) (**6**), a high-valent iron-oxo complex. This Fe(IV)O porphyrin cation radical initiates the oxygen atom transfer to the substrate (**7**) and the initial state is restored.

However, the depicted cycle is not always complete, there are three "uncoupling" pathways which can abort the catalytic cycle, being unproductive regarding substrate oxidation, yet still consuming NAD(P)H. The first one is the auto-oxidation of the oxy-ferrous complex (**4**) while forming the superoxide radical. The second one is known as the peroxide shunt, in which hydrogen peroxide is released from the hydroperoxo intermediate (**5b**) resulting in the substrate-bound high spin complex (**2**). Some P450s utilize the peroxide shunt in reverse, as a short cut for their reactions, introducing the oxygen to the substrate directly from the hydrogen peroxide [28]. The third possibility is the so-called oxidase shunt, where the activated oxygen atom of Cpd I (**6**) is protonated and reduced to form water rather than being inserted into the substrate.

1.1.4.Biotechnological application of cytochromes P450

Throughout their long evolution, P450s became versatile biocatalysts, performing a large variety of reactions, such as: hydroxylations, dehydrogenations, epoxidations, sulfoxidations, deaminations, N-, O-, S-dealkylations and many more [4, 29] (**Figure 6**). In addition to their diverse reaction spectrum they convert a broad range of substrates, from fatty acids, terpenes and steroids to drugs, organic solvents and even toxins. Nevertheless, what makes these enzymes particularly interesting for industrial biocatalysis is the ability to incorporate molecular oxygen into non-activated carbons in a regio- and/or stereoselective fashion at neutral pH and moderate temperatures [30-33]. Such selective hydroxylation of aromatic or aliphatic C-H bonds is hard to achieve by classical chemical synthesis, which often requires functional group protection, suffers from side reactions and high temperature operation [34-36].

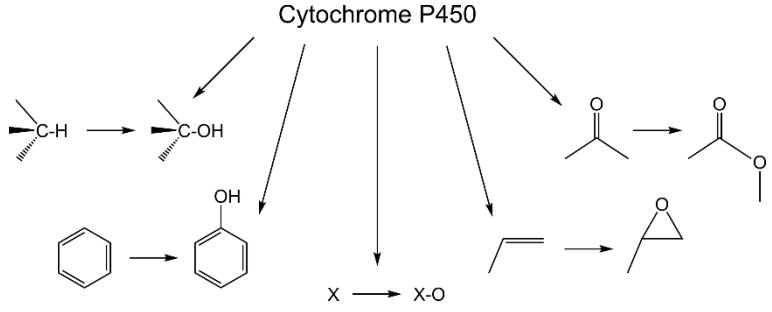

Figure 6 - Examples of the diverse oxidation reactions catalyzed by P450s.
X: -C, -N, -S. (Figure adapted from Bornschauer and Buchholz, 2005 [37])

In the last few years, significant progress has been made to reduce limitations and expand the application of P450s for synthetic processes [29, 38]. By means of protein engineering, such as site-directed mutagenesis or by directed (molecular) evolution techniques, the enzyme activity, stability,

substrate specificity and solvent tolerance has been successfully improved [39]. Yet, despite their impressive synthetic potential, it was also recognized that isolated P450s are challenging to implement in industry. Their constant need for the expensive cofactor supply and for the corresponding redox partners along with their instability and low activity under process conditions all raise limitations for such an approach [31, 40]. To circumvent this, the focus was shifted to the whole-cell system application of P450s. The application of a microbial host has proven to be a promising strategy by providing endogenous cofactor regeneration, potential co-expression of homologous or heterologous redox partners and protected environment for the biocatalyst [41]. In addition, the P450 stability was shown to be enhanced in the cellular milieu, since the H_2O_2 formed during uncoupling reactions is rendered harmless by the cellular catalase [42]. In spite of its many advantages, whole-cell catalysis also faces some important limitations, such as the transcellular transport limitation, low solubility/inhibition/toxicity of both substrate and product, inadequate NAD(P)H supply and unwanted side-reactions [40, 43].

Since cytochrome P450 substrates are mostly hydrophobic organic compounds, their transport in proximity of the whole-cell catalyst, present in the aqueous phase, as well as through the cell membrane, is a major challenge. To enable the substrate uptake, different membrane permeabilization methods (physical, chemical, and molecular engineering approaches) can be applied, depending on the microorganism. These methods may include the disintegration of the membrane by ultrasonication, freeze-thawing, using surface active substances such as Triton X, Tween, saponins or chelating agents such as ethylenediaminetetraacetic acid (EDTA) and even the co-expression of membrane transport proteins [44-48]. The faster transport of the substrate to the catalyst can be facilitated by using immiscible or miscible organic solvents. Two-phase systems with immiscible solvents are of particular interest, in which the organic phase serves as a substrate reservoir and facilitates the product removal, while the aqueous phase protects the biocatalyst from degradation [49, 50]. Another option is to apply an organic co-solvent such as ethanol, methanol or dimethyl sulfoxide (DMSO) in higher concentrations to increase substrate solubility. However, in these cases the solvent tolerance of the biocatalyst has to be considered.

A further possibility, which circumvents the use of damaging organic solvents, yet still increases both membrane permeability and substrate solubility, is the use of cyclodextrins (CD). CDs are oligosaccharides, consisting of cyclically arranged (α-1,4)-linked α-D-glucopyranose units, forming a lipophilic central cavity and a hydrophilic outer surface. Depending on the number of units they are called α-, β- and γ-CDs containing six, seven or eight glucopyranose units, respectively. These basic CDs can be further improved by chemical modifications resulting in derivatives with improved solubility and stability such as 2-hydroxypropyl-β-cyclodextrin (2-HP-β-CD) [51, 52]. Due to their hydrophobic cone-like cavity, CDs are able to form inclusion complexes with a variety of organic molecules. Based on this outstanding property, they have been widely used in medicine and healthcare for improved solubility, chemical stability and bioavailability of drugs [53]. Since CDs are inert to microorganisms and were shown to be beneficial to respiratory-chain activity [54] their use in microbial transformations of hydrophobic substrates has also been exemplified [55-57]. Besides improving substrate solubility, they

have also been used to avoid substrate/product toxicity and/or inhibition during the biocatalytic process by complexation of the corresponding molecule in the hydrophobic central cavity, thus removing it from the aqueous environment present in the cell [58].

At present, the practical application of P450s is limited mostly to the production of fine chemicals such as pharmaceuticals, flavors, fragrances and (human) drug metabolites [42]. Among the remarkable examples of biotechnological P450 applications is the artificial multi-enzyme cascade for the production of the anti-malarial drug artemisinic acid in *Saccharomyces cerevisiae* (*S. cerevisiae*) [59], the synthesis of a taxol precursor in *Escherichia coli* (*E. coli*) [60] and the production of pregnenolone, progesterone and finally hydrocortisone using *S. cerevisiae* [61, 62]. Several further developments have also contributed to raise attention to the commercial potential of P450s, such as the 11β-hydroxlation of cortexolone to hydrocortisone by *Curvularia sp*. [43, 63], the 6β-hydroxylation of compactin to pravastatin [64, 65], the biotransformation of Vitamin D3 to 1α,25-dihydroxyvitamin D3 [66, 67], or their role in anthocyanin biosynthesis in blue or violet flowers [68, 69]. The production of human drug metabolites is also a significant aspect of P450 applications due to their importance in diagnostics and drug development, for the assessment of drug-induced side effects, toxicity and possible drug-drug interactions. Their production by classical chemistry or using liver homogenates faces limitations, yet, the recombinant expression of human drug-metabolizing P450s turned out to be a promising alternative. This was successfully demonstrated by Novartis Pharma AG (Basel, Switzerland), who established an *E. coli* host co-expressing human P450s with human CPR [70]. Nonetheless, these mammalian systems might be limited due to the insufficient expression of the membrane-associated enzymes, hence bacterial, soluble P450s could be considered as suitable alternatives.

1.2. Cytochromes P450 from *Bacillus megaterium*

Bacillus megaterium (*B. megaterium*) is a gram-positive, rod shaped soil-bacterium which has been proven to be an ideal expression host for industrial biotechnology, mainly applied to protein production [71, 72]. It is used as a production strain for industrial enzymes such as, penicillin G acylase or different amylases, polyhydroxybutirate and vitamin B12 [73]. Beyond these applications, in the past decade *B. megaterium* has gained interest as host for novel recombinant enzymes and therapeutic proteins due to its many advantageous properties: it has a stable plasmid replication system, is not a pathogen, lacks alkaline proteases, does not form endotoxins, has a high protein secretion capacity directly into the medium and it is able to grow on a variety of carbon sources, which allows for low cost cultivation [74-77].

Amongst the most interesting proteins present in *B. megaterium* are P450s [78] such as: CYP102A1 (P450 BM3), a self-sufficient and so far one of the most thoroughly studied bacterial P450 [79]; CYP106A1 (P450 BM1) [80], recently functionally characterized by Brill *et al.* (2014) [81] and Lee *et al.* (2014) [82]; and finally CYP106A2 from *B. megaterium* ATCC 13368 [83, 84], which was

extensively investigated in the past four decades and its biotechnological relevance has been demonstrated in the conversion of steroids, di- and triterpenes [48, 85-89].

1.2.1.CYP106A1 from *Bacillus megaterium* DSM 319

CYP106A1 from *B. megaterium* ATCC 14581 is a soluble ~47.7 kDa protein consisting of 410 amino acids. It was first identified by He *et al.* in 1989, and has been investigated at the level of gene regulation and gene expression in the following years [90, 91]. In 2011, the genome of *B. megaterium* DSM 319 was sequenced [92], which led to the identification of several P450 genes, including the one encoding CYP106A1. The enzyme was purified and characterized by Brill *et al.*, who demonstrated its successful application in a whole-cell system for the hydroxylation of the triterpene, 11-keto-β-boswellic acid, at 7β and 15α positions [81]. Recently, CYP106A1 was also isolated from the *B. megaterium* strain ATCC 14581 by Lee *et al.*, showing successful *in vitro* steroid transformations, however, the product structures were left unidentified [82]. Its closest homologue is the well-studied CYP106A2 from *B. megaterium* ATCC 13368, with whom it shares 63 % amino acid sequence identity and 76 % similarity. Based on the high sequence identity between the two subfamily members, CYP106A1 was proposed to be an equally or even more promising catalyst in terms of steroidal drug or drug metabolite production, leading to a possible transition of the pharmaceutical industry towards greener processes.

1.2.2.CYP106A2 from *Bacillus megaterium* ATCC 13368

CYP106A2 from *B. megaterium* ATCC 13368 is a soluble ~47 kDa protein consisting of 410 amino acids. It is one of the few cloned bacterial steroid hydroxylases, also known as 15β-hydroxylase, which originates from its favored hydroxylation position on 3-oxo-Δ^4 steroids. The discovery of *B. megaterium* ATCC 13368-mediated steroid oxidation goes back to 1958, when the 15β-hydroxylation of progesterone was described by McAleer *et al.* (1958) [93]. Only later, in 1975 was the role of the cytochrome P450 as steroid hydroxylase recognized by Berg *et al.*, who also identified the potential components of the steroid hydroxylase system [83] followed by the isolation, purification and functional characterization of the enzyme [84, 94, 95]. Finally in 1993, the cloning, sequencing and heterologous expression of CYP106A2 took place in *E.coli* and *B. subtilis* [96]. Although its natural electron transfer partners are not known, its activity was successfully reconstituted using bovine adrenal redox partners, as well as by putidaredoxin and putidaredoxin reductase [48, 97-99].

In the past two decades, CYP106A2 was profoundly investigated as a potential industrial biocatalyst, applying the enzyme in whole-cell systems using both *E. coli* [48, 86, 98] and *B. megaterium* as expression hosts [87-89, 100]. Using *E.coli*, the transport of hydrophobic substrates across the outer membrane was found to be limited [101], thus further approaches were focused on using the gram-positive *B. megaterium* as host. The substrate spectrum of CYP106A2 was originally thought to be limited to 3-oxo-Δ^4-steroids [83], yet recent studies have shown that the hydroxylation of 3-hydroxy-Δ^5-steroids, di- and triterpenes is also feasible [87-89, 100]. The native substrate of CYP106A2 and its biological function are still unidentified. However, as a consequence of on-going

natural substrate library screenings, the list of its substrates is steadily growing. An overview of the so far identified CYP106A2 substrates is shown in **Table 1**.

Table 1 - Overview of the formerly identified substrates of CYP106A2
(Table adapted from Janocha, 2013 [102])

CYP106A2 substrates	References
Testosterone	Berg et al. 1976, Berg et al. 1979a
Progesterone	Berg et al. 1976, Berg et al. 1979a
17α-Hydroxyprogesteron	Berg et al. 1976, Berg et al. 1979a
20α-Dihydroprogesterone	Berg et al. 1976, Berg et al. 1979a
Deoxycorticosterone (DOC)	Berg et al. 1976, Berg et al. 1979a
Corticosterone	Berg et al. 1976, Berg et al. 1979a
Androstendione	Berg et al. 1976, Berg et al. 1979a
Anilin	Berg und Rafter 1981
6-Fluor-16-Methyl-DOC	Rauschenbach et al. 1993
Betulinic acid	Chatterjee et al. 2000
6β-Hydroxyprogesterone	Lisurek 2004
15β-Hydroxyprogesterone	Lisurek 2004
Cholestenone	Lisurek 2004
Spironolactone	Lisurek 2004
11-Deoxycortisol	Virus 2006
4-Pregnen-20β-ol-3-one	Bleif 2007
11-Keto-β-boswellic acid	Bleif 2007
Dihydrochinopimaric acid	Bleif 2007
Ethisterone	Bleif 2007
17α-Methyltestosterone	Bleif 2007
4-Pregnen-17α,20α,21-triol-3-one	Bleif 2007
Abietic acid	Bleif 2012
Oleanolic acid	Bleif 2012
Ursolic acid	Bleif 2012
Glycyrrhetinic acid	Bleif 2012
Digitoxigenin	Schmitz 2013
Prednisone	Schmitz 2013
Dexamethasone	Schmitz 2013
Dehydroepiandrosterone	Schmitz 2013
Pregnenolone	Schmitz 2013
Dipterocarpol	Schmitz 2013
Betulin	Schmitz 2013

Though its original name, 15β-hydroxylase, suggests hydroxylation at the 15β position, the long-thought strict regioselectivity was contradicted by the identification of 6β, 7α/β, 9α, 11α and 15α-hydroxy derivatives [85, 103, 104]. This by-product formation has been extensively studied for progesterone, where the 6β, 9α and 11α derivatives are of pharmaceutical interest (contraceptives, hormone replacement therapy) [103]. To enhance the previously observed C11-hydroxylation, a combinatory strategy was applied, joining directed evolution and rational protein design to change the selectivity of the enzyme

from 15β to 11α in the hydroxylation of progesterone [85]. An impressive increase in regioselectivity towards C11 was achieved forming a particularly interesting reaction product due to its inhibitory effect on 11β-hydroxysteroid dehydrogenase [105].

1.3. Steroid hormones and steroidal drugs

Steroids are terpenoid lipids with a characteristic gonane skeleton comprising seventeen carbon atoms in a four-ring structure, forming three cyclohexane rings (rings A, B, and C) and one cyclopentane ring (ring D) (**Figure 7**). Various derivatives exist, which principally differ in the oxidation state of the rings and in the functional groups attached to the four-ring system.

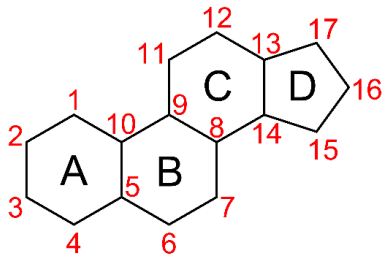

Figure 7 - Sterane, the parent ring structure of steroid compounds.
The four-ring structure (A-D) and the numbering of the carbon atoms (1-17) are shown.

Steroids play an important role as biological and chemical compounds in many living systems and have been identified in animals (e.g.: cholesterol, corticosteroids, sex hormones, bile acids, vitamin D, neurosteroids), plants (e.g.: phytosterols, diosgenin) and lower eukaryotes such as yeast and fungi (e.g.: ergosterol, ergosteroids) [106, 107]. In humans, steroidal hormones are synthesized in steroidogenic tissues such as gonads and adrenal glands from cholesterol. Their natural roles include the regulation of electrolyte and water homeostasis, cholesterol levels, control of sexual differentiation and reproduction, as well as cardiovascular and neuroprotective functions [108-111]. Steroid hormones are also known to control cell proliferation and tissue differentiation, to regulate signal transduction pathways and cell-to-cell communication processes [112-114].

Drugs based on the steroid structure are of great pharmaceutical importance being widely used in almost all fields of healthcare, from anti-microbial, anti-viral, anti-fungal agents to the treatment of hormone-dependent cancer forms, autoimmune and allergic disorders [106]. To date, steroids represent one of the largest sectors in the pharmaceutical industry with more than 300 approved drugs known [115, 116]. Steroid analogues with altered functional groups are favored over their natural counterparts, due to their improved therapeutic features such as, reduced side effects, higher potency and better pharmacokinetics [117]. Moreover, steroid hydroxylation is considered to be one of the most important reactions in steroid functionalization, since the derivatives can have enhanced biological activity and/or be further modified in drug development [118-120]. The synthesis of these functionalized derivatives is a real challenge for synthetic steroid chemistry, suffering from low predictability and specificity, yet, the combination of classical chemistry and biocatalysis was found to be successful to produce these steroids

for the pharmaceutical industry [107]. Microbial steroid hydroxylation using heterologously expressed P450s is considered to be a promising tool to produce such hydroxysteroids. Unfortunately, the biotechnological application of eukaryotic P450s is restricted due to their membrane-associated assembly leading to limitations in their expression and catalytic activities [13, 29]. In contrast, bacterial P450s are soluble proteins, which can be overexpressed to very high amounts allowing higher productivities in biotransformation and representing a promising alternative for industrial applications [48, 99].

1.4. Aim and outline of the work

The global objective of this work was the in-depth characterization of the bacterial CYP106A subfamily in the bioconversion of steroid compounds to explore and expand their potential application as biocatalysts in industrial-scale steroid hydroxylations (**Figure 8**). CYP106A2 from *B. megaterium* ATCC 13368 was extensively studied since the late 1970s and shown to hydroxylate steroids, di- and triterpenes in a regio- and stereoselective manner. Its lesser known counterpart, CYP106A1 from *B. megaterium* DSM 319, sharing high sequence identity, was also recognized as a terpene- and steroid-hydroxylase, however, its potential as a biocatalyst was not fully investigated.

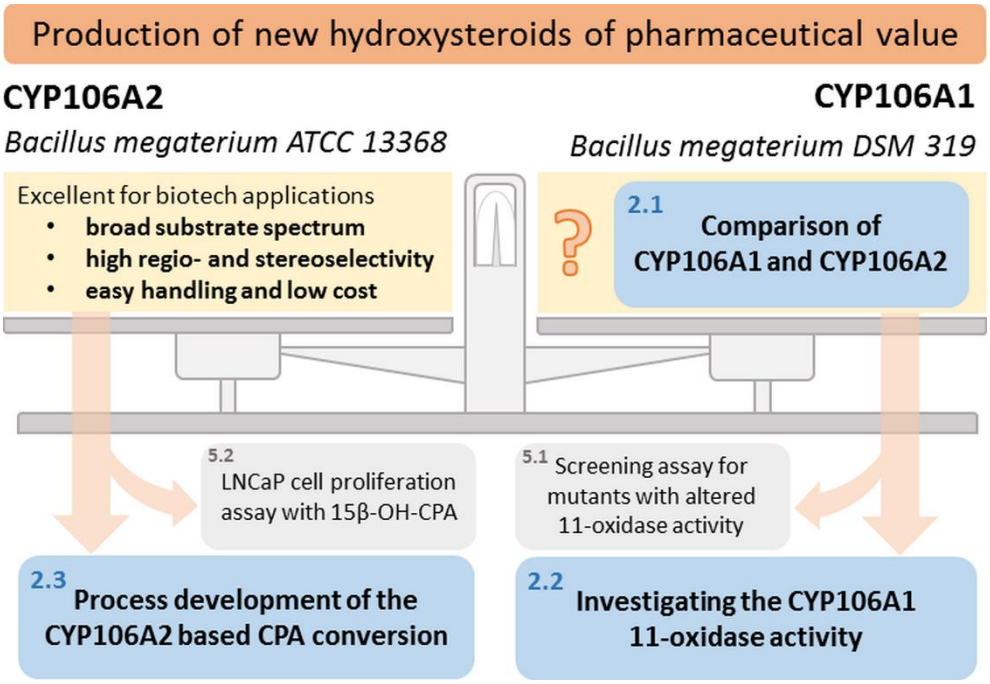

Figure 8 - Summary of the motivation, previous work and contents of this thesis. The orange box represents the global aim of the work, the yellow contains the state of the art. The blue and the grey rectangles symbolize the published and unpublished results, respectively, with the corresponding chapter number.

For a detailed analysis of the CYP106A subfamily members and a comparison of their steroid hydroxylating capacity, a focused steroid library was screened. The initial substrate-screening was based on their high-spin shift induction via difference spectroscopy, also allowing the determination of dissociation constants (K_D). Since type I shift-induction is a good indication but not a prerequisite for

successful conversion, all steroids were subjected to further *in vitro* assays and subsequent analysis of product formation by high performance liquid chromatography (HPLC). Out of the 19 converted steroids, 6 were chosen for further investigation. Since functionalized steroids could be of pharmaceutical importance as drugs or drug metabolites, the emphasis was placed on the analysis of enzyme activity and product identification for the evaluation of potential biotechnological applications. Substrate conversions were performed using formerly established *B. megaterium* MS941 whole-cell systems, overexpressing each CYP106 enzyme. The conversion products were isolated by preparative HPLC and their structural determination was achieved by NMR spectroscopy. The obtained results are summarized in **Chapter 2.1** of this thesis.

In **Chapter 2.2**, the newly identified CYP106A1 11-oxidase activity, obtained as a result in **Chapter 2.1**, was further investigated. Three 11β-hydroxysteroid-analogues (prednisolone, dexamethasone and 11β-hydroxyandrostenedione) were screened with CYP106A1. The 11-oxidation of the substrates was confirmed by NMR in all cases, however, single 11-keto product formation was only obtained for 11β-hydroxyandrostenedione. The latter reaction was chosen to investigate the mechanism of the reaction using kinetic solvent isotope effect.

The final section (**Chapter 2.3**) describes the results obtained in a collaborative project with the Technical University of Denmark, where the bioconversion of the pharmaceutically relevant antiandrogen, cyproterone acetate, was investigated using a CYP106A2-based *B. megaterium* whole-cell system. Since the product, 15β-hydroxycyproterone acetate, is of pharmaceutical interest, the aim was to scale-up the reaction from shake flasks to bioreactors to model an efficient, yet greener and cost-effective production. To improve the yield and product titers for a future large-scale application, the main bottlenecks of the reaction were identified and addressed.

2. Scientific articles

The obtained results presented in this work are published in the articles listed below:

2.1. Kiss *et al.* (2015)

Comparison of CYP106A1 and CYP106A2 from *Bacillus megaterium* - identification of a novel 11-oxidase activity

Flora Marta Kiss, Daniela Schmitz, Josef Zapp, Tobias K. F. Dier, Dietrich A. Volmer, Rita Bernhardt

Applied Microbiology and Biotechnology 2015 Apr 24 doi: 10.1007/s00253-015-6563-8

Comparison of CYP106A1 and CYP106A2 from *Bacillus megaterium* - identification of a novel 11-oxidase activity

Flora Marta Kiss[1], Daniela Schmitz[1], Josef Zapp[2], Tobias K. F. Dier[3], Dietrich A. Volmer[3], Rita Bernhardt[1*]

Abstract

The CYP106A subfamily hydroxylates steroids, di- and triterpenes in a regio- and stereoselective manner, which is a challenging task for synthetic chemistry. The well-studied CYP106A2 enzyme, from the *Bacillus megaterium* strain ATCC 13368, is a highly promising candidate for the pharmaceutical industry. It shares 63 % amino acid sequence identity with CYP106A1 from *B. megaterium* DSM319, which was recently characterized. A focused steroid library was screened with both, CYP106A1 and CYP106A2. Nineteen out of the 23 tested steroids were successfully converted by both enzymes during *in vitro* and *in vivo* reactions. Thirteen new substrates were identified for CYP106A1, while the substrate spectrum of CYP106A2 was extended by 7 new members. Finally, 6 chosen steroids were further studied on a preparative scale employing a recombinant *B. megaterium* MS941 whole-cell system, yielding sufficient amounts of product for structure characterization by nuclear magnetic resonance. The hydroxylase activity was confirmed at positons 6β, 7β, 9α and 15β. In addition, the CYP106A subfamily showed unprecedented 11-oxidase activity, converting 11β-hydroxysteroids to their 11-keto derivatives. This novel reaction and the diverse hydroxylation positions on pharmaceutically relevant compounds underline the role of the CYP106A subfamily in drug development and production.

Keywords: CYP106A1, CYP106A2, cortisol, cortisone, 11β-hydroxysteroid dehydrogenation

Introduction

For the past decade cytochrome P450 enzymes (P450s) have been studied as candidates for pharmaceutical drug and drug precursor development. This large superfamily of heme cofactor-containing monooxygenases (http://drnelson.uthsc.edu/CytochromeP450.html) is involved in the catalysis of a wide range of reactions from hydroxylations, epoxidations and deaminations to dealkylations and C-C bond cleavage. Not only do they perform versatile reactions, they also convert a broad range of substrates. P450s participate in the biosynthesis of endogenous steroids, fatty acids and vitamins as well as in the elimination of exogenous compounds, xenobiotics and drugs (Bernhardt, 2006; Urlacher et al., 2004). They are thus suitable for the production of pharmaceutical compounds and provide a more economically and ecologically sustainable alternative to chemical synthesis, even more so, where the latter has failed to produce sufficient amounts of product (Bernhardt and Urlacher, 2014; Urlacher and Girhard, 2012). The chemical synthesis of steroids is very complex and costly, particularly when performing regio- and stereo-selective hydroxylations. Microbial/enzymatic transformations are, therefore, favored by the industry as a straight-forward, greener and more cost-effective solution (Donova and Egorova, 2012; Tong and Dong, 2009).

The heterologous expression of bacterial P450 enzymes was shown to be successful in several host organisms, making the Class I bacterial P450 systems preferable over their membrane-bound mammalian counterparts, due to their solubility

[1]Institute of Biochemistry, Saarland University, D-66123 Saarbruecken, Germany

[2]Institute of Pharmaceutical Biology, Saarland University, D-66123 Saarbruecken, Germany

[3]Institute of Bioanalytical Chemistry, Saarland University, D-66123 Saarbruecken, German

*Address correspondence to: Professor Dr. Rita Bernhardt
Email: ritabern@mx.uni-sarland.de

and easy handling (Bernhardt, 2006; Hannemann et al., 2007; Venkataraman et al., 2014). Although their expression and purification is possible at an analytical scale, the use of isolated P450s in industrial applications is not feasible, mainly due to their instability under process conditions and the need for a constant supply of the rather expensive cofactor NADP(H) (Bernhardt and Urlacher, 2014; O'Reilly et al., 2011; Urlacher and Eiben, 2006). The latter has been addressed by both enzymatic and chemical methods (Chefson and Auclair, 2006; Hollmann et al., 2006), along with the progress towards improved thermostability (Li et al., 2007) and solvent tolerance (Seng Wong et al., 2004). A different possible workaround is the construction of whole-cell systems, where the P450 is expressed by a microbial host organism. These constructs have the advantage of stabilizing the P450 integrity and electron transfer and provide cofactor regeneration by the cellular metabolism. Numerous organisms have been described to realize the heterologous expression of P450s, including the most widely used, *Escherichia coli* (Agematu et al., 2006; Bracco et al., 2013; Makino et al., 2014). Nevertheless, there are cases when using *E. coli* can lead to limitations, such as the restricted transport of large hydrophobic molecules across the cell membrane (Janocha and Bernhardt, 2013; Zehentgruber et al., 2010). Another candidate, *Bacillus megaterium*, has recently aroused greater interest as a genetically modified host organism for biotechnological/industrial approaches, especially for the expression of heterologous proteins. On account of having its own P450 expression system, it does not require the addition of the heme-precursor (δ-aminolevulinic acid) in contrast to *E.coli* which lacks natural P450 genes and heme proteins. Its attractive characteristics also include: growth on various carbon sources, high plasmid stability and no alkaline protease or endotoxin production (Bleif et al., 2012; Korneli et al., 2013; Vary et al., 2007).

From a biotechnological standpoint, CYP106A2 from the *B. megaterium* strain ATCC 13368 (Berg et al., 1976; Berg et al., 1979) and its unique hydroxylating properties raised interest in the past years (Hannemann et al., 2006; Virus and Bernhardt, 2008). CYP106A2 being extensively studied since the late 1970s, is a highly active steroid hydroxylase, catalyzing mainly the 15β-hydroxylation of 3-oxo-Δ4-steroids (Berg et al., 1976; Berg et al., 1979). Furthermore, the enzyme was shown to hydroxylate di- and triterpenes (Bleif et al., 2011; Bleif et al., 2012; Schmitz et al., 2012) and recently was also described as a regioselective hydroxylase for the 3-hydroxy-Δ5 steroid dehydroepiandrosterone (Schmitz et al., 2014). Although its original name, 15β-hydroxylase, suggests mainly hydroxylation at the 15β position, the long-thought strict regioselectivity was contradicted by the identification of 6β, 7α/β, 9α, 11α and 15α-hydroxy products (Lisurek et al., 2004; Lisurek et al., 2008; Nguyen et al., 2012; Virus et al., 2006). Even though, these hydroxylations occur in lower proportions, the resulting products are of industrial interest. This means a unique potential for industrial applications, since there is a wide variety of compounds that could serve as substrates for this enzyme. Its natural substrate is yet to be identified and its substrate range is continuously broadening as a result of library screening (Schmitz et al., 2012; Schmitz et al., 2014).

The lesser known CYP106A1 shares 63 % amino acid sequence identity and 76 % similarity with its well-studied sibling, CYP106A2 (He et al., 1995; He et al., 1989). CYP106A1 from *B. megaterium* DSM319 was recently purified and characterized by our group (Brill et al., 2014) and successfully applied in a whole-cell system for the hydroxylation of a triterpene, 11-keto-β-boswellic acid (KBA), at 7β and 15α positions. The CYP106A1-dependent conversion showed a different product pattern compared with CYP106A2 (Bleif et al., 2012), resulting in two additional products, identified as 7β-hydroxy-KBA and 7β,15α-dihydroxy KBA. Furthermore, CYP106A1 was also characterized *in vitro* from another *B. megaterium* strain, ATCC 14581 by Lee *et al.*, who recognized some steroids as convertible substrates, but leaving product structures unidentified (Lee et al., 2014). Based on the high sequence identity between the two enzymes, CYP106A1 was proposed to be an

equally promising candidate in a possible transition of the pharmaceutical industry towards greener processes. In order to exploit the potential of CYP106A1 and to reveal the anticipated differences in activity and selectivity between the two subfamily members, we decided to focus on steroid conversions. Steroids are pharmaceuticals of great importance. Drugs based on the steroid structure are widely used in almost all fields of healthcare, from anti-microbial and anti-viral agents to the treatment of hormone-dependent cancer forms (Donova and Egorova, 2012). Moreover, steroid hydroxylation is considered to be one of the most important reactions in steroid functionalization, since the derivatives have enhanced biological activity or can be further modified in drug development (Choudhary et al., 2011; Choudhary et al., 2005; Janeczko et al., 2009).

Here we tested a focused substrate library with both CYP106A subfamily members and extended their substrate ranges with respect to different steroid molecules. Nineteen of the 23 screened steroids were successfully converted by both enzymes during *in vitro* and *in vivo* reactions. Using recombinant *B. megaterium* MS941 whole-cell systems, overexpressing each enzyme, sufficient amounts of product were obtained for structure characterization by nuclear magnetic resonance (NMR). Besides confirming the production of mono- and dihydroxylated products at 6β, 7β, 9α and 15β positions, we were able to demonstrate a previously unknown reaction among these P450s, an 11β-hydroxysteroid dehydrogenase activity. Our recent findings underline the role of the CYP106A subfamily in the field of drug development and production.

Materials and methods

Reagents and chemicals

All steroid substrates were purchased from Sigma-Aldrich (Sigma Aldrich Biochemie Gmbh, Germany), all other chemicals were obtained from standard sources and of highest grade available.

Expression and purification of the enzymes

The expression and purification of the CYP106A1 and CYP106A2 proteins was performed as described previously (Brill et al., 2014; Lisurek et al., 2004; Simgen et al., 2000). For the reconstituted *in vitro* system, a truncated form of bovine adrenodoxin ($Adx_{4\text{-}108}$) was used in combination with bovine adrenodoxin reductase (AdR). Their expression and purification was completed as described elsewhere (Sagara et al., 1993; Uhlmann et al., 1992).

UV-visible absorbance spectroscopy

To analyze the characteristics of the purified CYP106A family members, the UV-visible absorbance spectrum of the proteins was recorded in a range of 200-700 nm with a double beam spectrophotometer (UV-2101 PC, Shimadzu, Japan). The spectra were constantly analyzed during the purification process, approaching a Q value (A_{417}/A_{280}) higher then 1.5, suggesting a high amount of well-folded, heme-containing and active P450s. The concentration of the proteins for further experiments was determined by CO difference spectroscopy according to the method of Omura and Sato (Omura and Sato, 1964), using an extinction coefficient for the CO-bound P450 of 91 mM^{-1} cm^{-1}.

Substrate binding assay

The substrate binding difference spectra were investigated using a double-beam spectrophotometer (UV-2101PC, Shimadzu, Japan) and tandem quartz cuvettes. The reaction was carried out in 800 µl total volume. One chamber of each cuvette contained 10 µM solution of the enzymes in 50 mM potassium phosphate buffer pH 7.4, while the other chamber was filled with the buffer only. The substrate was dissolved in DMSO at a stock concentration of 20 mM. The enzyme solution was then titrated with increasing concentrations of the substrate. In each step the same amount of substrate was also added to the buffer-containing chamber of the reference cuvette. After each titration step, the spectrum was recorded between 350 nm and 500 nm. The K_d value was calculated after the titration of the substrate until saturation. The data was analyzed by plotting the peak-to-through differences against the concentrations of the substrate. The data was fitted in Origin (OriginLab Corporations,

Massachusetts, USA) using hyperbolic regression. The K_d values are averaged from three independent measurements.

***In vitro* conversions**

The *in vitro* conversion of the substrates was carried out with a reconstituted system in a final volume of 250 µL at 30 °C for 60 min in 50 mM potassium phosphate buffer (pH 7.4), containing 20 % (v/v) glycerol. The reconstituted system contained AdR (1 µM), the truncated form of bovine Adx_{4-108} (10 µM), CYP106A1 and CYP106A2 (1 µM), an NADPH-regenerating system [MgCl2 (1 mM), glucose-6-phosphate (5 mM), glucose-6-phosphate dehydrogenase (1 U), and NADPH (0.1 µM)] and the substrate (200 µM). The reaction was started by adding NADPH (100 µM) and stopped by the addition of 250 µl of ethyl acetate, mixed vigorously, and extracted twice. After evaporating the combined organic phases to dryness, the residues were dissolved in the high-performance liquid chromatography (HPLC) mobile phase and subjected to HPLC analysis.

In *vivo* conversions

The *in vivo* steroid conversions were performed using the recombinant *B. megaterium* MS941 strain, derived from the strain DSM319 (Wittchen and Meinhardt, 1995), lacking the major extracellular protease gene *nprM*. The *B. megaterium* MS941 strain was transformed with the corresponding plasmid pSMF2.1B (containing CYP106A1 cloned into SpeI/MluI sites (Brill et al., 2014)) or pSMF2.1C (containing CYP106A2 cloned into SpeI/MluI sites (Bleif et al., 2012)) applying a polyethylene glycol-mediated technique using protoplasts (Barg et al., 2005). To make sure that the conversion was catalyzed by the anticipated enzyme, the conversions were compared to transformations with the wild type strain MS941 (lacking the pSMF2.1 plasmid, but naturally containing cytochrome P450 genes) as a control. According to these results, the wild type strain did not show any conversion.

Precultures were inoculated from -80 °C glycerol stock, using 25 ml complex TB medium (24 g/l yeast extract, 12 g/l soytone, 2.31 g/l KH_2PO_4 and 12.5 g/l K_2HPO_4) supplemented with 10 µg/ml tetracycline and incubated overnight, at 150 rpm, 30 °C. The main culture (supplemented with the corresponding amount of tetracycline) was inoculated with 1% of the culture volume from the overnight culture. Following the inoculation of the main culture, it was further incubated for 2-3 hours, until it reached an OD_{578} = 0.4 when 0.5 g/l xylose solution was added to induce the expression. Cells were cultivated for 24 h under the same conditions prior to the addition of the substrate. For analytical purposes, the experiments were performed in 2 ml reaction tubes with a 500 µl volume of the freshly aliquoted main culture. The transformations required the use of an Eppendorf thermomixer (Eppendorf, Hamburg, Germany) for the continuous mixing with 1000 rpm, keeping the temperature constant at 30°C, for 1-4 h. For the preparative scale conversions, 50 ml culture volume was used in 300 ml baffled shake flasks, inoculated with 500 µl of the precultures, induced and cultivated for 24 h at 30°C, before the addition of the substrates. Conversions at a larger scale were performed with resting cells, either adding the substrate directly 24 hours after the expression or after harvesting the cells and suspending them in 100 mM potassium phosphate buffer (pH 7.4). The steroids were added as ethanolic solution to the culture medium (the use of ethanol did not exceed 5% of the culture volume). Following the corresponding conversion time, the reaction was stopped and the steroids were extracted twice by the addition of 50 ml ethyl acetate. The organic phase was dried over anhydrous $MgSO_4$ and concentrated to dryness in a rotatory evaporator (Büchi R-114). The yellowish residue was dissolved in the mobile phase of the HPLC and filtered through a sterile syringe filter (Rotilabo syringe filter, 0.22 µm, Carl Roth GmbH, Karlsruhe, Germany). The products were separated by preparative HPLC, according to its retention time. The collected fractions were evaporated to dryness and analyzed by NMR spectroscopy and high-resolution mass spectrometry (HRMS).

HPLC analysis

The HPLC analysis was performed on a Jasco system consisting of a Pu-980 HPLC pump, an AS-950 sampler, a UV-975 UV/Vis detector, and an LG-980–02 gradient unit (Jasco, Gross-Umstadt, Germany). A reversed-phase ec MN Nucleodor C_{18} (3µM, 4.0x125mm) column (Macherey-Nagel, Betlehem, PA, USA) was used to carry out the experiments, kept at an oven temperature of 40 °C. The steroids were eluted from the column using a gradient method, starting with a mobile phase ratio of 1:9 of ACN:H_2O and increasing it to 1:1. The used flow rate was 1 ml/min and the UV detection of the substrate and product was accomplished at 240 or 254 nm. In the case of the isolation of conversion products the conditions of the preparative reversed-phase HPLC (ec MN Nucleodur C_{18} VP (5µM, 8x250mm), Macherey-Nagel, Betlehem, PA, USA) varied according to the size of the column, consequently the maximum injectable amount of sample could reach 1 ml and the flow rate 2.5 ml/min.

The conversion and product distribution were calculated from the relative peak area (area %) of the HPLC chromatograms. Following the conversion, all peak areas were summed up and the respective product peak area was divided by the total area of all peaks. The results are presented as conversion % and product formation %.

HRMS analysis

Analyses were performed using a solariX 7 Tesla FTICR mass spectrometer (Bruker Daltonik, Bremen, Germany). All samples were ionized by atmospheric pressure chemical ionization (APCI) in negative ionization mode, using the following parameters: dry temperature 350 °C, vaporizing temperature 350 °C, corona needle 40000 nA, capillary voltage 2000 V, end plate offset -500 V, estimated R. P. (400 m/z) 70000. The calculated exact and measured accurate masses are presented next to each identified compound name in the NMR section.

NMR characterization of the metabolites

The NMR spectra were recorded in $CDCl_3$ or CD_3OD with a Bruker DRX 500 or a Bruker Avance 500 NMR spectrometer at 300 K. The chemical shifts were relative to $CHCl_3$ at δ 7.26 or CH_3OD at δ 3.30 (^{1}H NMR) and $CDCl_3$ at δ 77.00 or CD_3OD at δ 49.00 (^{13}C NMR) respectively using the standard δ notation in parts per million. The 1D NMR (^{1}H and ^{13}C NMR, DEPT135) and the 2D NMR spectra (gs-HH-COSY, gs-NOESY, gs-HSQCED, and gs-HMBC) were recorded using the BRUKER pulse program library. All assignments were based on extensive NMR spectral evidence. (For detailed substrate and product structures, see Table 4.)

6β-hydroxyandrost-4-ene-3,17-dione

Product A4 (2.6 mg) in the conversion of androstenedione with CYP106A1 (HRMS (APCI) calculated exact mass [Da] $C_{19}H_{26}O_3$ $[M+TFA-H]^-$ 415.1732; measured accurate mass [Da] 415,1733, error [ppm] -0.44). Its ^{1}H NMR data matched those in literature (Kirk et al., 1990). ^{1}H NMR ($CDCl_3$, 500 MHz): δ 0.95 s (3xH-18), 0.98 ddd (12.3, 10.8 and 4.2 Hz, H-9), 1.29 m (H-12a), 1.31 m (H-14), 1.33 m (H-7a), 1.41 s (3xH-19), 1.53 m (H-11a), 1.63 m (H-15a), 1.66 m (6-OH), 1.70 m (H-11b), 1.73 m (H-1a), 1.89 ddd (13.3, 4.2 and 3.0 Hz, H-12b), 1.99 ddd (13.2, 4.0 and 3.0 Hz, H-15b), 2.06 ddd (13.3, 5.0 and 3.0 Hz, H-1b), 2.12 m (H-16a), 2.14 m (H-7b), 2.18 m (H-8), 2.41 m (H-2a), 2.49 m (H-16b), 2.53 m (H-2b), 4.41 ddd (3x2.5 Hz, H-6), 5.84 brs (H-4). ^{13}C NMR ($CDCl_3$, 125 MHz): δ 13.79 (CH_3, C-18), 19.59 (CH_3, C-19), 20.29 (CH_2, C-11), 21.72 (CH_2, C-15), 29.43 (CH, C-8), 31.30 (CH_2, C-12), 34.20 (CH_2, C-2), 35.76 (CH_2, C-16), 37.13 (CH_2, C-1), 37.22 (CH_2, C-7), 38.05 (C, C-10), 47.63 (C, C-13), 50.93 (CH, C-14), 53.68 (CH, C-9), 72.94 (CH, C-6), 126.64 (CH, C-4), 167.43 (C, C-5), 199.97 (C, C-3), 220.33 (C, C-17).

7β-hydroxyandrost-4-ene-3,17-dione

Product A2 (3 mg) in the conversion of androstenedione with CYP106A1 (HRMS (APCI) calculated exact mass [Da] $C_{19}H_{26}O_3$ $[M+TFA-H]^-$ 415.1732; measured accurate mass [Da] 415,1731, error [ppm] 0.06). Its ^{1}H NMR data matched those in literature (Kirk et al., 1990): ^{1}H NMR ($CDCl_3$, 500 MHz): δ 0.95 s (3xH-18), 1.01 ddd (12.4, 10.5 and 4.0 Hz, H-9), 1.24 s (3xH-19), 1.26 ddd

(2x13.3 and 4.2 Hz, H-12a), 1.47 m (H-14), 1.50 m (H-11a), 1.57 m (7-OH), 1.67 ddd (13.5, 13.5 and 5.0 Hz, H-1a), 1.75 m (H-11b), 1.76 ddd (3x10.5 Hz, H-8), 1.88 ddd (13.3, 5.0 and 3.3 Hz, H-12b), 1.94 m (H-15a), 2.06 ddd (13.5, 5.0 and 3.3 Hz, H-1b), 2.13 ddd (19.5 and 2x9.5 Hz, H-16a), 2.32 m (H-15b), 2.39 m (H-2a), 2.45 m (H-2b), 2.48 m (H-16b), 2.49 m (H-6a), 2.58 dd (14.0 and 5.2 Hz, H-6b), 3.59 m (H-7), 5.78 d (2.0 Hz, H-4). ^{13}C NMR ($CDCl_3$, 125 MHz): δ 13.96 (CH_3, C-18), 17.38 (CH_3, C-19), 20.37 (CH_2, C-11), 24.98 (CH_2, C-15), 31.22 (CH_2, C-12), 33.89 (CH_2, C-2), 35.65 (CH_2, C-1), 35.97 (CH_2, C-16), 38.04 (C, C-10), 42.59 (CH, C-8), 42.69 (CH_2, C-6), 48.01 (C, C-13), 50.52 (CH, C-14), 50.78 (CH, C-9), 74.37 (CH, C-7), 125.09 (CH, C-4), 166.35 (C, C-5), 198.95 (C, C-3), 220.39 (C, C-17).

15β-hydroxyandrost-4-ene-3,17-dione

Product B6 (3.7 mg) in the conversion of androstenedione with CYP106A2 (HRMS (APCI) calculated exact mass [Da] $C_{19}H_{26}O_3$ $[M+TFA-H]^-$ 415.1732; measured accurate mass [Da] 415,1752, error [ppm] 4.78). Its ^{13}C NMR data matched those in literature (Mineki et al., 1995) ^{1}H NMR ($CDCl_3$, 500 MHz): δ 1.04 ddd (14.8, 10.7 and 4.2 Hz, H-9), 1.22 m (H-7a), 1.23 s (3xH-18), 1.26 s (3xH-19), 1.29 m (H-12a), 1.30 m (H-14), 1.52 m (H-11a), 1.74 m (H-1a), 1.75 m (H-11b), 1.85 ddd (13.2, 4.8 and 3.2 Hz, H-12b), 2.06 m (H-1b), 2.11 m (H-8), 2.15 m (H-7b), 2.36 m (H-2a), 2.37 m (H-6a), 2.43 m (H-2b), 2.50 m (H-6b), 2.52 dd (19.6 and 6.0 Hz, H-16a), 2.59 dd (19.6 and 1.3 Hz, H-16b), 4.59 ddd (6.0, 4.5 and 1.3 Hz, H-15), 5.77 brs (H-4). ^{13}C NMR ($CDCl_3$, 125 MHz): δ 17.26 (CH_3, C-19), 17.59 (CH_3, C-18), 20.26 (CH_2, C-11), 30.47 (CH_2, C-7), 31.44 (CH, C-8), 32.46 (CH_2, C-6), 32.61 (CH_2, C-12), 33.91 (CH_2, C-2), 35.73 (CH_2, C-1), 38.80 (C, C-10), 46.70 (C, C-13), 47.06 (CH_2, C-16), 54.24 (CH, C-9), 54.96 (CH, C-14), 67.16 (CH, C-15), 124.23 (CH, C-4), 170.12 (C, C-5), 199.30 (C, C-3), 219.05 (C, C-17).

7β, 15β-dihydroxyandrost-4-ene-3,17-dione

Product B3 (2 mg) in the conversion of androstenedione with CYP106A2 (HRMS (APCI) calculated exact mass [Da] $C_{19}H_{26}O_4$ $[M+TFA-H]^-$ 431.1682; measured accurate mass [Da] 431,1685, error [ppm] 0.81. The ^{1}H and ^{13}C NMR spectra showed signals for two secondary hydroxyl groups with similar chemical shifts to those of the monohydroxylated androstenedione derivatives A2 and B6. The positions of the hydroxyl groups at C-7 and C-15 were supported by the results of 2D NMR experiments (HHCOSY, HSQC and HMBC). For example, H-7 (δ_H 3.74 ddd) showed correlations to the H-6a and H-6b (2.58 m, 2H) and H-8 (2.12 ddd) in the HHCOSY, H-15 could be assigned by its vicinal couplings to H-14, H-16a and H-16b in the HHCOSY and its $^3J_{CH}$ correlation with carbonyl C-17 in the HMBC. The β-orientation for both hydroxyls could be concluded by results of the NOESY spectrum. H-7 and H-15 showed an effect to each other and both to the α-orientated H-14; H-7 showed an additional effect to the α-orientated H-9. Therefore, both H-7 and H-15 were in α-position and as a consequence their corresponding hydroxyls β-orientated. To our knowledge the structure of this dihydroxylated androstenedione has not been reported so far. ^{1}H NMR ($CDCl_3$, 500 MHz): δ 1.06 ddd (12.5, 10.7 and 4.2 Hz, H-9), 1.26 s (3xH-18), 1.27 m (H-12a), 1.28 s (3xH-19), 1.40 dd (10.7 and 4.5 Hz, H-14), 1.58 m (H-11a), 1.68 ddd (2x13.5 and 5.0 Hz, H-1a), 1.76 m (H-11b), 1.83 ddd (12.7, 4.0 and 2.5 Hz, H-12b),), 2.08 ddd (13.5, 5.0 and 3.3 Hz, H-1b), 2.12 ddd (3x 10.7 Hz, H-8) 2.38 m (H-2a), 2.44 m (H-2b), 2.53 dd (20.0 and 8.0 Hz, H-16a), 2.58 m (2H, H-6a and H-6b), 2.67 dd (20.0 and 1.2 Hz, H-16b), 3.74 ddd (9.5 and 2x8.0 Hz, H-7), 4.66 ddd (7.0, 4.5 and 1.2 Hz, H-15), 5.79 brs (H-4). ^{13}C NMR ($CDCl_3$, 125 MHz): δ 17.34 (CH_3, C-19), 17.65 (CH_3, C-18), 20.38 (CH_2, C-11), 32.16 (CH_2, C-12), 33.86 (CH_2, C-2), 35.58 (CH_2, C-1), 38.01 (C, C-10), 38.56 (CH, C-8), 42.46 (CH_2, C-6), 44.53 (CH_2, C-16), 47.06 (C, C-13), 51.01 (CH, C-9), 55.07 (CH, C-14), 68.52 (CH, C-15), 73.74 (CH, C-7), 125.37 (CH, C-4), 165.67 (C, C-5), 198.90 (C, C-3), 219.50 (C, C-17).

15β-hydroxycorticosterone

Product D1 (1.2 mg) in the conversion of corticosterone with CYP106A2 (HRMS (APCI)

calculated exact mass [Da] $C_{21}H_{30}O_5$ $[M-H]^-$ 361.2015; measured accurate mass [Da] 361.2020, error [ppm] 1.27). Its NMR data showed resonances for an additional hydroxyl group (δ_C 70.24; δ_H 4.41 m), which could be located at position 15β by means of 2D NMR. ^{1}H NMR ($CDCl_3$, 500 MHz): δ 1.02 m (H-14), 1.06 m (H-9), 1.15 m (H-7a), 1.19 s (3xH-18), 1.48 s (3xH-19), 1.62 dd (13.8 and 3.3 Hz, H-12a), 1.86 ddd (2x13.5 and 4.5 Hz, H-1a), 2.08 dd (13.8 and 2.8 Hz, H-12b), 2.21 ddd (13.5, 5.0 and 4.0 Hz, H-1b), 2.28 m (2H, H-6a and H-7b), 2.33 m (2H, H-16a and b), 2.34 m (H-17), 2.37 m (H-2a), 2.38 m (H-8), 2.49 m (H-2b), 2.55 m (H-6b), 3.23 dd (2x 4.5 Hz, 21-OH), 4.19 dd (18.5 and 4.5 Hz, H-21a), 4.24 dd (18.5 and 4.5 Hz, H-21b), 4.41 m (H-15), 5.70 d (2.0 Hz, H-4). ^{13}C NMR ($CDCl_3$, 125 MHz): δ 18.65 (CH_3, C-18), 20.80 (CH_3, C-19), 27.78 (CH, C-8), 31.70 (CH_2, C-7), 31.82 (CH_2, C-6), 33.79 (CH_2, C-2), 34.78 (C, C-10), 35.04 (CH_2, C-1), 35.53 (CH_2, C-16), 43.46 (C, C-13), 49.13 (CH_2, C-12), 56.64 (CH, C-9), 59.80 (CH, C-17), 61.74 (CH, C-14), 67.80 (CH, C-11), 69.22 (CH_2, C-21), 70.24 (CH, C-15), 122.55 (CH, C-4), 171.36 (C, C-5), 199.32 (C, C-3), 208.77 (C, C-20).

11-dehydrocorticosterone

Product C5 (2.5 mg) and D4 (1 mg) in the conversion of corticosterone with CYP106A1 and CYP106A2 respectively (HRMS (APCI) calculated exact mass [Da] $C_{21}H_{28}O_4$ $[M-H]^-$ 343.1909; measured accurate mass [Da] 343.1921, error [ppm] 3.34). The NMR spectra of C5 lacked of resonances for the 11-hydroxy group but revealed an additional carbonyl (δ_C 207.49) for C-11. ^{1}H NMR ($CDCl_3$, 500 MHz): δ 0.67 s (3xH-18), 1.27 m (H-7a), 1.41 s (3xH-19), 1.45 m (H-15a), 1.63 ddd (2x14.5 and 4.5 Hz, H-1a), 1.80 m (H-14), 1.92 m (2H, H-9 and H-16a), 1.93 m (H-8), 1.95 m (H-15b), 1.98 m (H-7b), 2.29 m (H-16b), 2.30 m (2H, H-2a and H-6a), 2.44 m (H-6b), 2.47 d (12.0 Hz, H-12a), 2.48 ddd (17.0, 14.5 and 5.0 Hz, H-2b), 2.56 d (12.0 Hz, H-12b), 2.68 dd (2x9.5 Hz, H-17), 2.77 ddd (14.5, 5.0 and 3.3 Hz, H-1b), 3.16 dd (2x 3.5 Hz, 21-OH), 4.14 dd (19.5 and 3.5 Hz, H-21a), 4.19 dd (19.5 and 3.5 Hz, H-21b), 5.73 brs (H-4). ^{13}C NMR ($CDCl_3$, 125 MHz): δ 14.35 (CH_3, C-18), 17.15 (CH_3, C-19), 23.34 (CH_2, C-16), 24.00 (CH_2, C-15), 32.13 (CH_2, C-7), 32.15 (CH_2, C-6), 33.69 (CH_2, C-2), 34.74 (CH_2, C-1), 36.74 (CH, C-8), 38.16 (C, C-10), 47.50 (C, C-13), 54.93 (CH, C-14), 56.20 (CH_2, C-12), 57.56 (CH, C-17), 62.67 (CH, C-9), 69.24 (CH_2, C-21), 124.70 (CH, C-4), 168.03 (C, C-5), 199.53 (C, C-3), 207.49 (C, C-11), 208.98 (C, C-20).

9α-hydroxy-11-dehydrocorticosterone

Product C2 (1 mg) in the conversion of corticosterone with CYP106A1 (HRMS (APCI) calculated exact mass [Da] $C_{21}H_{28}O_5$ $[M-H]^-$ 359.1859; measured accurate mass [Da] 343.1867, error [ppm] 2.45). C2 was the only product in our conversion study that formed a tertiary hydroxyl group with the P450 enzymes. Its resonance line at δ_C 79.31 showed $^3J_{CH}$ couplings to H-1a, H-12a and methyl H-19 in the HMBC spectrum indicating that C-9 bared the additional hydroxyl group. As H-9 in the substrate 9-OH of the conversion product C2 was α-oriented. This was obvious by the cross peaks found in NOESY spectrum. Key correlations were found between H-8 and the methyls H-18 and H-19, which therefore must be positioned on the same side of the steroid skeleton. Only two citations from the fifties could be found for the structure of 9α-hydroxy-11-dehydrocorticosterone but both without NMR data. ^{1}H NMR ($CDCl_3$, 500 MHz): δ 0.66 s (3xH-18), 1.39 m (H-15a), 1.49 s (3xH-19), 1.66 m (H-7a), 1.71 m (H-7b), 1.82 m (H-15b), 1.94 m (H-16a), 2.10 m (H-1a), 2.17 m (H-8), 2.22 m (H-14), 2.26 m (H-16b), 2.30 ddd (15.0, 4.7 and 2.0 Hz, H-6a), 2.37 m (H-2a), 2.38 d (12.0 Hz, H-12a), 2.47 m (H-2b), 2.48 m (H-6b), 2.50 m (H-1b), 2.73 dd (2x9.5 Hz, H-17), 3.05 dd (12.0 and 1.0 Hz, H-12b), 3.16 dd (2x 5.0 Hz, 21-OH), 4.13 dd (19.2 and 4.7 Hz, H-21a), 4.19 dd (19.2 and 4.7 Hz, H-21b), 5.86 d (2.0 Hz, H-4). ^{13}C NMR ($CDCl_3$, 125 MHz): δ 13.91 (CH_3, C-18), 18.89 (CH_3, C-19), 23.32 (CH_2, C-16), 23.72 (CH_2, C-15), 24.52 (CH_2, C-7), 28.15 (CH_2, C-1), 31.29 (CH_2, C-6), 33.74 (CH_2, C-2), 38.65 (CH, C-8), 43.66 (C, C-10), 47.11 (C, C-13), 48.73 (CH, C-14), 51.98 (CH_2, C-12), 57.41 (CH, C-17), 69.28 (CH_2, C-21), 79.31 (C, C-9), 127.68 (CH, C-

4), 165.89 (C, C-5), 198.83 (C, C-3), 206.83 (C, C-11), 209.09 (C, C-20).

6β-hydroxy-11-deoxycorticosterone (6β-hydroxy-DOC)

Product E5 (1.1 mg) in the conversion of 11-deoxycorticosterone with CYP106A1 (HRMS (APCI) calculated exact mass [Da] $C_{21}H_{30}O_4$ $[M-H]^-$ 345.2066; measured accurate mass [Da] 345.2076, error [ppm] 2.82). Selected ^{1}H NMR data were published by Matsuzaki (Matsuzaki et al., 1995). Our ^{1}H NMR of E4 matched these data. ^{1}H NMR ($CDCl_3$, 500 MHz): δ 0.73 s (3xH-18), 0.96 ddd (12.5, 11.0 and 4.5 Hz, H-9), 1.17 m (H-14), 1.28 m (H-7a), 1.38 m (H-12a), 1.39 s (3xH-19), 1.40 m (H-15a) 1.49 m (H-11a), 1.63 m (H-11b), 1.73 m (H-1a), 1.77 m (H-16a), 1.79 m (H-15b), 1.97 ddd (12.0, 3.5 and 2.5 Hz, H-12b), 2.01 m (H-8), 2.03 m (H-7b), 2.04 ddd (10.5, 5.0 and 2.8 Hz, H-1b), 2.23 m (H-16b), 2.40 dddd (17.3, 4.5, 3.0 and 1.0 Hz, H-2a), 2.47 brd (9.0 Hz, H-17), 2.49 m (H-16b), 2.53 ddd (17.3, 15.0 and 5.0 Hz, H-2b), 3.25 dd (2x4.5 Hz,far 19-OH), 4.17 dd (19.0 and 4.5 Hz, H-21a), 4.22 dd (19.0 and 4.5 Hz, H-21b), 4.37 dd (2x2.5 Hz, H-6), 5.83 brs (H-4). ^{13}C NMR ($CDCl_3$, 125 MHz): δ 13.50 (CH_3, C-18), 19.53 (CH_3, C-19), 20.87 (CH_2, C-11), 22.91 (CH_2, C-16), 24.43 (CH_2, C-15), 29.74 (CH, C-8), 34.20 (CH_2, C-2), 37.12 (CH_2, C-1), 37.94 (C, C-10), 38.35 (2xCH_2, C-7 and C-12), 44.75 (C, C-13), 53.38 (CH, C-9), 56.06 (CH, C-14), 59.09 (CH, C-17), 69.69 (CH_2, C-21), 73.03 (CH, C-6), 126.51 (CH, C-4), 167.60 (C, C-5), 200.08 (C, C-3), 210.06 (C, C-20).

15β-hydroxy-11-deoxycorticosterone (15β-hydroxy-DOC)

Product E4 (3.5 mg) and F5 (4 mg) in the conversion of 11-deoxycorticosterone with CYP106A1 and CYP106A2 respectively (HRMS (APCI) calculated exact mass [Da] $C_{21}H_{30}O_4$ $[M-H]^-$ 345.2066; measured accurate mass [Da] 345.2055, error [ppm] -3.06). In comparison to 11-deoxycorticosterone the NMR data of E4 and F5 showed signals for an additional secondary hydroxyl group (δ_H 4.38 ddd, δ_C 70.34). Its position at C-15 could be deduced by vicinal couplings of the methin proton with H-14 (δ_H 1.04) and H-16a (δ_H 2.32) in the HHCOSY and with C-13 (δ_C 44.29) and C-17 (δ_C 59.28) in HMBC. The β-orientation of the hydroxyl was obvious by the NOESY effects of H-15 with H-14 and H-16a, both in α-position. In addition to these results the chemical shifts of the epimeric 15α-hydroxy-11-deoxycorticosterone (Faramarzi et al., 2003) differed significantly from our values. ^{1}H NMR ($CDCl_3$, 500 MHz): δ 0.96 s (3xH-18), 1.04 m (H-9), 1.06 m (H-14), 1.16 m (H-7a), 1.22 s (3xH-19), 1.38 m (H-12a), 1.43 dddd (3x 13.5 and 3.5 Hz, H-11a), 1.66 dddd (13.5 and 3x 4.0 Hz, H-11b), 1.73 ddd (2x13.5 and 5.0 Hz, H-1a), 1.95 m (H-12b), 1.97 m (H-8), 2.05 ddd (13.5, 5.0 and 3.0 Hz, H-1b), 2.14 m (H-7b), 2.32 m (H-16a), 2.33 m (2H, H-6a and H-6b), 2.38 m (H-2a), 2.43 m (2H, H-2b and H-17), 2.49 m (H-16b), 4.18 d (19.0 Hz, H-21a), 4.24 d (19.0 Hz, H-21b), 4.38 ddd (3x5.5 Hz, H-15), 5.75 brs (H-4). ^{13}C NMR ($CDCl_3$, 125 MHz): δ 15.98 (CH_3, C-18), 17.29 (CH_3, C-19), 20.84 (CH_2, C-11), 31.11 (CH_2, C-7), 31.74 (CH, C-8), 32.61 (CH_2, C-16), 33.92 (CH_2, C-2), 35.78 (CH_2, C-1), 36.03 (CH_2, C-6), 38.69 (C, C-10), 39.87 (CH_2, C-12), 44.29 (C, C-13), 53.94 (CH, C-9), 59.28 (CH, C-17), 60.37 (CH, C-14), 69.39 (CH_2, C-21), 70.34 (CH, C-15), 124.09 (CH, C-4), 170.46 (C, C-5), 199.35 (C, C-3), 209.01 (C, C-20).

7β, 15β-dihydroxy-11-deoxycorticosterone (7β, 15β-dihydroxy-DOC)

Product E2 (1.8 mg) and F4 (3 mg) in the conversion of 11-deoxycorticosterone with CYP106A1 and CYP106A2 respectively (HRMS (APCI) calculated exact mass [Da] $C_{21}H_{30}O_5$ $[M-H]^-$ 361.2015; measured accurate mass [Da] 361.2019, error [ppm] 1.16). The NMR spectra of E2 and F4 were similar to those of E4, especially for the resonances of C-15 (δ_C 71.55) and H-15 (δ_H 4.50 ddd, 3x5.5 Hz) as well as the coupling pattern of H-15. But E2 beared an additional secondary hydroxyl group with resonances at δ_H 3.62 (ddd, 9.5 and 2x8.0 Hz) and δ_C 74.36. These resonances and the coupling pattern were close to those of the 7β-hydroxy group found for B3. Therefore, the structure of E2 was elucidated as 7β, 15β-dihydroxy-11-deoxycorticosterone, a structure which has not been published so far. 2D NMR

measurements supported the structure and led to the full assignments. ^{1}H NMR ($CDCl_3$, 500 MHz): δ 0.99 s (3xH-18), 1.03 m (H-9), 1.12 dd (10.8 and 5.0 Hz, H-14), 1.25 s (3xH-19), 1.33 ddd (2x13.0 and 4.0 Hz, H-12a), 1.50 dddd (3x 13.5 and 4.0 Hz, H-11a), 1.67 m (H-1a), 1.68 m (H-11b), 1.95 ddd (13.0, 4.0 and 3.0 Hz, H-12b), 2.05 m (H-8), 2.07 m (H-1b), 2.33 m (2H, H-16a and H-16b), 2.35 m (H-2a), 2.36 m (H-17), 2.41 m (H-2b), 2.55 m (2H, H-6a and H-6b), 3.62 ddd (9.5 and 2x8.0 Hz, H-7), 4.22 s (2H, H-21a and H-21b), 4.50 ddd (3x5.5 Hz, H-15), 5.77 brs (H-4). ^{13}C NMR ($CDCl_3$, 125 MHz): δ 15.63 (CH_3, C-18), 17.25 (CH_3, C-19), 20.74 (CH_2, C-11), 33.54 (CH_2, C-16), 33.89 (CH_2, C-2), 35.66 (CH_2, C-1), 37.95 (C, C-10), 38.52 (CH, C-8), 39.36 (CH_2, C-12), 42.60 (CH_2, C-6), 44.47 (C, C-13), 50.74 (CH, C-9), 59.01 (CH, C-17), 60.11 (CH, C-14), 69.35 (CH_2, C-21), 71.55 (CH, C-15), 74.36 (CH, C-7), 125.10 (CH, C-4), 166.10 (C, C-5), 198.99 (C, C-3), 209.24 (C, C-20).

15β-hydroxy-11-deoxycortisol
(15β-hydroxy-RSS)

Product G4 (5 mg) and H3 (5 mg) in the conversion of RSS with CYP106A1 and CYP106A2 respectively (HRMS (APCI) calculated exact mass [Da] $C_{21}H_{30}O_5$ $[M-H]^-$ 361.2015; measured accurate mass [Da] 361.2013, error [ppm] 0.72). Its NMR data showed resonances for an additional hydroxyl group (δ_C 70.29; δ_H 4.31 ddd), which could be located at position 15β by means of 2D NMR. Although 15β-hydroxy-11-deoxycortisol is a known structure NMR data were not available in literature. It should be mentioned that the coupling constants found for H-15α (7.8, 6.0 and 2.3 Hz) differed completely from those found for it in 15β-hydroxy-11-deoxycorticosterone (3x5.5 Hz) and in 15β-hydroxyandrost-4-ene-3,17-dione (6.0, 4.5 and 1.3 Hz). This is caused by the high flexibility of the trans-annulated cyclopentane ring and by the strong influence of the C-17 substitution pattern of its preferred configuration. ^{1}H NMR (CD_3OD, 500 MHz): δ 0.89 s (3xH-18), 1.04 ddd (12.3, 10.8 and 4.0 Hz, H-9), 1.13 dddd (13.8, 12.5, 11.5 and 4.0 Hz, H-7a), 1.25 s (3xH-19), 1.41 ddd (12.5, 4.0 and 2.8 Hz, H-12a), 1.48 ddd (2x 13.5 and 4.0 Hz, H-11a), 1.67 m (H-11b), 1.71 m (H-1a), 1.72 dd (11.5 and 6.0 Hz, H-14), 1.86 ddd (2x12.5 and 4.0 Hz, H-12b), 2.03 ddd (2x11.2 and 3.2 Hz, H-8), 2.06 dd (15.5 and 7.5 Hz, H-16a), 2.10 ddd (13.5, 5.2 and 3.0 Hz, H-1b), 2.20 dddd (12.5, 5.7 and 2x 2.8 Hz, H-7b), 2.30 m (H-2a), 2.32 m (H-6a), 2.48 ddd (17.0, 15.0 and 5.3 Hz, H-2b), 2.53 dddd (2x15, 5.5 and 1.7 Hz, H-6b), 2.73 dd (15.5 and 2.3 Hz, H-16b), 4.27 d (19.2 Hz, H-21a), 4.31 ddd (7.8, 6.0 and 2.3 Hz, H-15), 4.62 d (19.2 Hz, H-21b), 5.72 brs (H-4). ^{13}C NMR (CD_3OD, 125 MHz): δ 17.63 (CH_3, C-19), 18.04 (CH_3, C-18), 21.68 (CH_2, C-11), 32.66 (CH_2, C-7), 32.72 (CH_2, C-12), 32.94 (CH, C-8), 33.90 (CH_2, C-6), 34.73 (CH_2, C-2), 36.81 (CH_2, C-1), 40.16 (C, C-10), 47.54 (CH_2, C-16), 48.40 (C, C-13), 55.32 (CH, C-9), 55.73 (CH, C-14), 67.70 (CH_2, C-21), 70.29 (CH, C-15), 90.27 (C, C-17), 124.17 (CH, C-4), 175.17 (C, C-5), 202.35 (C, C-3), 212.64 (C, C-20).

7β, 15β-dihydroxy-11-deoxycortisol
(7β, 15β-dihydroxy-RSS)

Product G1 (3.5 mg) in the conversion of RSS with CYP106A1 (HRMS (APCI) calculated exact mass [Da] $C_{21}H_{30}O_6$ $[M-H]^-$ 377.1964; measured accurate mass [Da] 377.1976, error [ppm] 3.01). Its ^{1}H and ^{13}C NMR spectra revealed two additional secondary hydroxyl groups. One of them (δ_C 71.26; δ_H 4.56 ddd , 8.0, 5.6 and 2.6 Hz) gave similar values as found for the 15β-hydroxy group in H3. The other one (δ_C 74.67; δ_H 3.68 ddd, 2x10.0 and 6.5 Hz) showed vicinal couplings to the isochronic protons of H-6 (δ_H 2.56 m, 2H) and to H-8 (δ_H 2.06 m) in the HHCOSY. NOESY cross peaks between H-7 and the α-oriented H-9, H-14 and H-15 revealed the stereochemistry at C-7 with the hydroxy group in β-orientation. The structure of 7β, 15β-dihydroxy-11-deoxycortisol has not beeen published so far. ^{1}H NMR ($CDCl_3$, 500 MHz): δ 1.03 s (3xH-18), 1.06 ddd (2x12.0 and 3.7 Hz, H-9), 1.26 s (3xH-19), 1.39 m (H-12a), 1.48 m (H-11a), 1.67 m (H-1a), 1.70 m (H-12b), 1.72 m (H-11b), 1.77 dd (11.0 and 5.5 Hz, H-14), 2.06 m (H-8), 2.07 m (H-1b), 2.22 dd (15.5 and 8.0 Hz, H-16a), 2.40 m (H-2a), 2.45 m (H-2b), 2.56 m (2H, H-6a and H-6b), 2.63 dd (15.5 and 2.5 Hz, H-16b), 3.68 ddd (2x10.0 and 6.5 Hz, H-7), 4.36 d

(19.8 Hz, H-21a), 4.56 ddd (8.0, 5.6 and 2.6 Hz, H-15), 4.70 d (19.8 Hz, H-21b), 5.77 brs (H-4). ^{13}C NMR ($CDCl_3$, 125 MHz): δ 17.28 (CH_3, C-19), 17.62 (CH_3, C-18), 20.19 (CH_2, C-11), 30.22 (CH_2, C-12), 33.90 (CH_2, C-2), 35.65 (CH_2, C-1), 37.95 (C, C-10), 38.25 (CH, C-8), 42.65 (CH_2, C-6), 43.25 (CH_2, C-16), 48.70 (C, C-13), 50.33 (CH, C-9), 53.96 (CH, C-14), 67.71 (CH_2, C-21), 71.26 (CH, C-15), 74.67 (CH, C-7), 87.65 (C, C-17), 125.19 (CH, C-4), 165.99 (C, C-5), 198.98 (C, C-3), 212.29 (C, C-20)

Cortisone

Product I6 (1 mg) in the conversion of cortisol with CYP106A1 (HRMS (APCI) calculated exact mass [Da] $C_{21}H_{28}O_5$ $[M-H]^-$ 359.1858; measured accurate mass [Da] 359.1842, error [ppm] -4.62). Its ^{1}H NMR data matched those in literature (Kirk et al., 1990). ^{1}H NMR (CD_3OD, 500 MHz): δ 0.60 s (3xH-18), 1.33 m (H-7a), 1.42 s (3xH-19), 1.46 m (H-15a), 1.70 m (H-16a), 1.72 m (H-1a), 1.92 m (H-15b), 2.01 m (H-8), 2.02 m (H-7b), 2.04 d (12.5 Hz, H-12a), 2.11 d (10.5 Hz, H-9), 2.23 ddd (17.0 and 2x 3.8 Hz, H-2a), 2.33 ddd (15.0, 4.0 and 2.5 Hz, H-6a), 2.45 m (H-14), 2.50 m (H-2b), 2.52 m (H-6b), 2.70 m (H-1b), 2.72 m (H-16b), 2.95 d (12.5 Hz, H-12b), 4.22 d (19.5 Hz, H-21a), 4.60 d (19.5 Hz, H-21b), 5.71 brs (H-4). ^{13}C NMR (CD_3OD, 125 MHz): δ 16.15 (CH_3, C-18), 17.58 (CH_3, C-19), 24.14 (CH_2, C-15), 33.43 (CH_2, C-6), 33.58 (CH_2, C-7), 34.44 (CH_2, C-2), 35.23 (CH_2, C-16), 35.62 (CH_2, C-1), 37.88 (CH, C-8), 39.60 (C, C-10), 50.98 (CH, C-14), 51.45 (CH_2, C-12), 52.24 (C, C-13), 63.47 (CH, C-9), 67.88 (CH_2, C-21), 89.35 (C, C-17), 124.76 (CH, C-4), 172.87 (C, C-5), 202.45 (C, C-3), 212.01 (C, C-11), 212.78 (C, C-20).

6β-hydroxycortisone

The only under *in vivo* conditions observed product (2 mg) downstream K1 in the conversion of cortisone with CYP106A1 (HRMS (APCI) calculated exact mass [Da] $C_{21}H_{28}O_6$ $[M-H]^-$ 375.1808; measured accurate mass [Da] 375.1792, error [ppm] -4.22). Comparison of its ^{1}H and ^{13}C NMR data with those of the 6β-hydroxy derivatives, A4 and E5 showed striking similarities especially for the hydroxyl moiety. The results of 2D NMR analysis supported the structure. ^{1}H NMR ($CDCl_3$, 500 MHz): δ 0.69 s (3xH-18), 1.26 m (H-16a), 1.53 m (H-7a), 1.57 m (H-15a), 1.60 s (3xH-19), 1.64 m (H-1a), 1.88 m (H-9), 2.03 m (H-15b), 2.14 m (H-12a), 2.15 m (H-7b), 2.32 m (H-16b), 2.36 m (H-2a), 2.38 m (H-14), 2.42 m (H-8), 2.57 ddd (17.5, 15.0 and 5.0 Hz, H-2b), 2.81 m (H-12b), 2.82 m (H-1b), 4.29 d (19.8 Hz, H-21a), 4.38 dd (2x3.0 Hz, H-6), 4.65 d (19.8 Hz, H-21b), 5.83 brs (H-4). ^{13}C NMR ($CDCl_3$, 125 MHz): δ 16.00 (CH_3, C-18), 19.15 (CH_3, C-19), 23.42 (CH_2, C-15), 30.62 (CH, C-8), 32.06 (CH_2, C-16), 34.04 (CH_2, C-2), 35.98 (CH_2, C-1), 37.81 (C, C-10), 38.91 (CH_2, C-7), 49.37 (CH, C-14), 49.76 (CH_2, C-12), 51.68 (C, C-13), 62.17 (CH, C-9), 67.54 (CH_2, C-21), 72.41 (CH, C-6), 88.06 (C, C-17), 127.20 (CH, C-4), 166.06 (C, C-5), 199.94 (C, C-3), 208.47 (C, C-11), 211.53 (C, C-20).

15β-hydroxycortisone

Product K3 and L3 (1 mg) in the conversion of cortisone with CYP106A1 and with CYP106A2 respectively (HRMS (APCI) calculated exact mass [Da] $C_{21}H_{28}O_6$ $[M-H]^-$ 375.1808; measured accurate mass [Da] 375.1822, error [ppm] 3.87). Due to the low amount only a ^{1}H NMR and a HHCOSY could be recorded for the samples, indicating an additional secondary hydroxyl group for the conversion product. Comparison of the chemical shift and the coupling pattern of the C*H*OH resonance (4.62 dd 7.5, 5.5 and 2.0 Hz) with those of all the other conversion products led to the structure of 15β-hydroxycortisone. ^{1}H NMR ($CDCl_3$, 500 MHz): δ 0.67 s (3xH-18) 1.47 s (3xH-19), 4.33 d (19.8 Hz, H-21a), 4.62 ddd (7.5, 5.5 and 2.0 Hz, H-15), 4.77 d (19.8 Hz, H-21b), 5.77 brs (H-4).

Results

Expression, purification and spectral characterization of the proteins

The proteins were expressed and purified (to homogeneity) using a recombinant *E. coli* C43 (DE3) strain. The UV-Vis spectra of both proteins showed characteristic absorbance peaks at 356, 417, 534, 567 nm in the oxidized form. In the carbon monoxide-bound reduced form, a peak at

450 nm was clearly observed without a visible peak at 420 nm suggesting no inactive P450 form (Schenkman and Jansson, 1998) (Fig. S1).

Substrate binding

To compare the steroid hydroxylating capacity of the CYP106A subfamily members, a focused library of 23 steroids was screened for high-spin shift induction using difference spectroscopy (Table 1). The study was performed using difference spectroscopy due to its higher sensitivity, since the extent of the obtained shifts was very small, in all cases less than 10 %. The library included 14 compounds formerly tested with CYP106A2 and 9 additional 3-oxo-steroids, derivatives of already known substrates of CYP106A2. P450 substrates usually induce a shift of the heme iron to the high-spin state, resulting in a so-called type I shift spectrum (Schenkman et al., 1981). It is known that type I shift-inducing compounds are converted more often than those which do not induce a high spin shift. However, it has been shown previously that even compounds which do not induce a clear type I shift can be converted by P450s (Ferrero et al., 2012; Girhard et al., 2010; Schmitz et al., 2014; Simgen et al., 2000), yet the induction of a type I shift does not necessarily lead to product formation (Khatri et al., 2013; Schmitz et al., 2012). In our case, there are two examples listed in Table 1, where type I shift-inducing compounds were not converted (adrenosterone, 19-hydroxyandrostenedione), while successful conversion was observed with pregnenolone and 17-hydroxypregnenolone inducing no shift. The type I binding assay allows us a straight forward comparison of the binding behavior of CYP106A1 and CYP106A2. Only four steroids, β-estradiol, estrone, pregnenolone and 17β-hydroxypregnenolone, did not induce any spin-shift alteration in CYP106A1 and CYP106A2. There was only one steroid, 19-nortestosterone, which despite being converted by both enzymes, did not induce any spectral shift with CYP106A2, but induced a type I shift with CYP106A1. Out of 23 steroids tested, 18 showed a clear type I shift induction by both enzymes and product formation was observed with all but four steroids (Table 1). As expected, the two CYP106A family members show similar steroid binding behavior according to spin-state alterations, caused by the displacement of the water molecule as sixth heme iron ligand.

Catalytic activity and dissociation constants

The catalytic activity of the CYP106A subfamily was compared with respect to all 23 steroids (Table 1). Most of the steroids contained the 3-oxo-Δ4 moiety, others possessed 3-oxo-Δ2,4 or 3-hydroxy-Δ5 structures. Following the HPLC analysis, 19 out of 23 steroids, except 19-hydroxyandrostenedione, adrenosterone, β-estradiol and estrone, were observed to be converted by both subfamily members, with detectable conversion products. Though all 19 steroids were converted both by CYP106A1 and CYP106A2, differences in the product pattern and/or activity were observed when studying 3-oxo-Δ4-steroids (Table 2). There was no clear correlation found between the steroid structures, the differences in conversion velocity or side product formation.

However, testing C18-, C19-, C20- or C21-steroids, CYP106A2 seemed in all cases to be more selective than CYP106A1, showing one or two main products. In most cases CYP106A1 produced the same main product, but a higher number of side-products. CYP106A2 also showed slightly higher conversion velocity in all transformations except for 11β-hydroxysteroids.

To get deeper insight into the structural basis for the activity and selectivity of steroid hydroxylation, the substrates were narrowed down to six 3-oxo-Δ4 steroids (Table 4) whose conversion showed significant differences between CYP106A1 and CYP106A2, either in product pattern or enzyme activity. Since the main product of CYP106A2 was already identified for some of these substrates (Table 1), the recognized differences in the product pattern produced by CYP106A1 suggested hidden potentials in terms of novel products. The dissociation constant of these steroids and their in vitro and in vivo conversion with the resulting product(s) was therefore further investigated.

The binding of the six substrates induced a type I shift with both CYP106A enzymes (Table 1).

Table 1 Overview of the 23 tested steroids concerning their binding and conversion with CYP106A1 and CYP106A2

Steroid	*In vitro* conversion		Known product formation by CYP106A2	Induction of high spin shift	
	CYP106A1	CYP106A2		CYP106A1	CYP106A2
Testosterone	+	+	15β[a]	+	+
17α-methyltestosterone	+	+	n.d.	+	+
19-nortestosterone	+	+	n.d.	+	-
Ethisterone	+	+	n.d.	+	+
Progesterone	+	+	15β[a] (11α, 6β, 9α)	+	+
17α-hydroxyrogesterone	+	+	15β[a]	+	+
Androstenedione	+	+	15β[a]	+	+
11-deoxycorticosterone (DOC)	+	+	15β[a]	+	+
11-deoxycortisol (RSS)	+	+	n.d	+	+
Corticosterone	+	+	15β[a]	+	+
Cortisol	+	+	n.d.	+	+
Cortisone	+	+	n.d.	+	+
Prednisolone	+	+	n.d.	+	+
Prednisone	+	+	n.d.	+	+
Dexamethasone	+	+	n.d.	+	+
11β-hydroxyandrostenedione	+	+	n.d.	+	+
19-hydroxyandrostenedione	-	-	-	+	+
Adrenosterone	-	-	-	+	+
β-estradiol	-	-	-	-	-
Estrone	-	-	-	-	-
Pregnenolone	+	+	7β[b]	-	-
17α-hydroxypregnenolone	+	+	7β (7α)[b]	-	-
Dehydroepiandrosterone	+	+	7β (7α)[b]	+	+

+ / - = positive and negative outcomes of what is stated in the column headers, respectively, *n.d* hydroxylation position not determined
[a] Berg et al. (1976)
[b] Schmitz et al. (2014)

The equilibrium dissociation constants were determined to investigate the binding affinities towards both enzymes (Table 3), each of which was titrated with increasing concentrations of the corresponding substrates. Saturation of binding was observed in all cases and the binding constants were estimated by hyperbolic regression. In Fig. S2, the binding curves of three substrates tested in this study (corticosterone, cortisol and cortisone to CYP106A1 and CYP106A2) are shown as an example. Interestingly, both enzymes bind the six steroids with similar affinities, with dissociation constants ranging from 50 µM for 11-deoxycorticosterone (DOC) to 543 µM for cortisol (CYP106A2) and from 68 µM for DOC to 464 µM for cortisone (CYP106A1). The binding affinities of corticosterone, cortisone and cortisol showed the highest differences, being 2.5 fold and 1.7 fold higher for corticosterone and cortisone, respectively, with CYP106A1 compared with CYP106A2, whereas for cortisol the K_d value was 0.6 fold lower with CYP106A1 than with CYP106A2. The binding affinities are in the higher micromolar range with both enzymes, except for androstenedione and DOC.

Table 2 Summary of the *in vitro* substrate conversion of steroid compounds with the CYP106A subfamily members

Steroids	Conversion with CYP106A1 and CYP106A2
3-oxo-Δ^4 steroids	Conversion, similar or same product pattern and activity with exceptions (generally more side-product formation for CYP106A1)
3-oxo-$\Delta^{2,4}$ steroids	Conversion, same product pattern
3-hydroxy-Δ^5 steroids	Conversion, same product pattern
Other steroids	No conversion (19-hydroxyandrostenedione, adrenosterone, β-estradiol, estrone)

Table 3 Overview of the substrate binding to CYP106A1 and CYP106A2 showing the respective K_d values ($R^2 \geq 0.98$ in all cases)

Steroid	K_d value [µM]	
	CYP106A1	CYP106A2
Androstenedione	77 ± 2[a]	81 ± 10[b]
Corticosterone	471 ± 14[c]	185 ± 8[c]
11-deoxycorticosterone (DOC)	68 ± 2[a]	50 ± 1[c]
11-deoxycortisol (RSS)	161 ± 5[a]	102 ± 4[c]
Cortisol	307 ± 19[c]	543 ± 31[c]
Cortisone	464 ± 8[c]	260 ± 7[c]

[a] Brill (2013)
[b] Schmitz et al. (2014)
[c] Tested in this work

In vitro conversions

To shed more light on the differences in the hydroxylation pattern of both CYP106A subfamily members, the *in vitro* conversion of the six chosen steroids was further investigated and the main and some minor conversion products were identified. In order to compare both enzymes with one another and with previously published results, the redox system from bovine adrenals, known to be an efficient electron supplier for bacterial P450s, especially for CYP106A2 (Ewen et al., 2012; Virus et al., 2006), was used in this work as described elsewhere (Bleif et al., 2012; Schmitz et al., 2012).

Androstenedione was successfully converted by both enzymes, but with different velocities. Using equal enzyme concentrations, after 30 minutes CYP106A2 converted nearly 100 % of the substrate, producing two main products, B3 and B6, as well as several side products (Fig. 1b). In contrast, CYP106A1 could reach a maximal 84 % total conversion after 60 minutes (Fig. 1a). Consequently, the activity of CYP106A1 was considered to be lower towards androstenedione, though it also formed two main products, A2 and A4, besides a few minor metabolites. A2, A4 and A6 showed very similar retention times as the CYP106A2's products, B3, B6 and B7 respectively. The minor products A2 and B3 had shorter retention times, thus higher hydrophobicity.

Within 30 minutes, CYP106A1 converted 41 % of corticosterone into one main product (C5) with low amounts of minor product formation (C1-C4). No significant increase in conversion was observed with longer incubation times (Fig. 1c). The conversion with CYP106A2 resulted in a rather different product pattern. After 30 minutes, CYP106A2 converted 47 % of the substrate mainly to D1 and D2, whose peaks increased over time, resulting in 57 % conversion within 60 minutes (Fig. 1d). The CYP106A1 main and minor products (except for C1) showed matching retention times with the CYP106A2 metabolites.

The activity of the CYP106A subfamily members was considered to be similar towards DOC, since they both converted 100 % of the substrate within 60 minutes to one main (E4, F5) and several minor products (Fig. 1e, f). The main product (E4, F5) of both enzymes, as well as the minor products (E2, F4), had identical retention times. In addition, the minor product ratios increased from 30 to 60 minutes of conversion, along with the decrease of the main product peak, hence these products were thought to be further oxidized derivatives of the main product.

CYP106A2 showed complete conversion of 11-deoxycortisol (RSS) into one main (H3) and four minor products (H1-H5), already within 30 minutes (Fig. 1h). CYP106A1 showed similar activity towards the substrate with lower conversion rate and produced a main product (G4) with the same retention time as the CYP106A2 main product (H3) (Fig. 1g). Both enzymes showed side product formation of which G1 and H2 also had identical retention times.

After 4 hours CYP106A1 transformed 77 % of cortisol, while CYP106A2 converted only 55 %. Therefore, the activity of CYP106A2 was considered to be lower towards cortisol. CYP106A1 produced two main products, I5 downstream and I6 upstream the substrate peak and four side products (I1-I4) (Fig. 1i). Interestingly, using CYP106A1 only the ratio of I3, I4 and I5 increased, while the amounts of the substrate and I6 simultaneously decreased over time. According to the used reversed-phase HPLC system, I6 was believed to be more hydrophobic than the substrate (Fig. 1i). Cortisol conversion with CYP106A2 produced somewhat different results. After 1 hour, cortisol was converted into

J1 and J3 with low amounts of J2 and J4. The amount of J1 and J3 increased throughout the substrate conversion, showing again more hydrophobic side-product formation (Fig. 1j). The CYP106A1 products I2, I5 and I6 showed exactly the same retention times as J1, J3 and J4 from CYP106A2, suggesting identical structures.

When studying the conversion of cortisone, 93% of the substrate was converted by CYP106A2 within 1 hour, while CYP106A1 showed significantly lower activity with 58% conversion and reaching only 76% during the 4 hour reaction time (Fig. 1k, l). Besides the difference in their activities, both subfamily members produced one main product (K3 and L3) with the same retention time and two-three minor side products. Interestingly, the main products, K3 and L3 had matching retention times not only with each other, but also with I5 and J3 from the cortisol conversion (Fig. 1i, j).

In vivo whole-cell conversions and product identification

Following the comparison of the *in vitro* activities of both enzymes, which revealed some differences in the product pattern, we aimed to identify the main products via NMR spectroscopy. For this, 200 µM final concentration of the substrate was added to *B. megaterium* resting cells overexpressing the corresponding P450, 24 hours after induction. Samples were taken at 1 h, 2 h, 4 h, 8 h and 24 h to follow the main and side product formations over time for the final isolation of the main products. Compared with the *in vitro* results, the product pattern slightly differed using the whole-cell catalyst (Fig. S3). However, the main products remained present in all cases. The novel peaks observed in the *in vivo* system are most likely further metabolized intermediate products by enzymes naturally present in the strain or remaining traces of the cultivation medium. For this reason, we decided to purify the corresponding main products and some of the minor products already identified during the *in vitro* experiments. To avoid confusion, the products seen *in vitro* (Fig. 1) were labelled the same fashion as on the *in vivo* HPLC chromatograms (Fig. S3). The structures of all six substrates and their identified conversion products are summarized in Table 4.

In vivo, CYP106A1 showed a lower conversion rate with androstenedione compared with CYP106A2, consistent with the *in vitro* observations. However, both enzymes reached 100 % substrate consumption after 24 hours (data not shown). CYP106A1 showed the same product distribution after 4 hours (Fig. S3a) as *in vitro* (Fig. 1a), while CYP106A2 showed a slightly altered one (Fig. S3b). The main metabolite of androstenedione by CYP106A2 was identified as 15β-hydroxyandrostenedione (B6), confirming the results by Berg *et al.* (1976). After 8 hours, a significant increase in the minor product B3 formation was observed (Fig. S3b), identified as 7β, 15β-dihydroxyandrostenedione. Interestingly, CYP106A1 did not show 15β-hydroxylase activity towards its novel substrate. It produced the pharmaceutically promising 6β- and 7β-hydroxyandrostenedione (A4 and A2 respectively) as main metabolites, highlighting the difference in selectivity between the two subfamily members (Fig. S3a).

CYP106A1 applied in the whole-cell system showed 89 % conversion of corticosterone in 8 hours compared with a maximum 45 % product formation *in vitro*. The product pattern within 4 hours was similar to the one seen *in vitro*, showing C5 as main product. However, after 8 hours it shifted towards the minor products (C1-C4) (Fig. S3c). CYP106A2 converted 56 % of the substrate within 8 hours under *in vivo* conditions, comparable to the *in vitro* conversion. The product distribution was similar as seen before, with D1 and D2 as main products and a small amount of D4 formation. An additional product peak was also observed downstream D1, having the same retention time as C1 (Fig. S3d). The main product of CYP106A1 (C5) with matching retention time to the minor metabolite of CYP106A2 (D4) were both identified as 11-dehydrocorticosterone, justifying the assumption of Lee *et al.* (2014), that a dehydrogenation takes place during the corticosterone conversion. This is the first case where an 11β-hydroxysteroid dehydrogenation is observed, an unexampled transformation by the CYP106A subfamily. In addition, the main

metabolite of CYP106A2 (D1) was characterized as the 15β-hydroxylated derivative, matching the results of Berg *et al.* (1976). The minor metabolite of CYP106A1 was also successfully characterized as 9α-hydroxy-11-dehydrocorticosterone (C2).

Both CYP106A enzymes showed high activity towards DOC, with complete conversion within 2 hours (Fig. S3e, f) and the same product pattern as seen *in vitro* (Fig. 1e, f). The NMR characterization of the CYP106A1 main product exposed the 15β-hydroxy derivative (E4) just like in the case of CYP106A2 (F5) which was formerly identified by Berg *et al.* (1976). CYP106A1 showed 6β-hydroxy metabolite formation as well (E5), demonstrating again a stronger affinity for B-ring oxidations compared to CYP106A2.

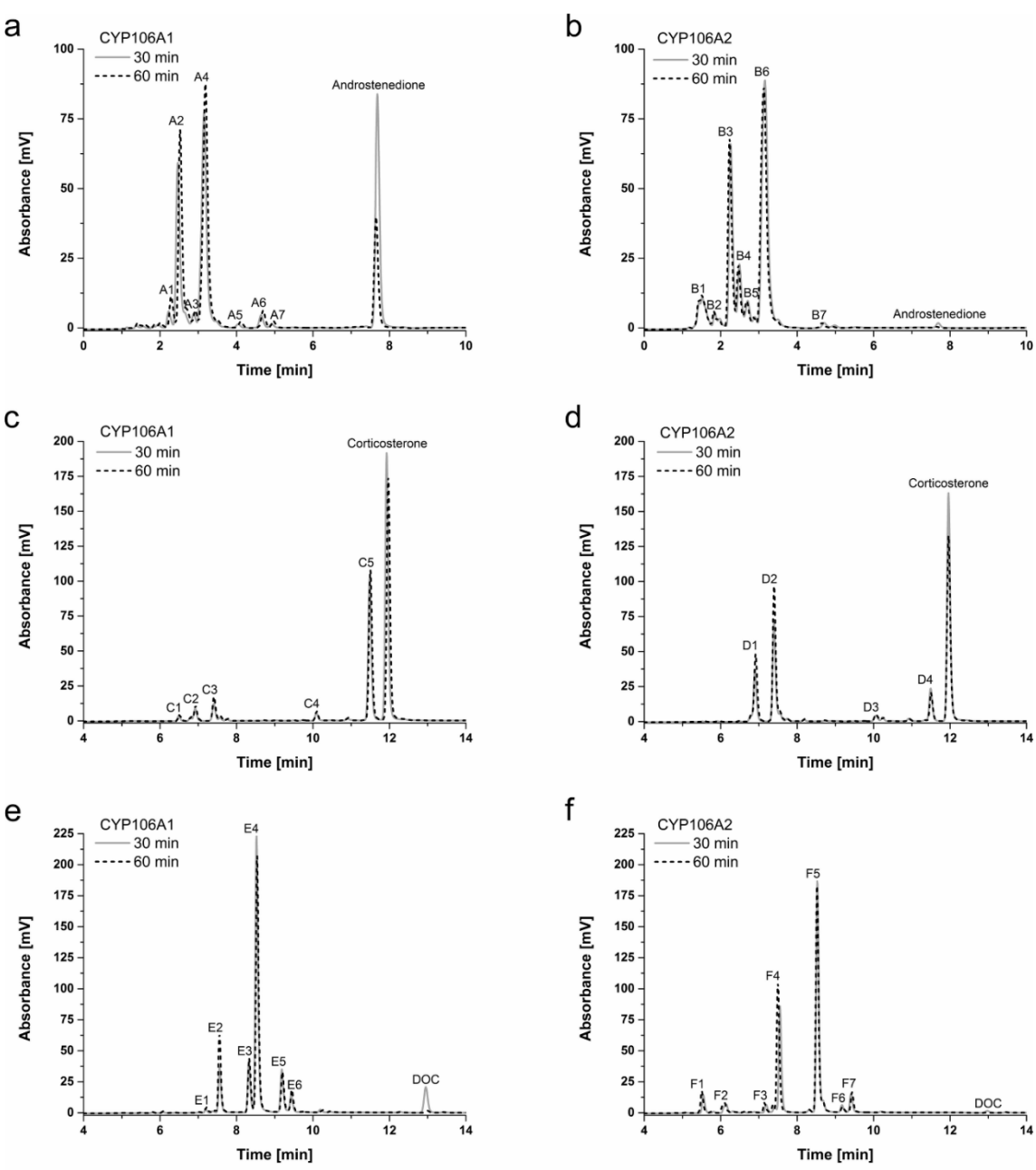

Fig. 1 HPLC chromatograms of the *in vitro* conversion of androstenedione (**a**, **b**), corticosterone (**c**, **d**), 11-deoxycorticosterone (**e**, **f**), 11-deoxycortisol (**g**, **h**), cortisol (**i**, **j**) and cortisone (**k**, **l**) by CYP106A1 and CYP106A2 respectively. The reaction was performed in 50 mM potassium-phosphate buffer containing 20 % glycerol at 30 °C, using 1 µM AdR, 10 µM $Adx_{4\text{-}108}$ and 0.5 µM CYP106A enzymes.

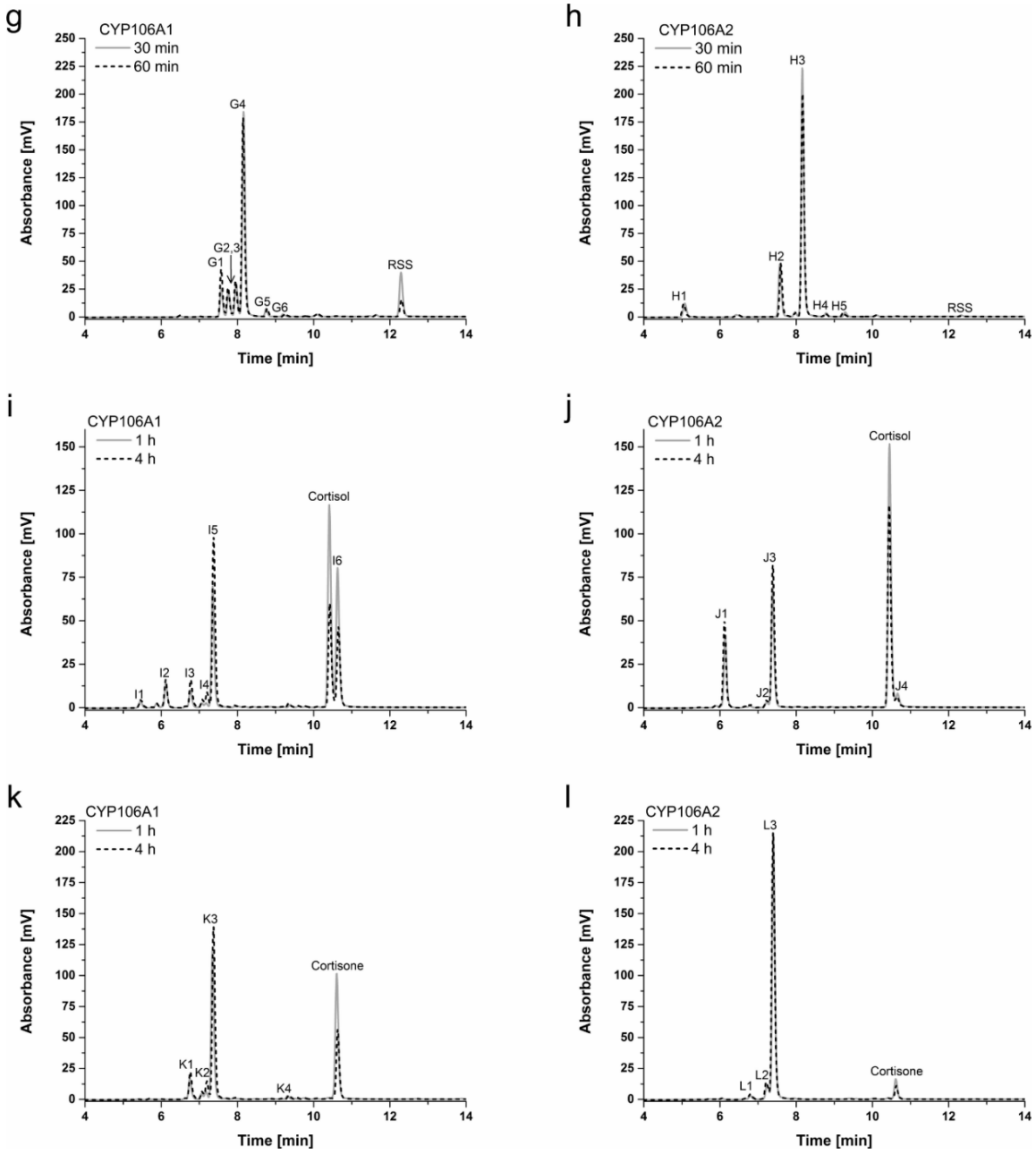

Fig. 1 (continued)

The latter also produced a metabolite (F6) with the same retention time as the 6β-hydroxy-DOC but in significantly minor amounts. The minor metabolites, E2 and F4, increased over time, while the 15β-hydroxy-DOC decreased, indicating further hydroxylation of the main metabolite (Fig. S3e, f). These minor products (E2, F4) were successfully purified and identified as 7β, 15β-dihydroxy-DOC.

In vivo, the CYP106A enzymes displayed similarly high activity to RSS, both completing the conversion after 4 hours. Within the first hour of conversion both enzymes displayed similar product distribution as observed *in vitro*. G4 and H3 were identified as main metabolites with the same retention time, and their structure was elucidated as 15β-hydroxy-RSS (Fig. S3g, h). In the case of CYP106A1 additional minor products appeared downstream the main product, increasing over time, together with the decrease of the main metabolite (Fig. S3g, h). From these, G1, with identical retention time to H2 produced by CYP106A2, was obtained in sufficient purity and quantity to be elucidated and turned out to be the 7β,15β-dihydroxy-RSS (Fig. S3g, h).

Table 4 Overview of the 6 studied steroids, including their conversion products by the CYP106A1 and CYP106A2 enzymes. (The product distribution is given in % after 4 h of conversion, if not otherwise indicated.)

Converted steroids	Identified conversion products	
	CYP106A1	CYP106A2
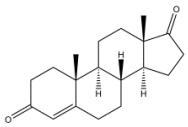 Androstenedione	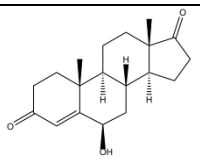 6β-hydroxyandrostenedione (31 %) 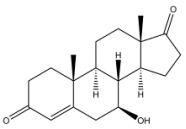 7β-hydroxyandrostenedione (22 %)	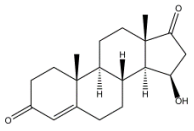 15β-hydroxyandrostenedione * (67 %) 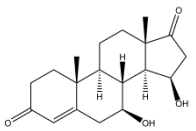 7β,15β-dihydroxyandrostenedione (9 %)
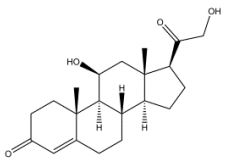 Corticosterone	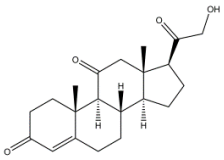 11-dehydrocorticosterone (38 %) 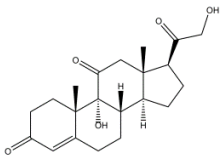 9α-hydroxy-11-dehydrocorticosterone (4 %)	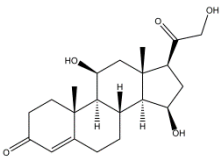 15β-hydroxycorticosterone * (16 % in 4h, 26 % in 8h) 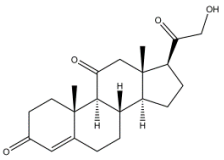 11-dehydrocorticosterone (7 % in 4h, 5 % in 8h)
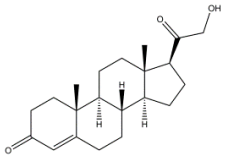 11-deoxycorticosterone (DOC)	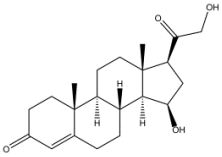 15β-hydroxy-DOC (28 %) 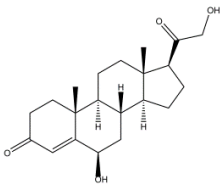 6β-hydroxy-DOC (9 %) 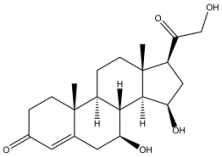 7β,15β-dihydroxy-DOC (37 %)	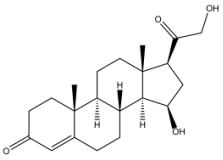 15β-hydroxy-DOC * (66 %) 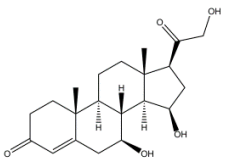 7β,15β-dihydroxy-DOC (21%)
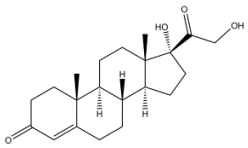 11-deoxycortisol (RSS)	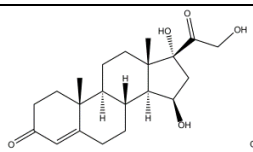 15β-hydroxy-RSS (36 % in 1h, 9 % in 4h) 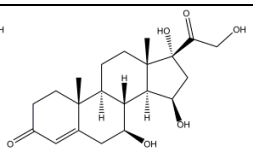 7β,15β-dihydroxy-RSS (8 % in 1h, 18 % in 4h)	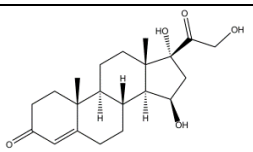 15β-hydroxy-RSS (76 % in 1h, 33 % in 4h)
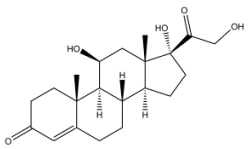 Cortisol	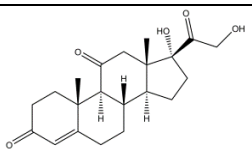 11-dehydrocortisol (cortisone) (19 %)	n.d.
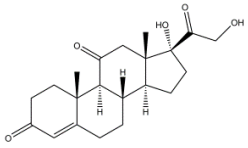 Cortisone	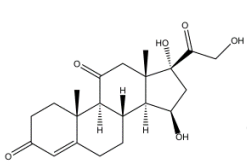 15β-hydroxycortisone (14 %) 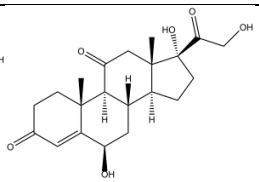 6β-hydroxycortisone (6 %)	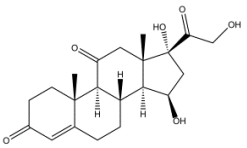 15β-hydroxycortisone (40 %)

*Also identified by Berg et al. (1976)

n.d. product structure not determined

CYP106A1 reached 38 % *in vivo* cortisol conversion within 4 hours. After 24 hours, the substrate was entirely converted, but the product distribution seen in the *in vitro* study was completely altered. The products had the same retention times, but the *in vivo* observed ratios

(I5, 4 % and I6, 20 %) were lower (Fig. 1i) compared with the *in vitro* results (I5, 22 % and I6, 28 %) (Fig. 1i). The main product (I6) of this newly identified CYP106A1 substrate was characterized as 11-dehydrocortisol (cortisone). CYP106A2 showed lower activity towards cortisol with only 16 % conversion within 4 hours and no complete substrate consumption even after 24 hours. Unlike the product distribution *in vitro* (Fig. 1j), here J1 was present as main product (Fig. 3Sj). However, CYP106A2 also produced a minor metabolite (J4) with matching retention time to 11-dehydrocortisol (I6), which was suggested to be the 11-keto compound.

Regarding cortisone, CYP106A1 converted 80 % of the substrate, while CYP106A2 performed complete conversion within 8 hours. Both enzymes produced the main metabolite as observed *in vitro* (K3 and L3), whose structure was elucidated as 15β-hydroxycortisone (Fig. 3Sk, l). *In vivo* the highest 15β-hydroxy product formation was 14 % by CYP106A1 within 4 hours, while *in vitro* it reached 56 % (Fig. S3k). CYP106A2 produced 40% of the 15β-hydroxy metabolite in 4 hours and two previously undetected minor metabolites were also observed, one showing the same retention time as K4, the other downstream L1 (Fig. S3l). A CYP106A1 product observed only *in vivo*, downstream K1 was also purified and characterized as the 6β-hydroxylated compound. Interestingly, the minor products from the previous cortisol conversion (I2, I5 for CYP106A1 and J1, J3 for CYP106A2, see Fig. S3k, l) showed the exact same retention times as the 6β- and 15β-hydroxycortisone. This suggests that their structures are identical, consequently, that both enzymes convert cortisol to cortisone, but the resulting 11-oxo steroid is further hydroxylated to its 6β- and 15β-hydroxy derivatives.

Discussion

The present paper reveals that out of 23 steroids studied, 19 were successfully converted by the CYP106A subfamily members, with 13 novel substrates identified for CYP106A1 and 7 for CYP106A2. Thus, CYP106A1, similarly to CYP106A2, is a highly active steroid hydroxylase, with 19 identified steroid substrates. A focused steroid library was used to compare both the CYP106A subfamily members, including 14 steroids formerly tested with CYP106A2 and 9 additional 3-oxo-steroids, derivatives of testosterone, corticosterone and androstenedione with distinct functional groups at C11, C17 and C19 positions. Difference spectroscopy revealed similar binding behaviors for all steroids towards both, CYP106A1 and CYP106A2 (Table 1). Out of 23 steroids tested, only four, namely β-estradiol, estrone, pregnenolone and 17α-hydroxypregnenolone, do not shift the heme iron into the high-spin form. Interestingly, all four compounds are 3-hydroxy steroids, either having an aromatic A-ring or a double bond between C5 and C6 (Fig. 2). Why the other tested 3-hydroxy-Δ5 steroid, DHEA, was able to induce a type I shift with both enzymes, is subject of further investigations and cannot be explained at this point.

Although not inducing an alteration of the spin-state, pregnenolone and 17α-hydroxypregnenolone were converted with both enzymes, supporting previous observations that type I binding is not necessary for conversion (Ferrero et al., 2012; Girhard et al., 2010; Schmitz et al., 2014; Simgen et al., 2000). Interestingly, the similarly functionalized 3-oxo-steroids progesterone and 17α-hydroxyprogesterone, induced a type I shift and were also converted. It is possible that the lacking hydrogen bond acceptor in the pregnenolone structure leads to a much weaker binding to the heme iron, thus not being able to displace the water and shift the spectrum. In contrast, estrogens (β-estradiol, estrone) are most probably not bound by CYP106A1 and CYP106A2, because no type I shift and no conversion have been observed for either substance. A possible explanation can be the lower flexibility of the aromatic A-ring, interfering with the binding of the substrate (Fig. 2) (Schmitz et al., 2014).

Although 3-oxo-Δ4-steroids are described as suitable substrates of CYP106A2, no conversion was observed for either 19-hydroxyandrostenedione or adrenosterone. These steroids have nearly identical structure to

androstenedione (which is converted by both CYP106A enzymes) beside the hydroxyl group at C19 position and the keto-function at C11 position, respectively (Fig. 3). This suggests that these additional functional groups (perhaps in combination with other structural properties present on the steroid molecule) are responsible for disabling the conversion.

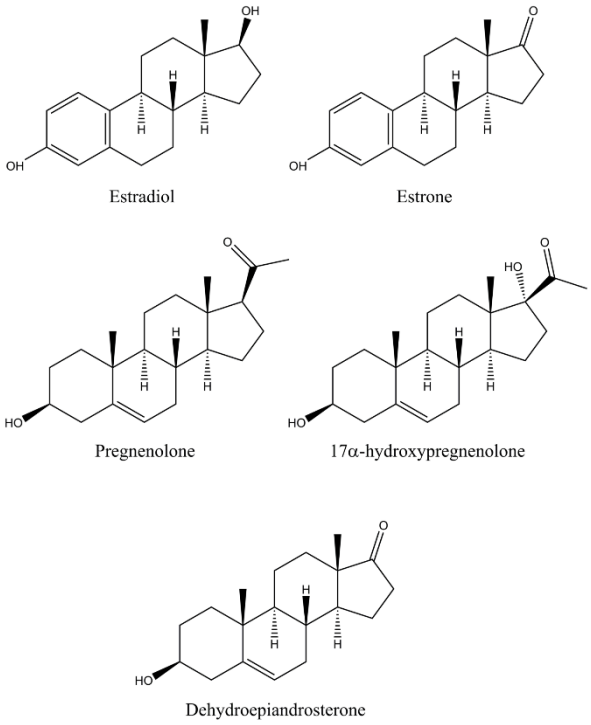

Fig. 2 Investigated 3-hydroxy steroids, not inducing any spectral shift with either of the CYP106A subfamily members, except for dehydroepiandrosterone, showing a type I shift and conversion with both enzymes.

Interestingly, the substrate spectrum was the same for both enzymes, although the activities and product patterns were not alike in several cases. Focusing on the identification of differences between the CYP106A enzymes, the 19 substrates were narrowed down to those 6, whose conversion resulted in different product patterns or changed activities (Table 4). As a first step, the dissociation constants of these 6 substrates (androstenedione, corticosterone, DOC, RSS, cortisol and cortisone) were determined. Steroid binding turned out to be similar with both CYP106A subfamily members, reflected by similar dissociations constants (Table 3). Strongest binding with both enzymes is observed for androstenedione (77 ± 2 µM with CYP106A1 and 81 ± 10 µM with CYP106A2) and DOC (68 ± 2 µM and 50 ± 1 µM respectively), while the other chosen substrates with a functional group either at C11 or C17 show a rather weak interaction. Corticosterone and cortisone bind stronger to CYP106A2, whereas cortisol binds stronger to CYP106A1. However, the differences are within one order of magnitude and, therefore, relatively small. Unfortunately, the role of the CYP106A enzymes in *B. megaterium* - whose knockout is not lethal, but leads to significantly reduced growth rates - is a question that remains to be solved. Most likely CYP106A enzymes play a role in the growth of *B. megaterium* strains on alternative carbon and energy sources such as steroids and terpenoids. This assumption is supported by the fact that endogenous CYP106A2 is expressed only in the stationary phase of growth, when carbon and energy sources are depleted in the medium (Berg and Rafter, 1981).

To obtain the hydroxylation products in sufficient amounts for NMR studies, whole-cell biotransformations were performed and the product structures elucidated (Table 4). Both enzymes favored the 15β-position when using C21-steroids such as DOC, RSS and cortisone. However, differences were observed with corticosterone and androstenedione. In the case of corticosterone, the main product was 11-dehydrocorticosterone using CYP106A1, while for CYP106A2 the main product was identified as 15β-hydroxycorticosterone. Androstenedione was hydroxylated at position 15β by CYP106A2 and both at positions 6β and 7β with CYP106A1.

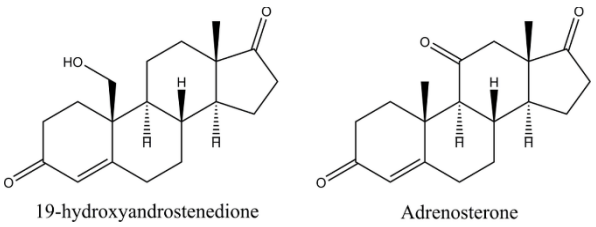

Fig. 3 Derivatives of the CYP106A-substrate androstenedione, which induce a type I shift but show no conversion

In order to get insight into the differences in steroid conversion between the CYP106A enzymes, an alignment was performed, where all conserved features of P450s were recognized in

Fig. 4 Alignment of the amino acid sequences of CYP106A1 and CYP106A2, showing the SRS regions identified by Gotoh (1992). The identical residues in the SRS region are shown in light blue, the different ones shown in red and the residues identified as lining the CYP106A2 active site by Janocha (2013) are marked with dark blue. The hΦ-Pro motif is shown with a blue frame

both enzymes (Fig. 4). Focusing on the substrate recognition sites (SRS), previously identified by Gotoh (1992), the SRS1 and SRS4-6 regions of CYP106A1 showed considerable differences in the amino acid pattern from the ones present in CYP106A2 (Fig. 4). The different residues in the SRS1 region, being responsible for the final stabilization of the substrate in the active site and in the SRS4-6 regions, involved in the initial substrate recognition and binding, could provide an explanation for the different regio- and stereoselectivity of the isoenzymes. We also examined the hΦ-Pro motif in SRS1, where a hydrophobic residue precedes the amino acid proline before the B´helix, which is usually associated with high substrate selectivity or regio- and stereospecificity (Pochapsky et al., 2010). In CYP106A2, the hydrophobic residue is valine at position 82, followed by the proline while in CYP106A1 position 82 is occupied by a threonine, followed by a serine. This difference might contribute to the lower selectivity of CYP106A1. In case of androstenedione, for instance, CYP106A2 hydroxylates the C-ring at position 15β preferentially, whereas CYP106A1 attacks at the B-ring with less selectivity resulting in 6β- and 7β-hydroxysteroids as main products.

Both enzymes hydroxylated the steroids mainly at the C- and B-rings. However, in the case of steroids with a hydroxyl group at C11, a completely different reaction was observed: The CYP106A1 enzyme enabled the dehydrogenation of cortisol and corticosterone, whereas CYP106A2 performed the same reaction only with corticosterone, converting these 11β-hydroxysteroids into their 11-keto forms (Scheme 1). This reaction was not yet described for the CYP106A subfamily and was only suggested to occur in one other case of P450s (Suhara et al., 1986). The mechanism is still unidentified and a highly interesting topic for further research. Yet, a very similar oxidation mechanism was studied by Bellucci *et al.*, where the model reaction was the oxidation of an allylic alcohol and by Matsunaga *et al*., where the oxidation mechanism of hydroxy-Δ^8-tetrahydrocannabinols was investigated. Both studies concluded that the so-called *gem*-diol pathway could be an explanation of the mechanism, while as an alternative they proposed a combination of the *gem*-diol and the double hydrogen abstraction pathway (Bellucci et al., 1996; Matsunaga et al., 2001).

Besides the reaction mechanism, the transformation of cortisol to cortisone is also notable, since both steroid hormones have important roles as pharmaceutical agents (Carballeira et al., 2009). Although, the

11-oxidase reaction catalyzed by CYP106A1 has shown only 19 % selectivity towards cortisone formation, we are confident that following the optimization of the *B. megaterium* whole-cell system, in combination with enzyme engineering tools, the selectivity of the enzyme could be increased towards an alternative route for this reaction.

In summary, in this work we extended the substrate range of the CYP106A subfamily, identifying 13 new steroidal substrates for CYP106A1 and 7 for CYP106A2. The enzymes produced hydroxylated metabolites at positions 6β, 7β, 9α and 15β and showed furthermore an unprecedented 11-oxidase activity. The hydroxyl groups introduced selectively in the steroid backbone make these derivatives valuable for the pharmaceutical industry. Either used as standards for human drug metabolites or as drug precursors for further functionalization, the production of these compounds with the help of the CYP106A subfamily has undoubtable advantage over chemical approaches. Our results strongly support the importance of the CYP106A1 and CYP106A2 enzymes for the pharmaceutical industry, especially for the production of human drug metabolites and drug precursors.

Aknowledgements

This work was generously supported by the People Programme (Marie Curie Actions) of the European Union's 7th Framework Programme (FP7/2007-2013), P4FIFTY - FP7 PEOPLE ITN 2011-289217. The authors thank Wolfgang Reinle and Birgit Heider-Lips for the excellent expression and purification of AdR and Adx_{4-108} and Nicolas Souza Carmona for the thorough revision of the language.

Conflict of interest

The authors declare no conflict of interest.

References

Agematu H, Matsumoto N, Fujii Y, Kabumoto H, Doi S, Machida K, Ishikawa J, Arisawa A (2006) Hydroxylation of testosterone by bacterial cytochromes P450 using the *Escherichia coli* expression system. Biosci Biotech Bioch 70(1):307-311

Barg H, Malten M, Jahn M, Jahn D (2005) Protein and vitamin production in *Bacilllus megaterium* Microbial processes and products. vol 18, 1 edn. Humana, Totowa, pp 205-223

Bellucci G, Chiappe C, Pucci L, Gervasi PG (1996) The Mechanism of Oxidation of Allylic Alcohols to α,β-Unsaturated Ketones by Cytochrome P450†. Chem Res Toxicol 9(5):871-874

Berg A, Gustafsson J, Ingelman-Sundberg M (1976) Characterization of a cytochrome P-450-dependent steroid hydroxylase system present in *Bacillus megaterium*. J Biol Chem 251:2831-2838

Berg A, Ingelman-Sundberg M, Gustafsson J (1979) Isolation and characterization of cytochrome P-450meg. Acta Biol Med Ger 38:333-344

Berg A, Rafter JJ (1981) Studies on the substrate specificity and inducibility of cytochrome P-450meg. Biochem J 196 (3) 781-786

Bernhardt R (2006) Cytochromes P450 as versatile biocatalysts. J Biotechnol 124(1):128-145

Bernhardt R, Urlacher V (2014) Cytochromes P450 as promising catalysts for biotechnological application: chances and limitations. Appl Microbiol Biotechnol 98(14):6185-6203

Bleif S, Hannemann F, Lisurek M, Kries J, Zapp J, Dietzen M, Antes I, Bernhardt R (2011) Identification of CYP106A2 as a regioselective allylic bacterial diterpene hydroxylase. ChemBioChem 12:576-582

Bleif S, Hannemann F, Zapp J, Hartmann D, Jauch J, Bernhardt R (2012) A new *Bacillus megaterium* whole-cell catalyst for the hydroxylation of the pentacyclic triterpene 11-keto-beta-boswellic acid (KBA) based on a recombinant cytochrome P450 system. Appl Microbiol Biotechnol 93:1135-1146

Bracco P, Janssen D, Schallmey A (2013) Selective steroid oxyfunctionalisation by CYP154C5, a bacterial cytochrome P450. Microb Cell Fact 12(1):95

Brill E (2013) Identifizierung und Charakterisierung neuer Cytochrom P450 Systeme aus *Bacillus megaterium* DSM319 Universität des Saarlandes

Brill E, Hannemann F, Zapp J, Bruning G, Jauch J, Bernhardt R (2014) A new cytochrome P450 system from *Bacillus megaterium* DSM319 for the hydroxylation of 11-keto-beta-boswellic acid (KBA). Appl Microbiol Biotechnol 98:1701-1717

Carballeira JD, Quezada MA, Hoyos P, Simeó Y, Hernaiz MJ, Alcantara AR, Sinisterra JV (2009) Microbial cells as catalysts for stereoselective red–ox reactions. Biotech Adv 27(6):686-714

Chefson A, Auclair K (2006) Progress towards the easier use of P450 enzymes. Mol Biosyst 2(10):462-469

Choudhary MI, Erum S, Atif M, Malik R, Khan NT, Atta ur R (2011) Biotransformation of (20S)-20-hydroxymethylpregna-1,4-dien-3-one by four filamentous fungi. Steroids 76(12):1288-1296

Choudhary MI, Sultan S, Khan MTH, Rahman A-u (2005) Microbial transformation of 17α-ethynyl- and 17α-ethylsteroids, and tyrosinase inhibitory activity of transformed products. Steroids 70(12):798-802

Donova M, Egorova O (2012) Microbial steroid transformations: current state and prospects. Appl Microbiol Biotechnol 94:1423-1447

Ewen K, Ringle M, Bernhardt R (2012) Adrenodoxin-A versatile ferredoxin. IUBMB Life 64:506-512

Faramarzi MA, Tabatabaei Yazdi M, Amini M, Zarrini G, Shafiee A (2003) Microbial hydroxylation of progesterone with *Acremonium strictum*. FEMS Microbiol Lett 222(2):183-186

Ferrero VEV, Di Nardo G, Catucci G, Sadeghi SJ, Gilardi G (2012) Fluorescence detection of ligand binding to labeled cytochrome P450 BM3. Dalton Trans 41(7):2018-2025

Girhard M, Klaus T, Khatri Y, Bernhardt R, Urlacher V (2010) Characterization of the versatile monooxygenase CYP109B1 from *Bacillus subtilis*. Appl Microbiol Biotechnol 87(2):595-607

Gotoh O (1992) Substrate recognition sites in cytochrome P450 family 2 (CYP2) proteins inferred from comparative analyses of amino acid and coding nucleotide sequences. J Biol Chem 267(1):83-90

Hannemann F, Bichet A, Ewen KM, Bernhardt R (2007) Cytochrome P450 systems--biological variations of

electron transport chains. Biochim Biophys Acta 1770(3):330-344

Hannemann F, Virus C, Bernhardt R (2006) Design of an *Escherichia coli* system for whole cell mediated steroid synthesis and molecular evolution of steroid hydroxylases. J Biotechnol 124(1):172-181

He J, Liang Q, Fulco A (1995) The molecular cloning and characterization of BM1P1 and BM1P2 proteins, putative positive transcription factors involved in barbiturate-mediated induction of the genes encoding cytochrome P450BM-1 of *Bacillus megaterium*. J Biol Chem 270:18615-18625

He J, Ruettinger R, Liu H, Fulco A (1989) Molecular cloning, coding nucleotides and the deduced amino acid sequence of P-450BM-1 from *Bacillus megaterium*. Biochim Biophys Acta 1009(3):301-303

Hollmann F, Hofstetter K, Schmid A (2006) Non-enzymatic regeneration of nicotinamide and flavin cofactors for monooxygenase catalysis. Trends Biotechnol 24(4):163-171

Janeczko T, Dmochowska-Gładysz J, Kostrzewa-Susłow E, Białońska A, Ciunik Z (2009) Biotransformations of steroid compounds by *Chaetomium* sp. KCH 6651. Steroids 74(8):657-661

Janocha S, Bernhardt R (2013) Design and characterization of an efficient CYP105A1-based whole-cell biocatalyst for the conversion of resin acid diterpenoids in permeabilized *Escherichia coli*. Appl Microbiol Biotechnol 97:7639-7649

Khatri Y, Hannemann F, Girhard M, Kappl R, Même A, Ringle M, Janocha S, Leize-Wagner E, Urlacher V, Bernhardt R (2013) Novel family members of CYP109 from *Sorangium cellulosum* So ce56 exhibit characteristic biochemical and biophysical properties. Biotechnol Appl Biochem 60(1):18-29.

Kirk DN, Toms HC, Douglas C, White KA, Smith KE, Latif S, Hubbard RWP (1990) A survey of the high-field 1H NMR spectra of the steroid hormones, their hydroxylated derivatives, and related compounds. J Chem Soc, Perkin Trans 2 (9):1567-1594

Korneli C, David F, Biedendieck R, Jahn D, Wittmann C (2013) Getting the big beast to work—Systems biotechnology of *Bacillus megaterium* for novel high-value proteins. J Biotechnol 163(2):87-96

Lee G-Y, Kim D-H, Kim D, Ahn T, Yun C-H (2014) Functional characterization of steroid hydroxylase CYP106A1 derived from *Bacillus megaterium*. Arch Pharm Res:1-10

Li Y, Drummond DA, Sawayama AM, Snow CD, Bloom JD, Arnold FH (2007) A diverse family of thermostable cytochrome P450s created by recombination of stabilizing fragments. Nat Biotechnol 25(9):1051-6

Lisurek M, Kang M, Hartmann R, Bernhardt R (2004) Identification of monohydroxy progesterones produced by CYP106A2 using comparative HPLC and electrospray ionisation collision-induced dissociation mass spectrometry. Biochem Biophys Res Commun 319:677-682

Lisurek M, Simgen B, Antes I, Bernhardt R (2008) Theoretical and experimental evaluation of a CYP106A2 low homology model and production of mutants with changed activity and selectivity of hydroxylation. ChemBioChem 9:1439-1449

Makino T, Katsuyama Y, Otomatsu T, Misawa N, Ohnishi Y (2014) Regio- and Stereospecific Hydroxylation of Various Steroids at the 16α Position of the D Ring by the *Streptomyces griseus* Cytochrome P450 CYP154C3. Appl Environ Microbiol 80(4):1371-1379

Matsunaga T, Tanaka H, Higuchi S, Shibayama K, Kishi N, Watanabe K, Yamamoto I (2001) Oxidation Mechanism of 7-Hydroxy-Δ8-tetrahydrocannabinol and 8-Hydroxy-Δ9-tetrahydrocannabinol to the Corresponding Ketones by CYP3A11. Drug Metab Dispos 29(11):1485-1491

Matsuzaki K, Arai T, Miyazaki T, Yasuda K (1995) Formation of 6β-OH-deoxycorticosterone from deoxycorticosterone by A6 cells. Steroids 60(7):457-462

Mineki S, Iida M, Kato K, Fukaya F, Kita K, Nakamura J, Yoshihama M (1995) Microbial production of hydroxy-C19-steroids as estrogen synthetase (P-450 · aromatase) inhibitors. J Ferment Bioengineer 80(3):223-228

Nguyen K, Virus C, Gunnewich N, Hannemann F, Bernhardt R (2012) Changing the regioselectivity of a P450 from C15 to C11 hydroxylation of progesterone. ChemBioChem 13:1161-1166

O'Reilly E, Kohler V, Flitsch SL, Turner NJ (2011) Cytochromes P450 as useful biocatalysts: addressing the limitations. Chem Commun 47(9):2490-2501

Omura T, Sato R (1964) The carbon monoxide-binding pigment of liver microsomes. I. Evidence for its hemoprotein nature. J Biol Chem 239:2370-2378

Pochapsky T, Kazanis S, Dang M (2010) Conformational Plasticity and Structure/Function Relationships in Cytochromes P450. Antioxid Redox Signal 13(8):1273-1296

Sagara Y, Wada A, Takata Y, Waterman M, Sekimizu K, Horiuchi T (1993) Direct expression of adrenodoxin reductase in *Escherichia coli* and the functional characterization. Biol Pharm Bull 16:627-630

Schenkman J, Jansson I (1998) Spectral analyses of cytochromes P450. Meth Mol Biol (Clifton, NJ) 107:25

Schenkman J, Sligar S, Cinti D (1981) Substrate interaction with cytochrome P-450. Pharmacol Ther 12:43-71

Schmitz D, Zapp J, Bernhardt R (2012) Hydroxylation of the triterpenoid dipterocarpol with CYP106A2 from *Bacillus megaterium*. FEBS J 279:1663-1674

Schmitz D, Zapp J, Bernhardt R (2014) Steroid conversion with CYP106A2 - production of pharmaceutically interesting DHEA metabolites. Microb Cell Fact 13:81

Seng Wong T, Arnold FH, Schwaneberg U (2004) Laboratory evolution of cytochrome P450 BM-3 monooxygenase for organic cosolvents. Biotechnol Bioeng 85(3):351-358

Simgen B, Contzen J, Schwarzer R, Bernhardt R, Jung C (2000) Substrate binding to 15beta-hydroxylase (CYP106A2) probed by FT infrared spectroscopic studies of the iron ligand CO stretch vibration. Biochem Biophys Res Commun 269:737-742

Suhara K, Takeda K, Katagiri M (1986) P-45011β-dependent conversion of cortisol to cortisone, and 19-hydroxyandrostenedione to 19-oxoandrostenedione. Biochem Biophys Res Commun 136(1):369-375

Tong W, Dong X (2009) Microbial biotransformation: recent developments on steroid drugs. Recent Pat Biotechnol 3(2):141-53.

Uhlmann H, Beckert V, Schwarz D, Bernhardt R (1992) Expression of bovine adrenodoxin in *E. coli* and site-directed mutagenesis of/2 Fe-2S/cluster ligands. Biochem Biophys Res Commun 188:1131-1138

Urlacher VB, Eiben S (2006) Cytochrome P450 monooxygenases: perspectives for synthetic application. Trends Biotechnol 24:324-330

Urlacher VB, Girhard M (2012) Cytochrome P450 monooxygenases: an update on perspectives for synthetic application. Trends Biotechnol 30:26-36

Urlacher VB, Lutz-Wahl S, Schmid RD (2004) Microbial P450 enzymes in biotechnology. Appl Microbiol Biotechnol 64:317-325

Vary P, Biedendieck R, Fuerch T, Meinhardt F, Rohde M, Deckwer W-D, Jahn D (2007) *Bacillus megaterium*—from simple soil bacterium to industrial protein production host. Appl Microbiol Biotechnol 76:957-967

Venkataraman H, te Poele E, Rosłoniec K, Vermeulen N, Commandeur JM, van der Geize R, Dijkhuizen L (2014) Biosynthesis of a steroid metabolite by an engineered *Rhodococcus erythropolis* strain expressing a mutant cytochrome P450 BM3 enzyme. Appl Microbiol Biotechnol:1-9

Virus C, Bernhardt R (2008) Molecular evolution of a steroid hydroxylating cytochrome P450 using a versatile steroid detection system for screening. Lipids 43:1133-1141

Virus C, Lisurek M, Simgen B, Hannemann F, Bernhardt R (2006) Function and engineering of the 15beta-hydroxylase CYP106A2. Biochem Soc Trans 34:1215-1218

Wittchen K, Meinhardt F (1995) Inactivation of the major extracellular protease from *Bacillus megaterium* DSM319 by gene replacement. Appl Microbiol Biotechnol 42:871-877

Zehentgruber D, Hannemann F, Bleif S, Bernhardt R, Lütz S (2010) Towards preparative scale steroid hydroxylation with cytochrome P450 monooxygenase CYP106A2. ChemBioChem 11:713-721

Applied Microbiology and Biotechnology

Supplementary material

Comparison of CYP106A1 and CYP106A2 from *Bacillus megaterium* - identification of a novel 11-oxidase activity

Flora Marta Kiss[1], Daniela Schmitz[1], Josef Zapp[2], Tobias K. F. Dier[3], Dietrich A. Volmer[3], Rita Bernhardt[1*]

[1]Institute of Biochemistry, University of Saarland, D-66123 Saarbruecken, Germany

[2]Institute of Pharmaceutical Biology, University of Saarland, D-66123 Saarbruecken, Germany

[3]Institute of Bioanalytical Chemistry, University of Saarland, D-66123 Saarbruecken, Germany

*Address correspondence to: Professor Dr. Rita Bernhardt
Institute of Biochemistry, University of Saarland, Campus B 2.2, D-66123 Saarbruecken, Germany
Tel: +49 681 302 305
Fax: +49 681 302 4739
Email: ritabern@mx.uni-sarland.de

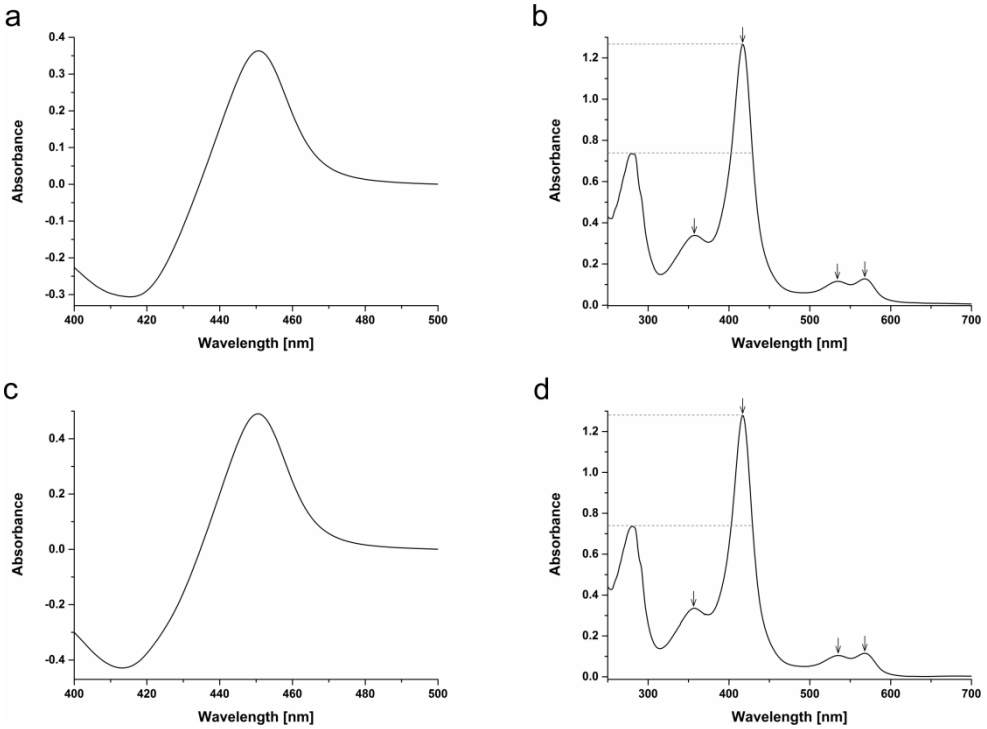

Fig. S1 UV-visible absorbance spectrum of the reduced and CO-bound form of the purified CYP106A1 (a) and CYP106A2 (c) enzyme, showing the characteristic peak at 450nm. UV-visible absorbance spectrum of the purified CYP106A1 (b) and CYP106A2 (d), showing the typical peaks at 356,417, 53 and 568 nm.

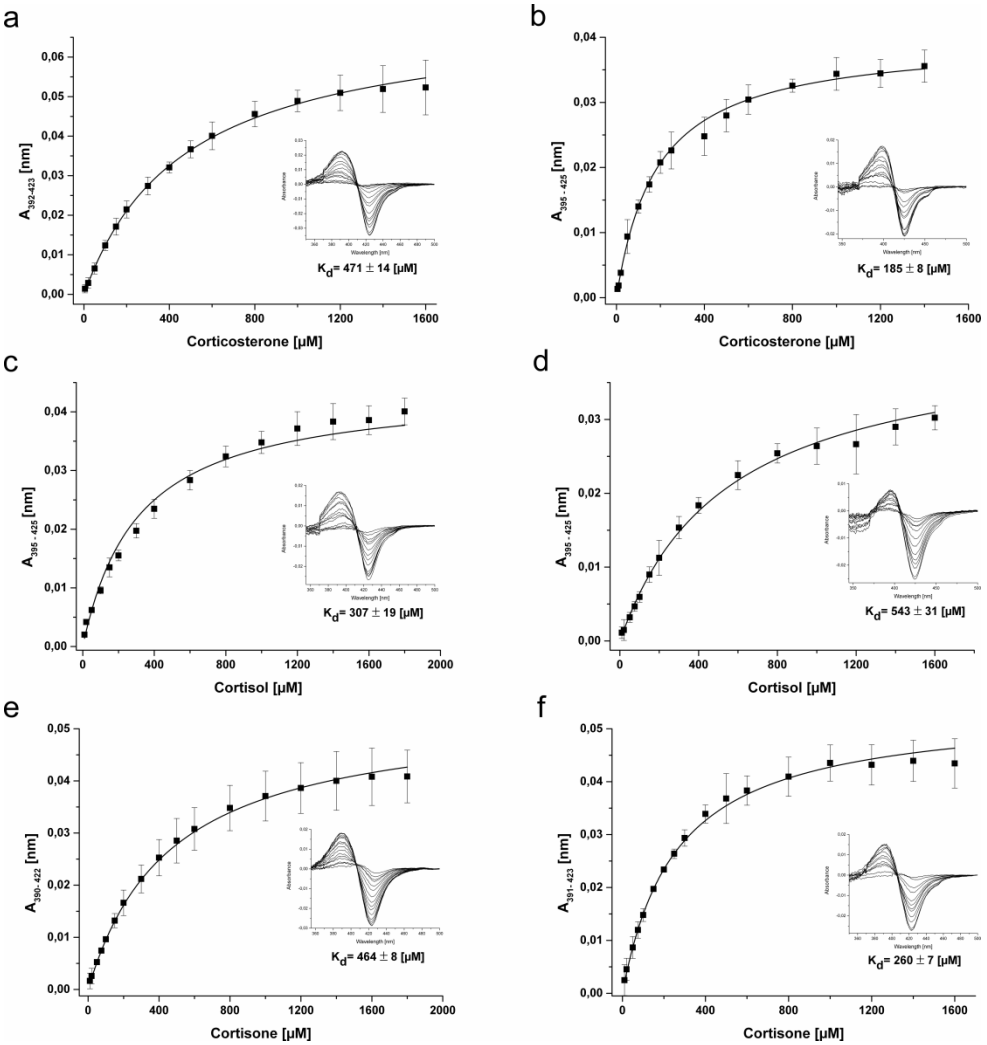

Fig. S2 Type I spectral shifts induced by the binding of corticosterone, cortisol and cortisone binding to CYP106A1 (a, c, e) and to CYP106A2 (b, d, f). Increasing amounts of substrates dissolved in DMSO were titrated (10 µM in 50 mM potassium phosphate buffer pH 7.4). The peak-to-through absorbance differences were plotted against the increasing concentrations of the substrate. The mean values of three independent measurements were fitted by hyperbolic regression.

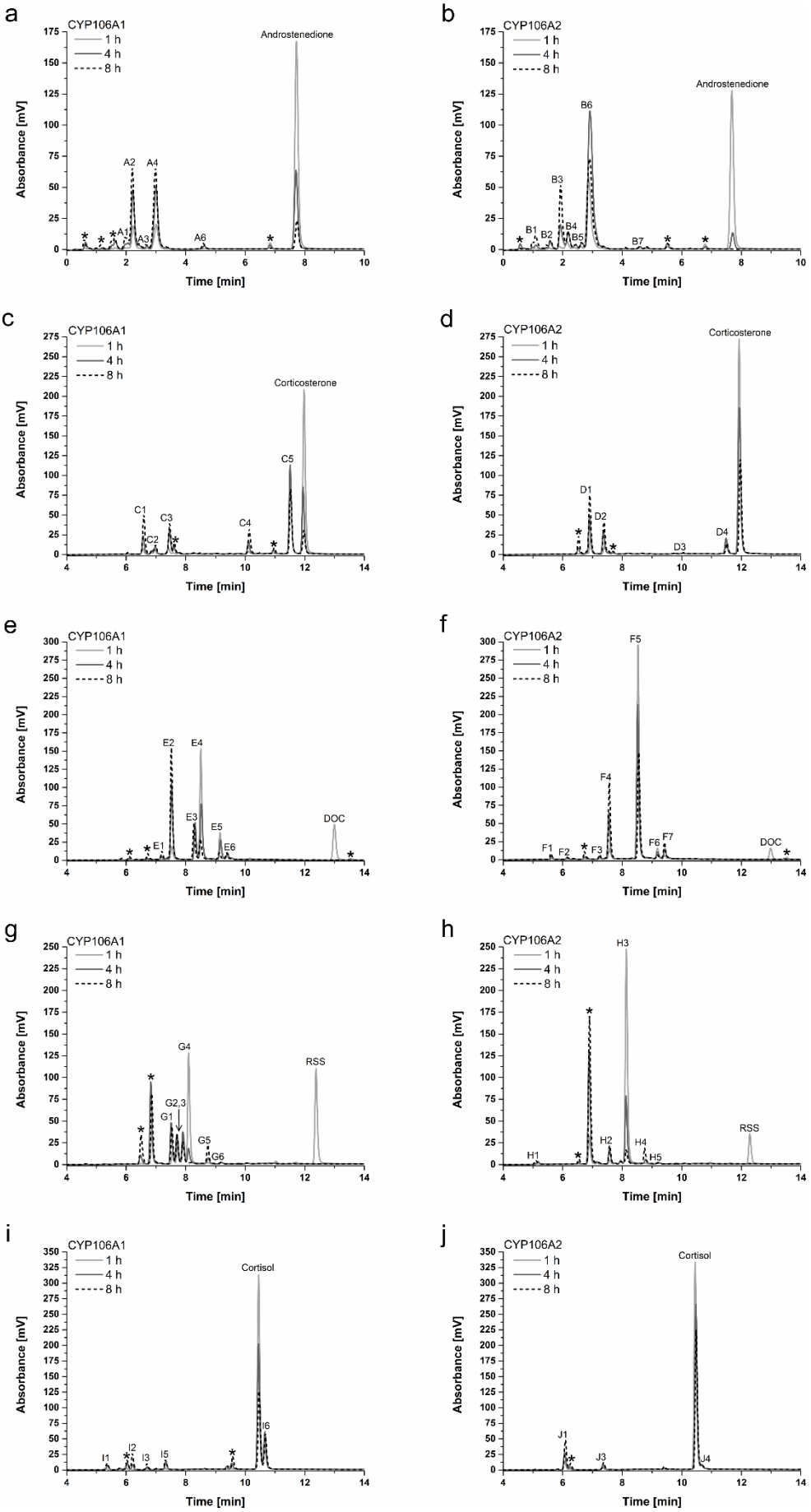
a
CYP106A1
1 h
4 h
8 h
Androstenedione
A1
A2
A3
A4
A6
b
CYP106A2
Androstenedione
B1
B2
B3
B4
B5
B6
B7
c
CYP106A1
Corticosterone
C1
C2
C3
C4
C5
d
CYP106A2
Corticosterone
D1
D2
D3
D4
e
CYP106A1
E1
E2
E3
E4
E5
E6
DOC
f
CYP106A2
F1
F2
F3
F4
F5
F6
F7
DOC
g
CYP106A1
G1
G2,3
G4
G5
G6
RSS
h
CYP106A2
H1
H2
H3
H4
H5
RSS
i
CYP106A1
Cortisol
I1
I2
I3
I5
I6
j
CYP106A2
Cortisol
J1
J3
J4
Absorbance [mV]
Time [min]

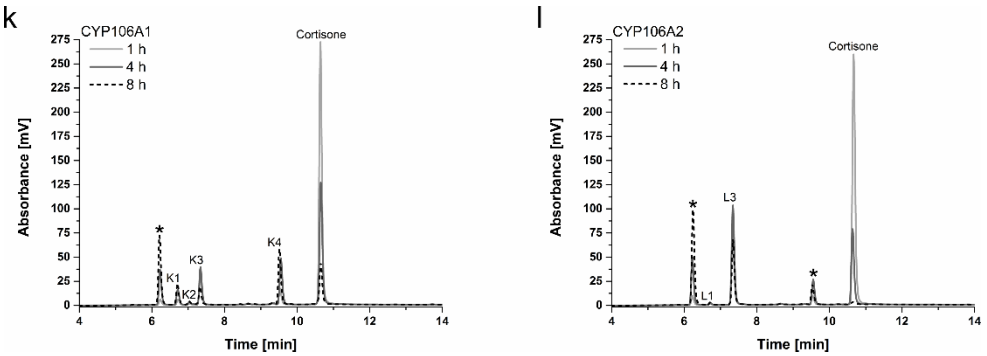

*The peaks labelled with an asterisk represent compounds which were not observed during the *in vitro* conversions, thus not treated as specific CYP106A enzyme products.

Fig. S3 HPLC chromatograms of the *in vivo* conversion of androstenedione (**a**, **b**), corticosterone (**c**, **d**), 11-deoxycorticosterone (**e**, **f**), 11-deoxycortisol (**g**, **h**), cortisol (**I**, **j**) and cortisone (**k**, **l**) by *Bacillus megaterium* MS941 strains, containing the plasmid pSMF2.1B (CYP106A1) or pSMF2.1C (CYP106A2). The reactions were performed with resting cells in 50 mM potassium phosphate buffer pH 7.4 at 30 °C for 24 hours with 200 µM substrate. Samples were collected at the indicated time points.

2.2. Kiss *et al.* (2015)

Identification of new substrates for the CYP106A1-mediated 11-oxidation and investigation of the reaction mechanism

Flora Marta Kiss, Yogan Khatri, Josef Zapp, Rita Bernhardt

FEBS letters 2015 doi:10.1016/j.febslet.2015.07.011

Identification of new substrates for the CYP106A1-mediated 11-oxidation and investigation of the reaction mechanism

Flora Marta Kiss[1], Yogan Khatri[1], Josef Zapp[2], Rita Bernhardt[1*]

Abstract

CYP106A1 from *Bacillus megaterium* DSM319 was recently shown to catalyze steroid and terpene hydroxylations. Besides producing hydroxylated steroid metabolites at positions 6β, 7β, 9α and 15β, the enzyme displayed previously unknown 11-oxidase activity towards 11β-hydroxysteroids. Novel examples for 11-oxidation were identified and confirmed by ^{1}H- and ^{13}C-NMR for prednisolone, dexamethasone and 11β-hydroxyandrostenedione. However, only 11β-hydroxyandrostenedione formed a single 11-keto product. The latter reaction was chosen to investigate the kinetic solvent isotope effect on the steady-state turnover of the CYP106A1-mediated 11-oxidation. Our results reveal a large inverse kinetic isotope effect (~0.44) suggesting the involvement of the ferric peroxoanion as a reactive intermediate.

Keywords: CYP106A1, 11β-hydroxysteroid, 11-oxidation, kinetic solvent isotope effect, cytochrome P450, ferric peroxoanion

Highlights:

- Novel substrates identified for the CYP106A1-mediated 11-oxidation
- Selective 11-oxidation of 11β-hydroxyandrostenedione observed
- 11-oxidation mechanism investigated via kinetic solvent isotope effect
- Inverse kinetic solvent isotope effect, suggesting the ferric peroxoanion as reactive intermediate

Introduction

The CYP106A1 enzyme from *Bacillus megaterium* DSM319 was recently isolated and characterized by our group (Brill et al. 2014). Its closest homologue, CYP106A2 from *B. megaterium* ATCC13368 has been extensively investigated and recognized as a highly potent catalyst for both steroid and terpene hydroxylations (Bernhardt 2006; Bleif et al. 2011; Bleif et al. 2012; Schmitz et al. 2014; Zehentgruber et al. 2010). Based on the 63 % amino acid sequence identity between the subfamily members, the functional characterization of CYP106A1 concerning tri-terpene hydroxylation (Brill et al. 2014), followed by the investigation of steroid hormone transformation (Kiss et al. 2015; Lee et al. 2014) was performed.

We have demonstrated the 6β, 7β, 9α and 15β steroid-hydroxylase activity of CYP106A1, in addition to the 11-oxidation of corticosterone and cortisol (Kiss et al. 2015). The latter reaction was also observed for the human CYP11B1, converting cortisol to cortisone (Suhara et al. 1986); however, the reaction mechanism has never been investigated. Since such 11-oxo steroid formation is uncommon in P450 catalysis, we were interested in studying the underlying mechanism by evaluating the kinetic solvent isotope effect (KSIE) in the CYP106A1-mediated 11-oxidation. The effect of hydrogen substitution by deuterium on the catalytic activity provides

[1]Institute of Biochemistry, Saarland University, D-66123 Saarbruecken, Germany

[2]Institute of Pharmaceutical Biology, Saarland University, D-66123 Saarbruecken, Germany

*Address correspondence to: Professor Dr. Rita Bernhardt
Email: ritabern@mx.uni-sarland.de

valuable information on proton involvement in the P450 catalytic steps.

The catalytic cycle of a P450 (**Fig. 1**), based on CYP101 (Denisov et al. 2005; Makris et al. 2002), starts with the ferric resting state of the enzyme (**1**) (Raag et al. 1991; Raag and Poulos 1989). Upon substrate binding, the six-coordinated low-spin complex is shifted to the five-coordinated high-spin state (**2**) and an electron transfer from an associated redox partner takes place (**3**) (Sligar 1976; Tsai et al. 1970). On subsequent binding of a molecular oxygen, the oxy-ferrous state (**4**) is formed (Champion et al. 1978; Macdonald et al. 1999), which is then reduced to a ferric peroxoanion (**5a**) leading to the formation of a hydroperoxo intermediate (**5b**), compound 0 (Cpd 0), on acceptance of a proton (Harris and Loew 1996). The availability of a second proton causes the release of a water molecule and generates compound I (Cpd I) (**6**) (Groves 2006; Rittle and Green 2010). Subsequently, the product is released (**7**) regenerating the ferric heme, thus allowing the next catalytic cycle to begin. Alternatively, the activated oxygen can be released through one of the "uncoupling" pathways (shunts, depicted in dashed grey in **Fig. 1**), which can abort the catalytic cycle, being unproductive regarding substrate oxidation, yet still consuming pyridine nucleotide, NADP(H)/NADH.

In general, standard P450-mediated reactions (e.g. hydroxylations) are considered to proceed through the classical Cpd I-mediated H-rebound mechanism, in which the reaction takes place with the help of two consecutive proton uptakes (Batabyal et al. 2013; Groves 2006; Liu and Ortiz de Montellano 2000; Vidakovic et al. 1998). However, the ferric peroxoanion (**5a**) can also intervene in the P450 catalysis, which has recently been observed in the CYP17A1-mediated lyase reaction (Gregory et al. 2013).

In this study, we investigated the underlying reaction mechanism of the CYP106A1-mediated 11-oxidation which has recently been described using corticosterone and cortisol as substrates (Kiss et al. 2015). Both steroid conversions displayed several hydroxy-derivatives in addition to the 11-keto-product. Therefore, further 11β-hydroxysteroid analogues were screened to obtain a regio-selective C11-oxidation. The chosen steroids, prednisolone, dexamethasone and 11β-hydroxyandrostenedione (11-OH-AD), were previously identified as high-spin-shift-inducing CYP106A1 substrates, yet, the reactions were not investigated in detail and the products were not characterized (Kiss et al. 2015).

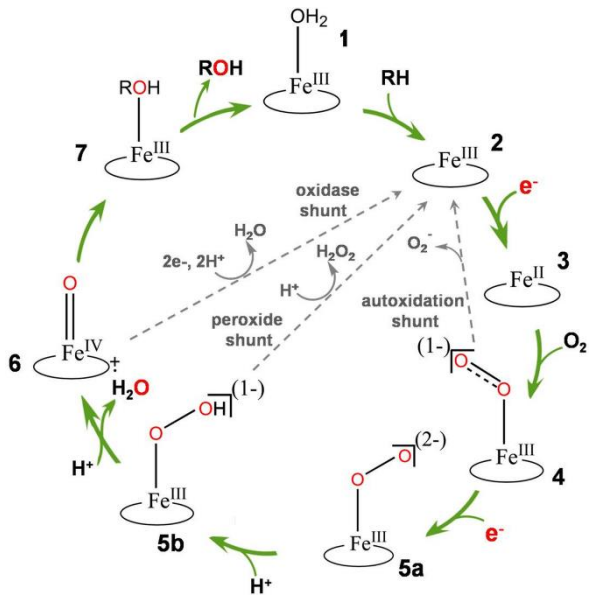

Fig. 1 – Cytochrome P450 catalytic cycle. The numbers (**1**-**7**) represent the actual state of the enzyme: **1** – Low-spin substrate-free state. **2** – High-spin enzyme-substrate complex. **3** - High-spin ferrous state. **4** – Oxy-ferrous state. **5a** - Ferric peroxo intermediate. **5b** – Ferric hydroperoxo intermediate/compound 0. **6** – High-valent iron-oxo state/compound I. **7** - Product oxidation and release. **RH** and **ROH** illustrate the substrate and the product, respectively. The three unproductive shunt-pathways are marked with dashed grey arrows and the reduced oxygen products are shown as outlets. (The cycle has been adapted from Makris *et al.* (2002) and Denisov *et al.* (2005).)

At first, we performed *in vitro* transformation of the substrates, followed by their *in vivo* turnover using a CYP106A1-based *B. megaterium* whole-cell system to obtain higher product yields required for the structural elucidation by nuclear magnetic resonance (NMR). The product structures confirmed the 11-oxidation of all substrates; however, only the 11-OH-AD conversion led to a single 11-keto-product, whereas prednisolone and dexamethasone displayed several hydroxy-metabolites as well. As a result, the regio-selective 11-oxidation of 11-OH-AD was chosen to study the reaction

mechanism employing the KSIE, a proven method to distinguish the involvement of P450 reaction intermediates Cpd I or the ferric peroxoanion during P450 catalysis (Aikens and Sligar 1994; Gregory et al. 2013; Khatri et al. 2014; Purdy et al. 2006; Schowen 1977; Vidakovic et al. 1998; Xiang et al. 2000).

Materials and methods

Protein expression and purification

The expression and purification of the CYP106A1 enzyme was performed as described elsewhere (Brill et al. 2014). The truncated bovine adrenodoxin (Adx_{4-108}) and the bovine adrenodoxin reductase (AdR) were expressed and purified as described by Uhlmann *et al*. (Uhlmann et al. 1992) and Sagara *et al*. (Sagara et al. 1993), respectively.

In vitro conversion and steady state kinetic turnover

Prednisolone, dexamethasone and 11-OH-AD were converted with a reconstituted system containing the CYP106A1 enzyme, AdR and Adx_{4-108} (in a ratio of 1:2:20), and a NADPH regenerating system, as formerly described by Kiss *et al*. (Kiss et al. 2015). The reaction was performed at 30 °C, for 60 min using 200 µM substrate. The final CYP106A1 concentration was 2 µM in the case of 11-OH-AD and 5 µM for both prednisolone and dexamethasone.

The steady state kinetic turnover of 11-OH-AD was performed in protiated and deuterated solvent systems using 2 µM enzyme and 50 µM final substrate concentration. To investigate the effect of radical scavengers on the catalytic rate, the *in vitro* conversions were performed with the addition of ascorbate (20 mM), catalase (20 U) and superoxide-dismutase (SOD) (3 U), individually as well as in combination. To determine whether hydrogen peroxide (H_2O_2) could be applied to reconstitute the activity of CYP106A1, H_2O_2 and cumene hydroperoxide were used in a final concentration of 50 µM. The reactions were stopped after 20 min and extracted twice by addition of 250 µL ethyl acetate. After evaporating the organic phases, the dried samples were dissolved in methanol and subjected to high-performance liquid chromatography (HPLC) analysis. An ec MN Nucleodor C_{18} (3 µM, 4.0x125 mm) column was used, with a mobile phase consisting of methanol, tetrahydrofuran and water in an 8:19:72 ratio. The steroids were eluted in an isocratic mode with a flow rate of 0.5 mL/min and detected at 240 nm. The conversions were analyzed using the peak areas (area %) of the HPLC chromatograms with the help of the ChromPass/Galaxie Chromatography Data System (Jasco, Gross-Umstadt,Germany).

In vivo conversion and product purification

The CYP106A1-based *B. megaterium* whole-cell system (harboring the plasmid pSMF2.1B) was used for biotransformation as described earlier (Brill et al. 2014; Kiss et al. 2015). The substrate was added in a final concentration of 400 µM to the *B. megaterium* resting cells in 100 mM potassium phosphate buffer (pH 7.4). The reaction was stopped after 24 h and extracted twice with ethyl acetate. The samples were dried and resuspended in the HPLC mobile phase. The product purification was performed with a preparative HPLC column (ec MN Nucleodur C_{18} VP (5 µM, 8x250 mm) using gradient elution (solvent A: 10 % acetonitrile (ACN), solvent B: 100 % ACN) with a flow rate of 2 mL/min.

NMR characterization of the metabolites

The NMR spectra were recorded in CD_3OD or in $CDCl_3$ with a Bruker DRX 500 or a Bruker Avance 500 NMR spectrometer at 300 K. The chemical shifts were relative to CH_3OD at δ 3.30 (^{1}H NMR) and CD_3OD at δ 49.00 (^{13}C NMR) or to $CHCl_3$ at δ 7.26 (^{1}H NMR) and $CDCl_3$ at δ 77.00 (^{13}C NMR) respectively, using the standard δ notation in parts per million. The 1D NMR (^{1}H and ^{13}C NMR, DEPT135) and the 2D NMR spectra (gs-HH-COSY, gs-NOESY, gs-HSQCED, and gs-HMBC) were recorded using the BRUKER pulse program library. All assignments were based on extensive NMR spectral evidence. For the detailed NMR data of the identified products see Supplementary Material.

Results and discussion

Substrate conversions, product purification and characterization by NMR

Since the previously identified substrates for the CYP106A1 11-oxidation (corticosterone and cortisol) gave rise to multiple product formation (Kiss et al. 2015), other 11β-hydroxysteroid analogues were investigated to identify a selective 11-keto product formation. The *in vitro* conversion of the pharmaceutically relevant glucocorticoids, prednisolone and dexamethasone, also resulted in several products (**Table 1, Fig. 2B and 3B**) in contrast to the transformation of 11-OH-AD, where only a single product was formed with a yield of 50 % (**Table 1, Fig. 4B**).

Even though single product formation was only observed with 11-OH-AD, we were interested in characterizing all 11β-hydroxysteroid metabolites by NMR, to identify novel 11-keto products and other glucocorticoid derivatives of potential pharmaceutical value. For the isolation and purification of the reaction products, the steroid bioconversions were performed via a CYP106A1-based *B. megaterium* whole-cell system.

The *in vivo* turnover of prednisolone led to ~51 % conversion resulting in a main product, P1 (35 %) with identical retention time (~3.6 min) to the one observed *in vitro*. Besides the major product, multiple side-products (<5%) were also detected, out of which P2 (~4.8 min) and P3 (~8.3 min) eluted at the same time as the respective *in vitro* metabolites (**Fig. 2 B, C**). Although both P1 and P2 were well resolved during the purification, the NMR analysis of their purified fractions showed a mixture of several steroids, containing 15β-hydroxyprednisolone as a major compound. Likewise, product P3, which was identified as a 2:3 mixture of 15β-hydroxyprednisone and 1,2-dihydro-15β-hydroxyprednisone displaying 11-oxidation catalyzed by CYP106A1 (**Scheme 1**).

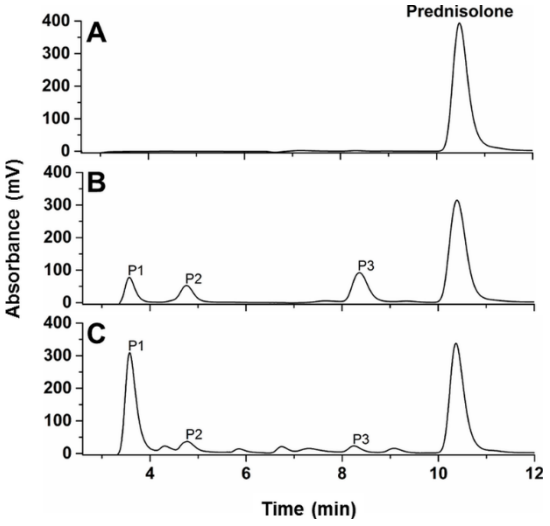

Fig. 2 - HPLC chromatograms of the CYP106A1 catalyzed prednisolone conversion. (A) Negative control, containing prednisolone only. (**B**) *In vitro* prednisolone conversion, using bovine $Adx_{4\text{-}108}$ (100 µM), bovine AdR (10 µM) and CYP106A1 (5 µM). (**C**) *In vivo* conversion of prednisolone using the CYP106A1-overexpressing *B. megaterium* MS941 strain.

The unusual 1(2)-double bond hydrogenation has not been observed in our previous studies (Kiss et al. 2015), hence, it was proposed to be the result of an uncharacterized enzyme present in the *B. megaterium* MS941 strain. It has been reported that 3-ketosteroid-dehydrogenases present in *Nocardia*, *Mycobacterium* and *Actinobacter sp.* can be responsible for both 1(2)-hydrogenase and reductase reactions (Arinbasarova et al. 1996; Goren et al. 1983; van der Geize et al. 2000). However, these enzymes have not been described so far for *B. megaterium*. Therefore, the origin of

Table 1 - *In vitro* conversion results showing relative conversion and product retention times, when applicable.

Substrate (RT/min)	**RC** (%)	**Product RT** (min)				**Remark**
		P1	**P2**	**P3**	**P4**	
Prednisolone (10.5)	33	3.6	4.8	8.4	-	Fig. 2B
Dexamethasone (20.4)	40	5.1	6.9	8.3	15.8	Fig. 3B
11-OH-AD (13.0)	50	10.5	-	-	-	Fig. 4B

*RT, Retention time; RC, Relative conversion

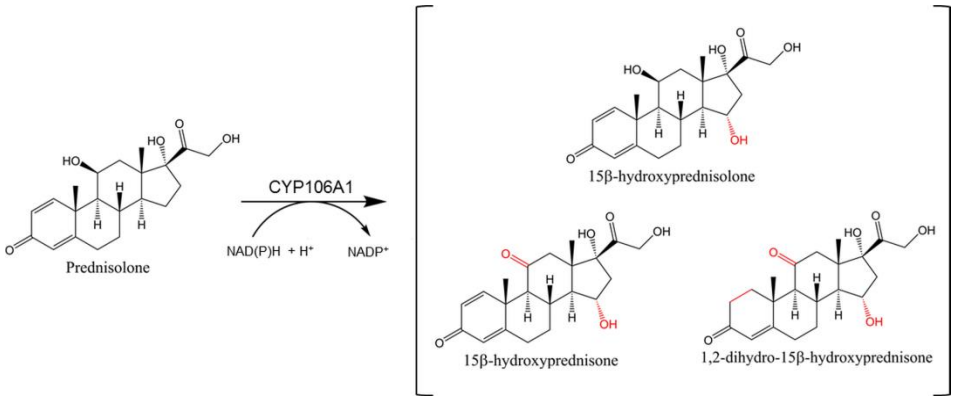

Scheme 1 – Oxidative transformation of prednisolone catalyzed by CYP106A1.

the 1(2)-hydrogenase reaction remains unclear. The above described prednisolone metabolites were previously unidentified, and therefore, no biotechnological applications are known to date. Nonetheless, the 15β-hydroxyl group attached to both prednisolone and prednisone structures provides a new reaction site for further functionalization, contributing to the development of novel glucocorticoids possessing anti-inflammatory/immunomodulatory activity with a potentially reduced risk of side effects.

Using the CYP106A1-based whole-cell system, nearly 50 % of dexamethasone was converted in 24 h, yielding four products, P1 to P4, which were all successfully isolated and characterized. Each of the identified metabolites showed identical retention times to the ones observed *in vitro*, eluting at 5.1, 6.9, 8.3 and 15.8 min, respectively (**Fig. 3 B, C**). The major product, P1 (37 %), and P2 (6 %) were identified as 15β-hydroxy- and 6β-hydroxy-derivatives of dexamethasone, respectively. The latter one also known as the major human metabolite of dexamethasone produced by CYP3A4 (Gentile et al. 1996; Minagawa et al. 1986; Tomlinson et al. 1997). Besides the hydroxylated derivatives, two minor 11-oxidized compounds were observed and characterized as 11-ketodexamethasone (P4, 2 %) and 15β-hydroxy-11-ketodexamethasone (P3, 3 %) (**Scheme 2**). The 11-keto compound was previously identified as a specific glucocorticoid receptor agonist, explaining the glucocorticoid effect of dexamethasone in tissues expressing the 11β-hydroxysteroid dehydrogenase type 2 enzyme, responsible for 11-oxidation in mammalian tissues (Rebuffat et al. 2004).

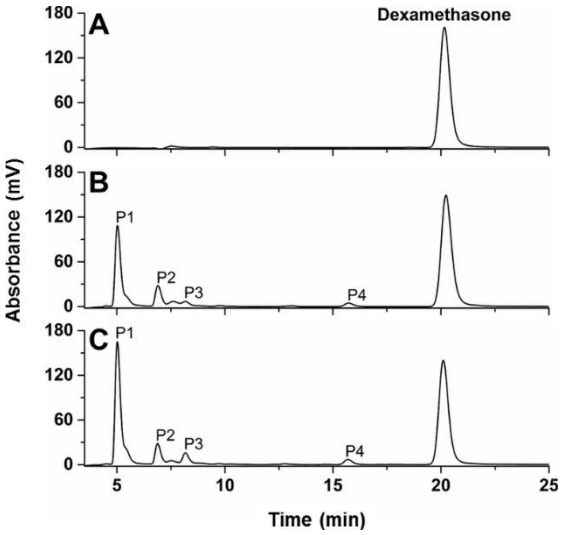

Fig. 3 - HPLC chromatograms of the CYP106A1-catalyzed dexamethasone conversion. (**A**) Negative control, containing dexamethasone only. (**B**) *In vitro* dexamethasone conversion, using bovine $Adx_{4\text{-}108}$ (100 µM), bovine AdR (10 µM) and CYP106A1 (5 µM). (**C**) *In vivo* conversion of dexamethasone using the CYP106A1-overexpressing *B. megaterium* MS941 strain.

The *in vivo* turnover of 11-OH-AD resulted in ~90 % conversion within 24 h and a single main product along with traces of minor side products, which were not observed in the *in vitro* system (**Fig. 4 C**). The major product, P1 (~10.5 min), showed identical retention time to that of the *in vitro* reaction (**Fig. 4 B**). The NMR characterization identified P1 as the 11-keto derivative, adrenosterone, supporting the previously observed 11-oxidase activity of CYP106A1 during the transformation of corticosterone and cortisol (Kiss et al. 2015) (**Scheme 3**). Adrenosterone is a weak androgen hormone found only in trace amounts in mammals, but in higher quantities in fish, where it

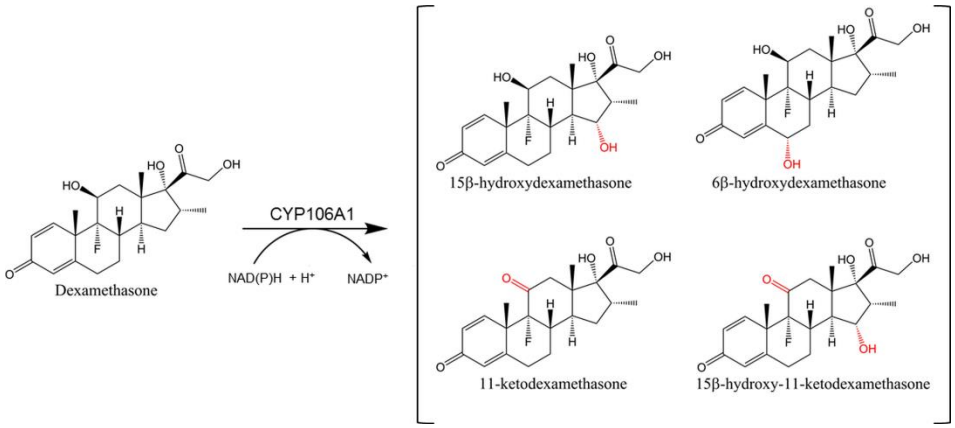

Scheme 2 – Oxidative transformation of dexamethasone catalyzed by CYP106A1.

acts as a precursor of 11-ketotestosterone, the endogenous androgenic sex hormone (Blasco et al. 2009; Borg 1994). It is sold as a dietary supplement, reducing body fat and increasing muscle mass and was also proposed to be a selective inhibitor of 11β-hydroxysteroid dehydrogenase type I enzyme (Brooker et al. 2009).

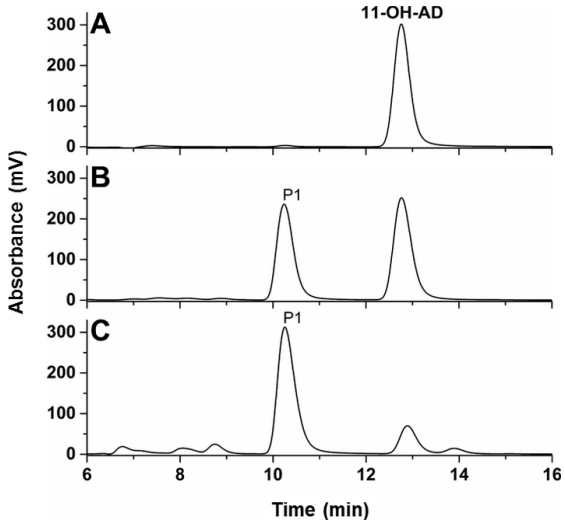

Fig. 4 - HPLC chromatograms of the CYP106A1 catalyzed 11β-hydroxyandrostenedione conversion. (**A**) Negative control, containing 11-OH-AD only. (**B**) *In vitro* 11-OH-AD conversion, using bovine Adx_{4-108} (40 µM), bovine AdR (4 µM) and CYP106A1 (2 µM). (**C**) *In vivo* conversion of 11-OH-AD using the CYP106A1-overexpressing *B. megaterium* MS941 strain.

Steady state kinetic turnover in protiated and deuterated solvent systems

The CYP106A1-mediated conversion of prednisolone and dexamethasone resulted in multiple products, in contrast to 11-OH-AD, where only the 11-keto product formation was detected. Thus, the latter reaction was chosen as a suitable model for the investigation of KSIE in CYP106A1-mediated 11-oxidation. The steady state turnover of 11-OH-AD by CYP106A1 was investigated with a time-dependent reaction in the presence of saturating substrate concentration. To study the catalytic activity, an incubation time of 20 min was chosen, representing the linear phase of the reaction (**Fig. 5 A**). The turnover was carried out in a protiated buffer system, in which an individual rate of adrenosterone formation of 0.36 ± 0.04 min^{-1} was observed. Interestingly, upon H_2O substitution for D_2O, the conversion demonstrated a significantly increased catalytic rate of 0.81 ± 0.03 min^{-1}, leading to a 2.25-times faster product formation upon H/D exchange. These rates correspond to an inverse KSIE (k_H/k_D) of 0.44 (**Fig. 5 B**) suggesting that the 11-oxidation reaction is mediated through the unprotonated ferric peroxo intermediate, in contrast to traditional hydroxylation reactions, which are believed to proceed through the classical Groves

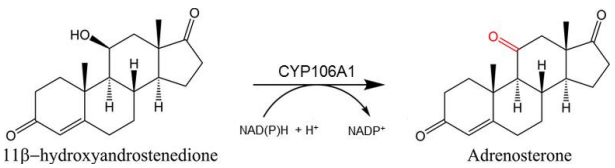

Scheme 3 – 11-oxidation of 11β-hydroxyandrostenedione catalyzed by CYP106A1.

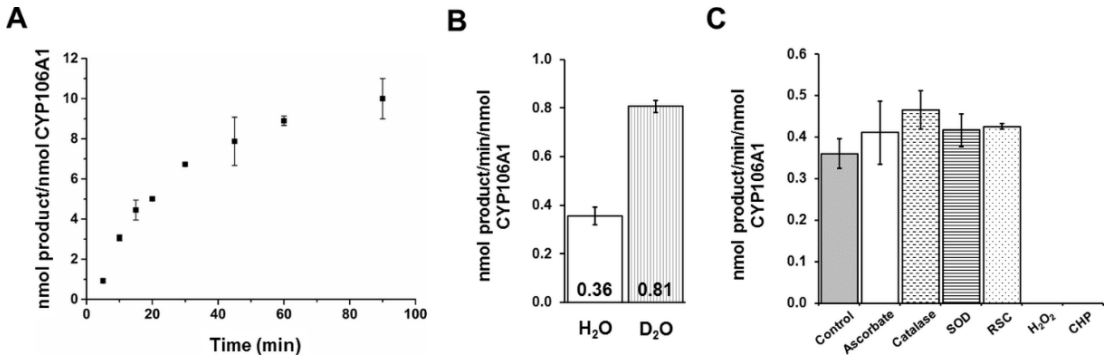

Fig. 5 - Investigation of the catalytic rate of 11-oxidation by CYP106A1. (**A**) Time dependent conversion of 11-OH-AD using CYP106A1 (2 µM) and 11-OH-AD (50 µM). (**B**) Steady-state kinetic solvent isotope effects observed for 11-oxidase CYP106A1 catalysis. The numbers inside the bars indicate the catalytic activity, while the error bars represent the standard deviation of 5 independent reactions. (**C**) The effect of radical scavengers on the catalytic rate of 11-OH-AD oxidation. The error bars represent the standard deviation of 3 independent measurements.
*SOD, superoxide-dismutase; RSC, radical scavengers in combination; CHP, cumene hydroperoxide

rebound mechanism with Cpd I as the reactive intermediate (Batabyal et al. 2013; Groves 2006; Liu and Ortiz de Montellano 2000; Vidakovic et al. 1998). The detected large inverse KSIE could be explained by the fact that inhibiting protonation of the peroxo-ferric species in deuterated solvents facilitates the productive oxidation rather than the uncoupling via proton-dependent unproductive pathways (peroxide shunt, oxidase shunt). Forming the nucleophilic peroxoanion intermediate (**Fig. 1, (5a)**) does not involve any protonation event, thus the catalytic activity would be expected to be the same in both H_2O and D_2O buffer systems. However, the slower rate of Cpd I formation in a deuterated solvent system in combination with inhibited unproductive pathways could result in the increase of the peroxoanion intermediate, along with the product formation (Gregory et al. 2013). The latter was described for tyrosine hydroxylase (Frantom and Fitzpatrick 2003) and putidamonooxin (Twilfer et al. 2000), where, as a result of the slower rate of uncoupling reactions compared with the productive pathway in D_2O, a large inverse KSIE was observed. Concerning P450 enzymes, the involvement of the ferric peroxoanion has only been observed for the CYP17-catalyzed C17-C20 lyase reaction (Gregory et al. 2013), its involvement in an oxidase reaction has not been demonstrated so far.

To exclude the role of unproductive pathways and the possible H_2O_2-mediated substrate oxidation (reverse peroxide shunt) and to support the participation of the ferric peroxo species in the CYP106A1-catalyzed 11-oxidation, the *in vitro* conversions were performed with the addition of radical scavengers and in the presence of H_2O_2 or cumene hydroperoxide. As scavenging agents ascorbate (neutralizing the superoxide radical, singlet oxygen and hydroxyl radicals), catalase (decomposing hydrogen peroxide to water and oxygen) and superoxide dismutase (SOD) (scavenger of superoxide anion) were applied, individually or in combination. No significant decrease in the catalytic rate was observed in comparison to the positive control, the 11-OH-AD conversion in protiated environment (**Fig. 5 C**). Using H_2O_2 or cumene hydroperoxide (CHP), no product formation was detected. These results suggest that the previously observed inverse KSIE is not the result of an inhibited uncoupling reaction but of the catalysis via a proton-independent intermediate. Since steroid 11-dehydrogenation by a P450 had never been investigated before, similar P450 dependent keto-product formations described in the literature have been considered for possible parallels. Interestingly, in contrast to our observations, the microsomal oxidation of cyclohex-2-en-1-ol (Bellucci et al. 1996), the CYP3A11 mediated hydroxy-Δ^8-tetrahydrocannabinol transformation (Matsunaga et al. 2001) and the CYP2E1-catalyzed ethanol oxidation (Wang et al. 2007) were all proposed to proceed through the gem-diol or the combination

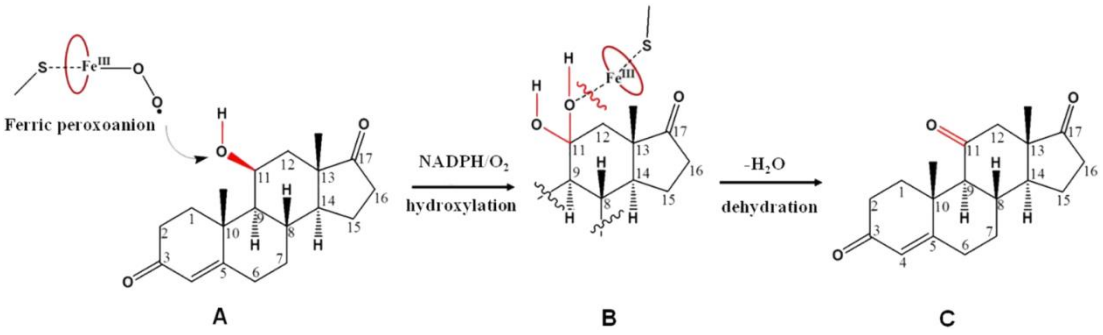

Scheme 4 - Proposed model for the 11-oxidation of 11-OH-AD by CYP106A1. The 11-oxidation proceeds throughh a nucleophilic attack at the C11 hydroxyl group of 11-OH-AD (**A**) by the ferric peroxo species. A subsequent hydroxylation step leads to the '*gem-diol*' (**B**). The '*gem-diol*' undergoes a dehydration reaction, abstracting the hydrogen and forming the 11-keto product, adrenosterone (**C**).

of gem-diol and double hydrogen abstraction pathways involving Cpd I (**Fig. 1, [6]**) as a reactive intermediate. However, the observed inverse KSIE and the absent role of proton-dependent uncoupling pathways in the CYP106A1 catalyzed 11-oxidation are not reconcilable with a proton-dependent, Cpd I-mediated mechanism. Therefore, we propose that the 11-oxidation reaction of 11-OH-AD is mediated by a nucleophilic attack of the ferric peroxoanion, as illustrated in **Scheme 4**. To provide additional evidence for the involvement of the ferric peroxo species, the spectroscopic characterization of the reactive intermediate could be a topic of further research, as reviewed elsewhere (Krest et al. 2013; Luthra et al. 2011; Sligar et al. 2005).

In conclusion, we present prednisolone, dexamethasone and 11-OH-AD as novel substrates for the 11-oxidation by CYP106A1. The enzyme performed selective 11-oxidation on 11-OH-AD, resulting in a single 11-keto product, while the conversion of prednisolone and dexamethasone displayed 6β- and 15β-hydroxylated derivatives, as well as the 11-keto steroids. Since the hydroxy metabolites can be developed into functionalized drugs with improved properties (e.g.: higher specificity, improved pharmacokinetics) (Bernhardt and Urlacher 2014), the production of such novel derivatives using CYP106A1 is considered a promising approach for the pharmaceutical industry. In addition, due to the selective conversion of 11-OH-AD, the 11-oxidation mechanism was also investigated. We observed an inverse KSIE (~0.44), suggesting that the 11-oxidation takes place without the involvement of proton uptake, proposing for the first time the ferric peroxoanion as a reactive intermediate in a P450-mediated oxidation reaction.

Author contributions

FMK carried out the experiments, analyzed and interpreted the data and drafted the manuscript. YK and RB designed the project, analyzed and interpreted the results, and assisted in drafting the manuscript. JZ performed the NMR measurements and the structure determination of the converted steroids. All authors read and approved the final manuscript.

Acknowledgements

This work was generously supported by the People Programme (Marie Curie Actions) of the European Union's 7th Framework Programme (FP7/2007-2013), P4FIFTY - FP7 PEOPLE ITN 2011-289217 and by a grant from the Federal Ministry of Education and Research (BMBF - 031A166A). The authors thank Birgit Heider-Lips for the expression and purification of AdR and Adx_{4-108} and Nicolas Souza Carmona for the language revision.

References

Aikens J, Sligar SG (1994) Kinetic Solvent Isotope Effects During Oxygen Activation by Cytochrome P-450Cam. Journal of the American Chemical Society 116(3):1143-1144

Arinbasarova AY, Karpov AV, Fokina VV, Medentsev AG, Koshcheyenko KA (1996) Kinetic Characteristics of 1-en-Dehydrogenation of 6-Alpha-Methylhydrocortisone by Cells of *Arthrobacter-Globiformis*-193. Enzyme Microb Technol 19(7):501-506

Batabyal D, Li H, Poulos TL (2013) Synergistic Effects of Mutations in Cytochrome P450cam Designed To Mimic CYP101D1. Biochemistry 52(32):5396-5402

Bellucci G, Chiappe C, Pucci L, Gervasi PG (1996) The Mechanism of Oxidation of Allylic Alcohols to α,β-Unsaturated Ketones by Cytochrome P450. Chemical Research in Toxicology 9(5):871-874

Bernhardt R (2006) Cytochromes P450 as versatile biocatalysts. J Biotechnol 124(1):128-145

Bernhardt R, Urlacher VB (2014) Cytochromes P450 as promising catalysts for biotechnological application:

chances and limitations. Applied microbiology and biotechnology 98(14):6185-6203

Blasco M, Carriquiriborde P, Marino D, Ronco AE, Somoza GM (2009) A quantitative HPLC–MS method for the simultaneous determination of testosterone, 11-ketotestosterone and 11-β hydroxyandrostenedione in fish serum. Journal of Chromatography B 877(14–15):1509-1515

Bleif S, Hannemann F, Lisurek M, Kries J, Zapp J, Dietzen M, Antes I, Bernhardt R (2011) Identification of CYP106A2 as a regioselective allylic bacterial diterpene hydroxylase. Chembiochem : a European journal of chemical biology 12(4):576-582

Bleif S, Hannemann F, Zapp J, Hartmann D, Jauch J, Bernhardt R (2012) A new *Bacillus megaterium* whole-cell catalyst for the hydroxylation of the pentacyclic triterpene 11-keto-beta-boswellic acid (KBA) based on a recombinant cytochrome P450 system. Applied microbiology and biotechnology 93(3):1135-1146

Borg B (1994) Androgens in teleost fishes. Comparative Biochemistry and Physiology Part C: Pharmacology, Toxicology and Endocrinology 109(3):219-245

Brill E, Hannemann F, Zapp J, Bruning G, Jauch J, Bernhardt R (2014) A new cytochrome P450 system from *Bacillus megaterium* DSM319 for the hydroxylation of 11-keto-beta-boswellic acid (KBA). Applied microbiology and biotechnology 98:1701-1717

Brooker L, Parr MK, Cawley A, Flenker U, Howe C, Kazlauskas R, Schänzer W, George A (2009) Development of criteria for the detection of adrenosterone administration by gas chromatography-mass spectrometry and gas chromatography-combustion-isotope ratio mass spectrometry for doping control. Drug Testing and Analysis 1(11-12):587-595

Champion PM, Gunsalus IC, Wagner GC (1978) Resonance Raman investigations of cytochrome P450CAM from *Pseudomonas putida*. Journal of the American Chemical Society 100(12):3743-3751

Denisov IG, Makris TM, Sligar SG, Schlichting I (2005) Structure and Chemistry of Cytochrome P450. Chem Rev 105(6):2253-2278

Frantom PA, Fitzpatrick PF (2003) Uncoupled Forms of Tyrosine Hydroxylase Unmask Kinetic Isotope Effects on Chemical Steps. Journal of the American Chemical Society 125(52):16190-16191

Gentile D, Tomlinson E, Maggs J, Park B, Back D (1996) Dexamethasone metabolism by human liver in vitro. Metabolite identification and inhibition of 6-hydroxylation. J Pharmacol Exp Ther 277(1):105-12

Goren T, Harnik M, Rimon S, Aharonowitz Y (1983) 1-Ene-steroid reductase of Mycobacterium sp. NRRL B-3805. J Steroid Biochem 19((6)):1789-97.

Gregory MC, Denisov IG, Grinkova YV, Khatri Y, Sligar SG (2013) Kinetic Solvent Isotope Effect in Human P450 CYP17A1-Mediated Androgen Formation: Evidence for a Reactive Peroxoanion Intermediate. Journal of the American Chemical Society 135(44):16245-16247

Groves JT (2006) High-valent iron in chemical and biological oxidations. Journal of Inorganic Biochemistry 100(4):434-447

Harris DL, Loew GH (1996) Investigation of the proton-assisted pathway to formation of the catalytically active, ferryl species of P450s by molecular dynamics studies of P450eryF. J Am Chem Soc 118(27):6377-6387

Khatri Y, Luthra A, Duggal R, Sligar SG (2014) Kinetic solvent isotope effect in steady-state turnover by CYP19A1 suggests involvement of Compound 1 for both hydroxylation and aromatization steps. FEBS Letters 588(17):3117-3122

Kiss F, Schmitz D, Zapp J, Dier TF, Volmer D, Bernhardt R (2015) Comparison of CYP106A1 and CYP106A2 from *Bacillus megaterium* – identification of a novel 11-oxidase activity. Applied microbiology and biotechnology:1-20

Krest CM, Onderko EL, Yosca TH, Calixto JC, Karp RF, Livada J, Rittle J, Green MT (2013) Reactive Intermediates in Cytochrome P450 Catalysis. Journal of Biological Chemistry 288(24):17074-17081

Lee G-Y, Kim D-H, Kim D, Ahn T, Yun C-H (2014) Functional characterization of steroid hydroxylase CYP106A1 derived from *Bacillus megaterium*. Arch Pharm Res:1-10

Liu Y, Ortiz de Montellano PR (2000) Reaction Intermediates and Single Turnover Rate Constants for the Oxidation of Heme by Human Heme Oxygenase-1. Journal of Biological Chemistry 275(8):5297-5307

Luthra A, Denisov IG, Sligar SG (2011) Spectroscopic features of cytochrome P450 reaction intermediates. Archives of Biochemistry and Biophysics 507(1):26-35

Macdonald IDG, Sligar SG, Christian JF, Unno M, Champion PM (1999) Identification of the Fe−O−O Bending Mode in Oxycytochrome P450cam by Resonance Raman Spectroscopy. Journal of the American Chemical Society 121(2):376-380

Makris TM, Davydov R, Denisov IG, Hoffman BM, Sligar SG (2002) Mechanistic Enzymology of Oxygen Activation by the Cytochromes P450 Drug Metabolism Reviews 34(4):691-708

Matsunaga T, Tanaka H, Higuchi S, Shibayama K, Kishi N, Watanabe K, Yamamoto I (2001) Oxidation Mechanism of 7-Hydroxy-Δ8-tetrahydrocannabinol and 8-Hydroxy-Δ9-tetrahydrocannabinol to the Corresponding Ketones by CYP3A11. Drug Metabolism and Disposition 29(11):1485-1491

Minagawa K, Kasuya Y, Baba S, Knapp G, Skelly J (1986) Identification and quantification of 6 beta-hydroxydexamethasone as a major urinary metabolite of dexamethasone in man. Steroids 47(2-3):175-88

Purdy MM, Koo LS, Ortiz de Montellano PR, Klinman JP (2006) Mechanism of O2 Activation by Cytochrome P450cam Studied by Isotope Effects and Transient State Kinetics. Biochemistry 45(51):15793-15806

Raag R, Martinis SA, Sligar SG, Poulos TL (1991) Crystal structure of the cytochrome P-450CAM active site mutant Thr252Ala. Biochemistry 30(48):11420-11429

Raag R, Poulos TL (1989) The structural basis for substrate-induced changes in redox potential and spin equilibrium in cytochrome P-450CAM. Biochemistry 28(2):917-922

Rebuffat AG, Tam S, Nawrocki AR, Baker ME, Frey BM, Frey FJ, Odermatt A (2004) The 11-ketosteroid 11-ketodexamethasone is a glucocorticoid receptor agonist. Molecular and cellular endocrinology 214(1–2):27-37

Rittle J, Green MT (2010) Cytochrome P450 Compound I: Capture, Characterization, and C-H Bond Activation Kinetics. Science 330(6006):933-937

Sagara Y, Wada A, Takata Y, Waterman M, Sekimizu K, Horiuchi T (1993) Direct expression of adrenodoxin reductase in Escherichia coli and the functional characterization. Biol Pharm Bull 16:627-630

Schmitz D, Zapp J, Bernhardt R (2014) Steroid conversion with CYP106A2 - production of pharmaceutically interesting DHEA metabolites. Microbial Cell Factories 13:81

Schowen R (1977) Solvent isotope effects on enzymic reactions. In: Cleland WW, O'Leary MH, Northrop DB (eds) Isotope Effects on Enzyme-Catalyzed Reactions. University Park Press, Baltimore, pp 64-99

Sligar SG (1976) Coupling of spin, substrate, and redox equilibriums in cytochrome P450. Biochemistry 15(24):5399-5406

Sligar SG, Makris TM, Denisov IG (2005) Thirty years of microbial P450 monooxygenase research: Peroxo-heme intermediates - The central bus station in heme oxygenase catalysis. Biochemical and biophysical research communications 338(1):346-354

Suhara K, Takeda K, Katagiri M (1986) P-45011β-dependent conversion of cortisol to cortisone, and 19-hydroxyandrostenedione to 19-oxoandrostenedione. Biochemical and biophysical research communications 136(1):369-375

Tomlinson ES, Lewis DFV, Maggs JL, Kroemer HK, Park BK, Back DJ (1997) In vitro metabolism of dexamethasone (DEX) in human liver and kidney: The involvement of CYP3a4 and CYP17 (17,20 LYASE) and molecular modelling studies. Biochemical Pharmacology 54(5):605-611

Tsai R, Yu CA, Gunsalus IC, Peisach J, Blumberg W, Orme-Johnson WH, Beinert H (1970) Spin-state changes in cytochrome P-450(cam) on binding of specific substrates. Proceedings of the National Academy of Sciences of the United States of America 66(4):1157-1163

Twilfer H, Sandfort G, Bernhardt F-H (2000) Substrate and solvent isotope effects on the fate of the active oxygen species in substrate-modulated reactions of putidamonooxin. European Journal of Biochemistry 267(19):5926-5934

Uhlmann H, Beckert V, Schwarz D, Bernhardt R (1992) Expression of bovine adrenodoxin in E. coli and site-directed mutagenesis of/2 Fe-2S/cluster ligands. Biochemical and biophysical research communications 188:1131-1138

van der Geize R, Hessels GI, van Gerwen R, Vrijbloed JW, van der Meijden P, Dijkhuizen L (2000) Targeted Disruption of the kstD Gene Encoding a 3-Ketosteroid Δ1-Dehydrogenase Isoenzyme ofRhodococcus erythropolis Strain SQ1. Applied and Environmental Microbiology 66(5):2029-2036

Vidakovic M, Sligar SG, Li H, Poulos TL (1998) Understanding the Role of the Essential Asp251 in Cytochrome P450cam Using Site-Directed Mutagenesis, Crystallography, and Kinetic Solvent Isotope Effect. Biochemistry 37(26):9211-9219

Wang Y, Yang C, Wang H, Han K, Shaik S (2007) A New Mechanism for Ethanol Oxidation Mediated by Cytochrome P450 2E1: Bulk Polarity of the Active Site Makes a Difference. Chembiochem : a European journal of chemical biology 8(3):277-281

Xiang H, Tschirret-Guth RA, Ortiz de Montellano PR (2000) An A245T Mutation Conveys on Cytochrome P450eryF the Ability to Oxidize Alternative Substrates. Journal of Biological Chemistry 275(46):35999-36006

Zehentgruber D, Hannemann F, Bleif S, Bernhardt R, Lütz S (2010) Towards preparative scale steroid hydroxylation with cytochrome P450 monooxygenase CYP106A2. Chembiochem : a European journal of chemical biology 11:713-721

FEBS letters

Supplementary material

Identification of new substrates for the CYP106A1-mediated 11-oxidation and investigation of the reaction mechanism

Flora Marta Kiss[1], Yogan Khatri[1], Josef Zapp[2], Rita Bernhardt[1*]

[1]Institute of Biochemistry, Saarland University, D-66123 Saarbruecken, Germany

[2]Institute of Pharmaceutical Biology, Saarland University, D-66123 Saarbruecken, German

*Address correspondence to: Professor Dr. Rita Bernhardt
Institute of Biochemistry, Saarland University, Campus B 2.2, D-66123 Saarbruecken, Germany
Tel: +49 681 302 305
Fax: +49 681 302 4739
Email: ritabern@mx.uni-sarland.de

NMR data of the identified products of:

Prednisolone:

- **15β-Hydroxyprednisolone**

Its NMR data matched perfectly with those of an authentic sample (Schmitz *et al.*, in preparation). ^{1}H NMR (CD_3OD, 500 MHz): δ 1.06 (m, H-9), 1.11 (s, 3xH-18), 1.16 (m, H-7a), 1.52 (s, 3xH-19), 1.57 (dd, 13.8 and 3.3 Hz, H-12a), 1.61 (dd, 11.2 and 6.0 Hz, H-14), 1.98 (dd, 15.5 and 7.5 Hz, H-16a), 1.99 (m, H-12b), 2.39 (m, H-6a), 2.44 (m, H-7b), 2.52 (m, H-8), 2.68 (tdd, 13.5, 5.0 and 2.0 Hz, H-6b), 2.73 (dd, 15.5 and 2.3 Hz, H-16b), 4.24 (d, 19.2 Hz, H-21a), 4.31 (ddd, 7.5, 6.0 and 2.3 Hz, H-15), 4.39 (q, 3.3 Hz, H-11), 4.62 (d, 19.2 Hz, H-21b), 6.01 (t, 2.0 Hz, H-4), 6.22 (dd, 10.0 and 2.0 Hz, H-2), 7.48 (d, 10.0 Hz, H-1).

- **15β-Hydroxyprednisone**

The NMR spectra of this prednisolone product revealed a carbonyl, instead of an alcohol function at C-11 (δ_C 208.01). A further hydroxyl group at position 15β could be deduced from the results of the 2D NMR measurements. ^{1}H NMR ($CDCl_3$, 500 MHz): δ 0.97 (s, 3xH-18), 1.35 (m, H-7a), 1.48 (s, 3xH-19), 1.74 (m, H-8), 2.04 (m, H-9), 2.09 (d, 11.7 Hz, H-12a), 2.29 (dd, 11.6 and 6.0 Hz, H-14), 2.35 (dd, 15.5 and 7.5 Hz, H-16a), 2.39 (m, H-7b), 2.40 (m, H-6a), 2.58 (tdd, 13.5, 5.0 and 1.7 Hz, H-6b), 2.75 (dd, 15.5 and 2.3 Hz, H-16b), 2.80 (d, 11.7 Hz, H-12b), 4.29 (d, 20.0 Hz, H-21a), 4.56 (ddd, 7.5, 6.0 and 2.3 Hz, H-15), 4.66 (d, 20.0 Hz, H-21b), 6.15 (t, 2.0 Hz, H-4), 6.22 (dd, 12.0 and 2.0 Hz, H-2), 7.68 (d, 10.2 Hz, H-1). ^{13}C NMR ($CDCl_3$, 125 MHz): δ 18.40 (CH_3, C-18), 18.83 (CH_3, C-19), 24.73 (CH, C-8), 32.15 (CH_2, C-6), 32.80 (CH_2, C-7), 42.41 (C, C-10), 47.07 (CH, C-16), 50.05 (CH_2, C-12), 51.35 (C, C-13), 53.33 (CH, C-14), 60.90 (CH, C-9), 67.44 (CH_2, C-21), 69.10 (CH, C-15), 87.36 (C, C-17), 124.74 (CH, C-4), 127.75 (CH, C-2), 154.98 (CH, C-1), 166.19 (C, C-5), 186.29 (C, C-3), 208.01 (C, C-11), 210.94 (C, C-20).

- **1,2-Dihydro-15β-hydroxyprednisone**

Its ^{1}H NMR spectrum showed some remarkable differences to that of the substrate, prednisolone. The resonances for the double bond between C-1 and C-2, as well as for the hydroxyl group at C-11 were absent. Signals of four additional methylene protons appeared in the spectrum and the doublet resonances of H-12a and H-12b showed an α-carbonyl induced downfield shift. These observations led to the structure of 1,2-dihydro-15β-hydroxyprednisone. ^{1}H NMR (CD_3OD, 500 MHz): δ 0.84 (s, 3xH-18), 1.34 (m, H-7a), 1.47 (s, 3xH-19), 1.70 (m, H-1a), 1.99 (d, 12.0 Hz, H-12a), 2.15 (m, H-9), 2.21 (dd, 15.5 and 7.5 Hz, H-16a), 2.24 (m, H-2a), 2.31 (m, H-7b), 2.33 (m, 2H, H-8 and H-14), 2.52 (m, H-2b), 2.55 (m, 2H, H-6a and H-6b), 2.72 (m, H-1b), 2.75 (dd, 15.5 and 2.3 Hz, H-16b), 2.96 (d, 12.0 Hz, H-12b), 4.20 (d, 19.5 Hz, H-21a), 4.42 (ddd, 7.5, 5.7 and 2.2 Hz, H-15), 4.60 (d, 19.5 Hz, H-21b), 5.72 (br s, H-4).

Dexamethasone:

- **15β-Hydroxydexamethasone**

Compared to the substrate, dexamethasone, the NMR data of the conversion product showed resonances for an additional hydroxyl group (δ_C 78.60; δ_H 3.67 dd). Its position at C-15 could be deduced by vicinal couplings of the methine proton with H-14 (δ_H 2.08 dd, 12.0 and 6.3 Hz,) and H-16 (δ_H 3.02 qd, 7.5 and 3.0 Hz). The β orientation of the hydroxyl was confirmed by the NOESY effects of H-15 to H-16 and H-14, all in a-position. ^{1}H NMR (CD_3OD, 500 MHz): δ 0.93 (d, 7.5 Hz, 3H, Me-16), 1.17 (s, 3xH-18), 1.43 (dd, 13.7 and 2.5 Hz, H-12a), 1.57 (m, H-7a), 1.60 (s, 3xH-19), 2.08 (dd, 12.0 and 6.3 Hz, H-14), 2.20 (m, H-7b), 2.29 (m, H-12b), 2.40 (tdd, 14.0, 5.0 and 2.0 Hz, H-6a), 2.73 (m, H-6b), 2.80 (dtd, 29.5, 12.0 and 4.5 Hz, H-8), 3.02 (qd, 7.5 and 3.0 Hz, H-16), 3.67 (dd, 6.3 and 3.0 Hz, H-15), 4.22 (d, 19.2 Hz, H-21a), 4.25 (m, H-11), 4.60 (d, 19.2 Hz, H-21b), 6.09 (t, 2.0 Hz, H-4), 6.28 (dd, 10.0 and 2.0 Hz, H-2), 7.41 (d, 10.0 Hz, H-1). ^{13}C NMR (CD_3OD, 125 MHz): δ 13.12 (CH_3, Me-16), 20.21 (CH_3, C-18), 23.67 (d, J_{CF}=6.0 Hz, CH_3, C-19), 27.66 (CH_2, C-7), 32.15 (CH_2, C-6), 32.27 (d, J_{CF}=19.3 Hz, CH, C-8), 38.12 (CH_2, C-12), 48.92 (C, C-13), 48.95 (CH, C-14), 49.47 (CH, C-16), 50.41 (d, J_{CF}=22.5 Hz, C, C-10), 67.89 (CH_2, C-21), 72.83 (d, J_{CF}=37.5 Hz, CH, C-11), 78.60 (CH, C-15), 92.01 (C, C-17), 103.02 (d, J_{CF}=176.0 Hz, C, C-9), 125.09 (CH, C-4), 129.81 (CH, C-2), 155.96 (CH, C-1), 171.16 (C, C-5), 189.07 (C, C-3), 211.95 (C, C-20).

- **6β-Hydroxydexamethasone**

Selected ^{1}H NMR data of this compound were published by Matsuzaki *et al.* [1]. Our ^{1}H NMR results matched these data. 2D NMR measurements led to the full assignments of the ^{1}H and ^{13}C NMR

spectra. ^{1}H NMR (CD_3OD, 500 MHz): δ 0.89 (d, 7.5 Hz, 3H, Me-16), 1.04 (s, 3xH-18), 1.22 (ddd, 12.0, 8.0 and 4.0 Hz, H-15d), 1.48 (dd, 13.8 and 2.0 Hz, H-12a), 1.76 (m, H-7a), 1.77 (s, 3xH-19), 1.78 (m, H-15b), 1.92 (ddd, 14.5, 4.5 and 2.3 Hz, H-7b), 2.23 (dd, 12.0 and 8.0, H-14), 2.30 (dt, 13.8 and 3.3 Hz, H-12b), 2.69 (dtd, 29.5, 12.0 and 4.5 Hz, H-8), 3.09 (dqd, 11.3, 7.5 and 4.0 Hz, H-16), 4.25 (d, 19.2 Hz, H-21a), 4.29 (m, H-11), 4.44 (dd, 3.8 and 2.2 Hz, H-6), 4.59 (d, 19.2 Hz, H-21b), 6.16 (t, 2.0 Hz, H-4), 6.26 (dd, 10.0 and 2.0 Hz, H-2), 7.37 (d, 10.0 Hz, H-1). ^{13}C NMR (CD_3OD, 125 MHz): δ 15.34 (CH_3, Me-16), 17.44 (CH_3, C-18), 25.12 (d, J_{CF}=5.5 Hz, CH_3, C-19), 31.86 (d, J_{CF}=20.0 Hz, CH, C-8), 33.54 (CH_2, C-15), 36.01 (CH_2, C-7), 37.05 (CH, C-16), 37.62 (CH_2, C-12), 45.07 (CH, C-14), 49.46 (C, C-13), 50.33 (d, J_{CF}=22.7 Hz, C, C-10), 68.08 (CH_2, C-21), 72.80 (d, J_{CF}=38.3 Hz, CH, C-11), 73.07 (CH, C-6), 92.09 (C, C-17), 102.42 (d, J_{CF}=172.5 Hz, C, C-9), 127.39 (CH, C-4), 128.95 (CH, C-2), 157.27 (CH, C-1), 167.85 (C, C-5), 189.38 (C, C-3), 212.69 (C, C-20).

- **11-Ketodexamethasone**

Due to the low amount of obtained product, only ^{1}H NMR and HHCOSY could have been measured for this sample. These revealed a C11-keto function as the only structural difference from the substrate. ^{1}H NMR (CD_3OD, 500 MHz): δ 0.74 (s, 3xH-18), 0.91 (d, 7.5 Hz, 3H, Me-16), 1.30 (m, H-15a), 1.55 (s, 3xH-19), 1.61 (m, H-7a), 1.78 (q, 12.0 Hz, H-15b), 1.89 (m, H-7b), 2.08 (dd, 11.7 and 1.5 Hz, H-12a), 2.73 (m, H-14), 3.09 (m, H-16), 2.45 (m, 2H, H-6a and H-8), 2.70 (m, H-6b), 3.35 (dd, 11.7 and 6.5 Hz, H-12b), 4.22 (d, 19.5 Hz, H-21a), 4.55 (d, 19.5 Hz, H-21b), 6.15 (t, 2.0 Hz, H-4), 6.23 (dd, 10.3 and 2.0 Hz, H-2), 7.50 (d, 10.3 Hz, H-1).

- **15β-Hydroxy-11-ketodexamethasone**

In contrast to dexamethasone, the NMR data of this conversion product missed resonances for the hydroxyl group at C-11. However, a supplemental carbonyl resonance appeared as a doublet at δ_C 206.81 exhibiting a J_{CF} = 27.5 Hz coupling with the fluorine atom at C-9. In addition, a hydroxyl group at 15β-position could be deduced from the comparison of its NMR data with those of 15β-hydroxydexamethasone and by means of 2D NMR. ^{1}H NMR (CD_3OD, 500 MHz): δ 0.91 (s, 3xH-18), 0.98 (d, 7.5 Hz, 3H, Me-16), 1.58 (s, 3xH-19), 1.66 (m, H-7a), 2.04 (dd, 11.7 and 1.5 Hz, H-12a), 2.22 (m, H-7b), 2.47 (ddd, 14.2, 4.5 and 2.3 Hz, H-6a), 2.63 (m, H-14), 2.67 (m, H-8), 2.72 (m, H-6b), 3.03 (qd, 7.5 and 3.0 Hz, H-16), 3.37 (dd, 11.7 and 6.5 Hz, H-12b), 3.74 (dd, 6.3 and 3.0 Hz, H-15), 4.21 (d, 19.2 Hz, H-21a), 4.57 (d, 19.2 Hz, H-21b), 6.16 (t, 2.0 Hz, H-4), 6.24 (dd, 10.3 and 2.0 Hz, H-2), 7.52 (d, 10.3 Hz, H-1). ^{13}C NMR (CD_3OD, 125 MHz): δ 13.08 (CH_3, Me-16), 18.30 (CH_3, C-18), 22.07 (d, J_{CF}=5.5 Hz, CH_3, C-19), 26.90 (CH_2, C-7), 32.38 (CH_2, C-6), 36.73 (d, J_{CF}=21.0 Hz, CH, C-8), 48.34 (CH, C-14), 48.69 (CH_2, C-12), 49.27 (d, J_{CF}=23.0 Hz, C, C-10), 51.27 (CH, C-16), 52.52 (C, C-13), 68.16 (CH_2, C-21), 77.07 (CH, C-15), 91.04 (C, C-17), 101.59 (d, J_{CF}=186.5 Hz, C, C-9), 126.62 (CH, C-4), 129.89 (CH, C-2), 154.63 (CH, C-1), 167.88 (C, C-5), 188.42 (C, C-3), 206.81 (d, J_{CF}=27.5 Hz, C, C-11), 211.70 (C, C-20).

11β-hydroxyandrostenedione:

- **Adrenosterone (Androst-4-ene-3,11,17-trione)**

Its ^{13}C NMR data matched those in literature [2, 3]. ^{1}H NMR ($CDCl_3$, 500 MHz): δ 0.88 (s, 3xH-18), 1.31 (m, H-7a), 1.49 (s, 3xH-19), 1.65 (m, H-1a), 1.70 (td, 12.5 and 9.3 Hz, H-15a), 1.90 (ddd, 12.5, 11.0 and 6.0 Hz, H-14), 1.92 (d, 11.0 Hz, H-9), 2.07 (m, H-8), 2.11 (m, H-7b), 2.14 (m, H-15b), 2.28 (dt, 19.5 and 9.2 Hz, H-16a), 2.32 (m, H-2a), 2.33 (m, H-12a), 2.35 (m, H-6a), 2.46 (m, H-6b), 2.47 (m, H-2b), 2.50 (d, 13.0 Hz, H-12b), 2.58 (ddd, 19.5, 9.2 and 1.3 Hz, H-16b), 2.77 (ddd, 13.5, 5.0 and 3.2 Hz, H-1b), 5.75 (s, H-4). ^{13}C NMR ($CDCl_3$, 125 MHz): δ 14.65 (CH_3, C-18), 17.30 (CH_3, C-19), 21.56 (CH_2, C-15), 30.92 (CH_2, C-7), 31.97 (CH_2, C-6), 33.68 (CH_2, C-2), 34.71 (CH_2, C-1), 35.93 (CH_2, C-16), 36.80 (CH, C-8), 38.30 (C, C-10), 49.83 (CH, C-14), 50.36 (C, C-13), 50.40 (CH_2, C-12), 63.34 (CH, C-9), 124.82 (CH, C-4), 167.80 (C, C-5), 199.50 (C, C-3), 207.49 (C, C-11), 216.77 (C, C-17).

References

1. Matsuzaki, K., Miyazaki, T. & Yasuda, K. (1991) Formation of 6 beta-hydroxydexamethasone from dexamethasone by A6 cells, *Endocrinol Jpn.* **38**, 131-135.

2. Al-Sanea, M. M., Abdel-Hafez, A. A., Omar, F. A. & Youssef, A. F. (2008) Biotransformation studies of prednisone using human intestinal bacteria Part I: Aerobic incubation *Bull Pharm Sci* **31**, 215-228.

3. Hanson, J. R. & Siverns, M. (1975) 13C nuclear magnetic resonance spectra of some steroidal unsaturated ketones, *J Chem Soc Perkin 1* 1956-1958.

2.3. Kiss *et al.* (2015)

Process development for the production of 15β-hydroxycyproterone acetate using *Bacillus megaterium* expressing CYP106A2 as whole-cell biocatalyst

Flora Marta Kiss, Marie T. Lundemo, Josef Zapp, John M. Woodley, Rita Bernhardt

Microbial Cell Factories 2015 Mar doi: 10.1186/s12934-015-0210-z

Process development for the production of 15β-hydroxycyproterone acetate using *Bacillus megaterium* expressing CYP106A2 as whole-cell biocatalyst

Flora M Kiss[1,†], Marie T Lundemo[3,†], Josef Zapp[2], John M Woodley[3], Rita Bernhardt[1*]

Abstract

Background: CYP106A2 from *Bacillus megaterium* ATCC 13368 was first identified as a regio- and stereoselective 15β-hydroxylase of 3-oxo-Δ^4-steroids. Recently, it was shown that besides 3-oxo-Δ^4-steroids, 3-hydroxy-Δ^5-steroids as well as di- and triterpenes can also serve as substrates for this biocatalyst. It is highly selective towards the 15β position, but the 6β, 7α/β, 9α, 11α and 15α positions have also been described as targets for hydroxylation. Based on the broad substrate spectrum and hydroxylating capacity, it is an excellent candidate for the production of human drug metabolites and drug precursors.

Results: In this work, we demonstrate the conversion of a synthetic testosterone derivative, cyproterone acetate, by CYP106A2 under *in vitro* and *in vivo* conditions. Using a *Bacillus megaterium* whole-cell system overexpressing CYP106A2, sufficient amounts of product for structure elucidation by nuclear magnetic resonance spectroscopy were obtained. The product was characterized as 15β-hydroxycyproterone acetate, the main human metabolite. Since the product is of pharmaceutical interest, our aim was to intensify the process by increasing the substrate concentration and to scale-up the reaction from shake flasks to bioreactors to demonstrate an efficient, yet green and cost-effective production. Using a bench-top bioreactor and the recombinant *Bacillus megaterium* system, both a fermentation and a transformation process were successfully implemented. To improve the yield and product titers for future industrial application, the main bottlenecks of the reaction were addressed. Using 2-hydroxypropyl-β-cyclodextrin, an effective bioconversion of 98 % was achieved using 1 mM substrate concentration, corresponding to a product formation of 0.43 g/L, at a 400 mL scale.

Conclusions: Here we describe the successful scale-up of cyproterone acetate conversion from shake flasks to bioreactors, using the CYP106A2 enzyme in a whole-cell system. The substrate was converted to its main human metabolite, 15β-hydroxycyproterone acetate, a highly interesting drug candidate, due to its retained antiandrogen activity but significantly lower progestogen properties than the mother compound. Optimization of the process led to an improvement from 55 % to 98 % overall conversion, with a product formation of 0.43 g/L, approaching industrial process requirements and a future large-scale application.

Keywords: Cytochrome P450, CYP106A2, *Bacillus megaterium*, Whole-cell biocatalyst, Steroid hydroxylase, Cyproterone acetate, Bioreactor, Cyclodextrin

[1] Institute of Biochemistry, Saarland University, Campus B 2.2, 66123 Saarbruecken, Germany

[2] Institute of Pharmaceutical Biology, Saarland University, Campus B 2.2, 66123 Saarbruecken, Germany

[3] CAPEC-PROCESS, Department of Chemical and Biochemical Engineering, Technical University of Denmark, DK-2800 Lyngby, Denmark

[†] Equal contributors.

[*] Corresponding author
Email: ritabern@mx.uni-sarland.de

Background

Cytochrome P450 monooxygenases (P450s) are hemeproteins that catalyze the oxidation of a wide variety of substrates, from endogenous compounds, such as steroids, vitamins and fatty acids, to xenobiotics and drugs. They have attracted interest in research due to their unique ability to activate molecular oxygen, introducing one atom into the substrate and reducing the second one to water [1]. The fact that they are able to introduce an oxygen atom into non-activated hydrocarbons without extreme conditions, in combination with their high regio- and stereoselectivity on complex molecules, makes their application particularly interesting to the pharmaceutical industry. P450s represent a suitable alternative over chemical synthesis, especially in the hydroxylation of steroidal pharmaceuticals, where the chemical methods are either time- and labor-intensive, expensive and complex or non-existent [2]. Steroid-based drugs are one of the largest groups of marketed pharmaceuticals [3]. There are about 300 approved steroid drugs to date and their number is constantly growing due to the production of diversely functionalized steroid cores, resulting in often altered therapeutic activity [4]. Thus, steroid-hydroxylating P450s could provide an alternative for the production of drug precursors and human drug metabolites.

The bacterial P450, CYP106A2 from *Bacillus megaterium* (*B. megaterium*) ATCC 13368, is one of the few cloned bacterial steroid hydroxylases that has been studied in detail and was announced to be a suitable biocatalyst for the production of hydroxysteroids [5]. CYP106A2, also known as 15β-hydroxylase, converts mainly 3-oxo-Δ^4-steroids [6-8] although recent studies have shown that it can perform di- and triterpenoid hydroxylation [9-11] and the conversion of 3-hydroxy-Δ^5-steroids [12]. Moreover, as a result of on-going screening of a natural substrate library, the substrate range of this enzyme is constantly extended. However, the native substrate of CYP106A2, and thus its biological function, is still unknown. Its natural electron transfer protein is also unknown, yet the activity was successfully demonstrated using megaredoxin and megaredoxin reductase [7] and it is also supported by the bovine adrenal redox partners as well as by putidaredoxin and putidaredoxin reductase [5,13,14].

In the past two decades CYP106A2 was profoundly investigated as a biocatalyst, applying the enzyme in whole-cell systems, efficiently using both *Escherichia coli* (*E. coli*) [5,13] and *B. megaterium* as expression hosts [9-12]. Whole-cell systems, in which the P450 is expressed by a microbial host, have the advantage of stabilizing the enzyme under process conditions and providing cofactor regeneration through cellular metabolism, avoiding the need for the expensive NADPH supply.

Since the transport of hydrophobic substances across the outer membrane of *E. coli* was found to be limiting [5], the attention was shifted to the gram-positive *B. megaterium* as host. This spore-forming, mainly aerobic bacterium became a long-term participant of the biotechnological industry, due to the fact that even the wild-type strains are capable of producing high titers of proteins of industrial interest [15,16]. Further attractive characteristics include the ability to grow on a variety of carbon sources, the GRAS status, high plasmid stability and the lack of endotoxin and extracellular protease production. These characteristics make this organism highly favored for industrial practice [17].

The endogenous CYP106A2 system in *B. megaterium* ATCC 13368 was used for *in vivo* transformation of the diterpene abietic acid producing 12β-hydroxyabietic acid and 12α- hydroxyabietic acid [10]. As a next step, the CYP106A2 gene was overexpressed in combination with bovine adrenal redox partners in *B. megaterium* MS941 for the hydroxylation of 11-keto-β-boswellic acid in the 15α position [9]. Another triterpenoid, dipterocarpol, was also hydroxylated by CYP106A2 in *B. megaterium* ATCC 13368 resulting in six products at a 1 L scale [11]. Recently reported, the regioselective hydroxylation of the 3-hydroxy-Δ^5 steroid dehydroepiandrosterone (DHEA) was achieved by CYP106A2 expressed in the natural host

B. megaterium ATCC 13368 and the recombinant *B. megaterium* MS941 [12].

In the present work, the conversion of a synthetic testosterone derivative, cyproterone acetate (CPA, 6-Chloro-1β,2β-dihydro-17-hydroxy-3'H-cyclopropa(1,2)-pregna-1,4,6-triene-3,20-dione acetate), was performed using a recombinant *B. megaterium* MS941 system overexpressing the CYP106A2 enzyme. The synthetic antiandrogen, CPA, was converted to 15β-hydroxy cyproterone acetate (15β-OH-CPA, 15β-hydroxy-6-Chloro-1β,2β-dihydro-17-hydroxy-3′H-cyclopropa(1,2)-pregna-1,4,6-triene-3,20-dione acetate) (Scheme 1). CPA is a synthetic derivative of 17α-hydroxyprogesterone, an anti-androgenic compound with additional progestogen and antigonadotropic properties [18,19]. It has antagonistic properties towards the androgen receptor, although it can also act as its partial agonist. It is generally used as a treatment for metastatic prostate cancer and for the control of libido in severe hypersexuality and/or sexual deviation in males, but it is also applied for the treatment of hirsutism and acne in female patients and in oral contraceptive pills. The main human metabolite of CPA in both plasma and urine is the 15β-OH-CPA. It shows only 10 % of the progestogenic potency of CPA but retains the anti-androgen activity [19]. These characteristics imply that the metabolite is potentially a better option for the treatment of androgen-induced problems, particularly in male patients.In 1982, the *B. megaterium* ATCC 13368 strain was already proposed for the bioconversion of 1α,2α-methylene steroids into their 15β-hydroxy derivatives, in order to produce new anti-androgenic steroids with minor progestogen activity [20]. According to our latest information, 1 mg 15β-hydroxy metabolite costs 300 $, while 250 mg of the original compound costs 199 $ (Santa Cruz Biotechnology, http://www.scbt.com/, 2014). Although we lack detailed information about the production, the price difference suggests an expensive procedure.

In the present work we perform process development of the CPA bioconversion in shake flasks and lab-scale bioreactors, thus providing an improved model for a greener yet cost-effective large-scale production of the 15β-hydroxy metabolite. The reaction was successfully carried out at 400 mL scale, although to further improve the conversion rate the bottlenecks of the system were identified. Working with P450s applied in whole-cell systems, the following difficulties have already been recognized [1,21]:

- NADP(H) depletion
- low substrate and product solubility
- problematic uptake of the substrate and efflux of the product
- substrate or product inhibition/toxicity.

To find the bottleneck of our system, we addressed each point separately. The cofactor limitation was investigated by adding NADPH in excess. Issues with solubility, toxicity or inhibition, related to substrate or product were investigated. Subsequently, substrate feeding strategies were evaluated in an attempt to overcome these effects. Moreover, the proposed transport restriction was addressed by using different membrane permeabilization methods (freeze-thawing, ultrasonication, acetone treatment). 2-hydroxypropyl-β-cyclodextrin (HP-β-CD) was also applied to improve the process performance since it was previously

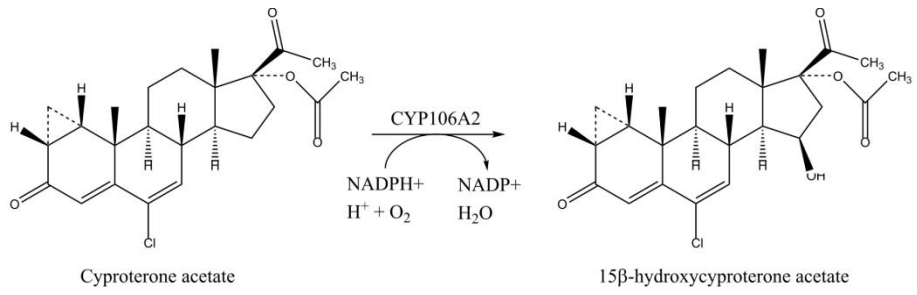

Scheme 1 Cyproterone acetate conversion to its main human metabolite 15β-hydroxycyproterone acetate by CYP106A2.

described to be successful as a solubilizing agent and was used for improved substrate transport across the cell membrane. By identifying the limitations of the system, the aim was to be able to improve the economic performance of the process by increasing the reaction yield at higher substrate concentrations.

Results

Purification and spectral characterization of CYP106A2

The CYP106A2 protein was expressed and purified using a recombinant *E. coli* C43 (DE3) strain. The UV–vis absorbance spectra recorded from 250 to 700 nm showed the characteristic absorbance peaks at 356, 417, 534 and 567 nm in the oxidized form. In the case of the reduced and carbon monoxide-bound form, the peak at 450 nm was observed, with no peak indicating inactive P450 at 420 nm.

In vitro conversion, reaction kinetics and inhibition studies

Using difference spectroscopy, the binding of CPA to CYP106A2's active site was studied *in vitro*. CPA did not induce any spectral shift, indicating that the steroid does not contribute to the replacement of the axial water molecule, hindering the determination of the dissociation constant. The catalytic activity of CYP106A2 towards CPA was first tested *in vitro*. The activity was reconstituted using bovine adrenal redox partners ($Adx_{4–108}$ and AdR) proven to be highly efficient electron suppliers for CYP106A2 [14,22]. The CYP106A2-dependent conversion of CPA was analyzed by high-performance liquid chromatography (HPLC) and resulted in one main product. Using 0.5 μM CYP106A2 and 400 μM substrate, the conversion reached 48.2 ± 2.8 % in 60 minutes (Figure 1).

The *in vitro* conversions were also performed with increasing substrate concentrations (50 μM-1.2 mM) to study the potential inhibitory effect of the substrate. Using 200 μM or higher substrate concentrations, the product concentration never exceeded 200 μM. These results suggest that the enzyme is inhibited above a certain product concentration, regardless of the amount of substrate, since the reaction stops after 150 to 200 μM product was formed (Figure 2).

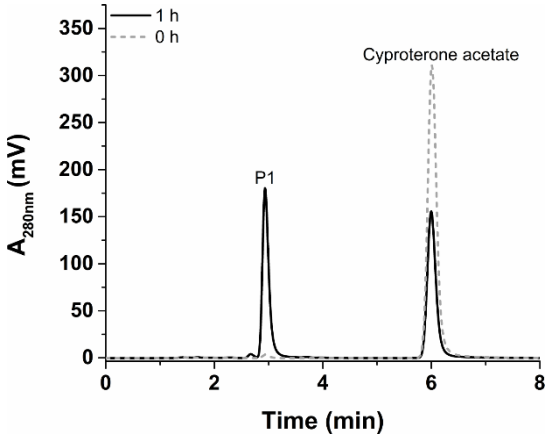

Figure 1 HPLC chromatogram of the in vitro conversion of cyproterone acetate by CYP106A2. The reaction was performed in 50 mM potassium phosphate buffer containing 20 % glycerol (pH 7.4) at 30 °C, using 0.5 μM CYP106A2, 10 μM $Adx_{4–108}$ and 1 μM AdR. The reaction was stopped and extracted twice by ethyl acetate directly after the addition of the substrate (grey dotted line, 0 h) and after 1 h (black line, 1 h). Cyproterone acetate (400 μM) was converted to one main product (P1).

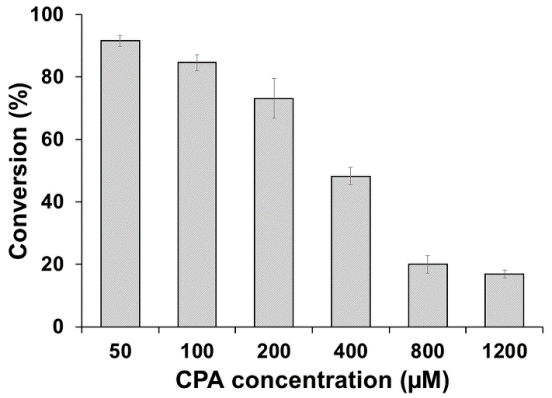

Figure 2 In vitro conversion of cyproterone acetate using increasing substrate concentrations. The reaction was performed using substrate concentrations, in a range of 50 μM to 1.2 mM for 60 min. Each bar represents the mean value of three independent measurements, with the corresponding standard deviation indicated by the error bars.

As a next step, the Michaelis-Menten parameters for the CYP106A2-dependent CPA conversion were determined. The catalytic activity of the CPA conversion showed a V_{max} of 61.65 ± 2.56 nmol product per nmol CYP106A2 per minute and a K_m of 103.14 ± 11.99 μM (Figure 3).

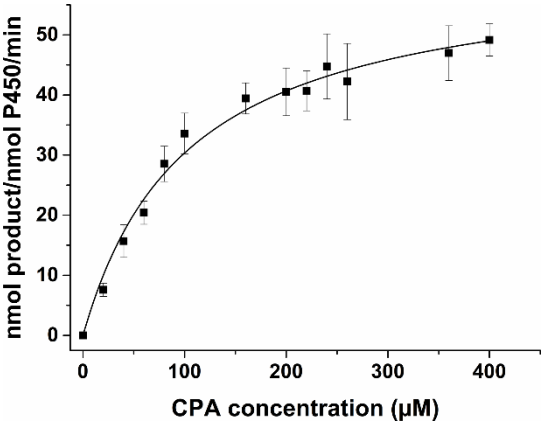

Figure 3 Determination of the kinetic parameters for the cyproterone acetate conversion catalyzed by CYP106A2. The reaction kinetics were performed in 50 mM potassium phosphate buffer containing 20 % glycerol (pH 7.4) at 30 °C for 2 min using 0.5 µM CYP106A2, 10 µM $Adx_{4–108}$ and 1 µM AdR. Cyproterone acetate was used in a concentration range of 0 to 400 µM. The data shown are the result of four independent measurements (R^2>0.98).

To investigate potential product inhibition, *in vitro* product inhibition experiments were performed using a fixed amount of substrate with increasing initial product concentrations (purified by preparative HPLC). The results confirmed the assumption that the product used in 200 µM or higher concentrations strongly inhibits the reaction. Using 200 µM 15β-OH-CPA, we could observe only a 25 ± 1.9 % conversion, which was roughly half of the product formation that was observed in the control sample (47 ± 4.3 %) containing only the substrate (400 µM). When increasing the product concentration to 1200 µM the conversion drastically decreased to 5 ± 0.12 %, one tenth of the control conversion (Figure 4).

In vivo conversion, product localization and catalyst reusability

Following the successful conversion of CPA by the CYP106A2-overexpressing *B. megaterium* strain (Figure 5), the product of the reaction was purified on preparative HPLC and its structure was identified by nuclear magnetic resonance (NMR) spectroscopy. The resulting main product (P1), 15β-OH-CPA, was used in the above-mentioned *in vitro* as well as in the *in vivo* product inhibition studies. The whole-cell catalyst was further characterized by examining the substrate and product localization. Both substrate and product were shown to be attached to the cell pellet fraction (data not shown). Adding more cells after 4 h of conversion did not improve the reaction yield, most likely since all remaining substrate was already inside or attached to the original cells (Figure 6). However, the addition of 3 times more cells (150 g/L wet cell weight (WCW)) and 2 times more substrate (1 mM) only doubled the product concentration thereby giving a lower biocatalyst yield.

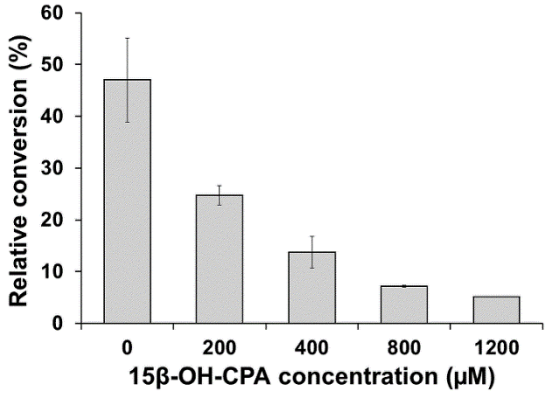

Figure 4 In vitro conversion of cyproterone acetate using increasing initial product concentrations. The reactions were performed using 400 µM substrate concentration and initial product concentrations ranging from 0 to 1200 µM for 60 min. The data represents the mean of three independent measurements with the corresponding standard deviation shown by the error bars.

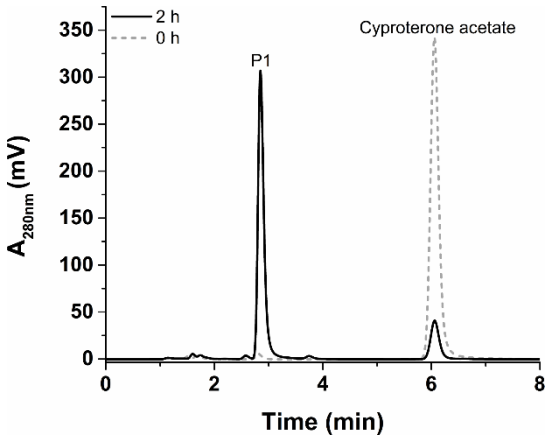

Figure 5 HPLC chromatogram of the cyproterone acetate conversion using B. megaterium MS941 overexpressing the CYP106A2 enzyme. The reaction was performed with resting cells in 100 mM potassium phosphate buffer (pH 7.4) at 30 °C, 150 rpm. Cyproterone acetate (400 µM) was added to the cells in DMSO solution (2 % v/v). Samples were collected directly at the point of substrate addition (grey dotted line) and after 2 h (black line). The substrate was converted to one main product (P1).

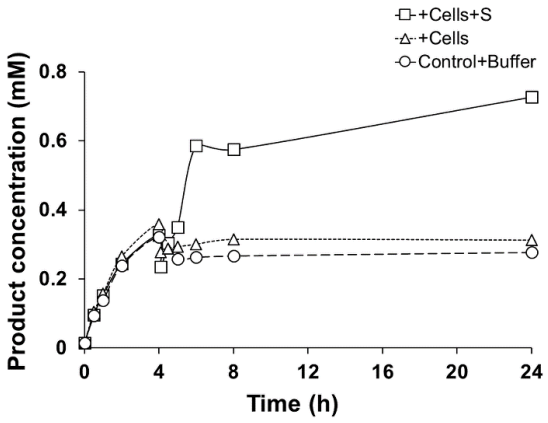

Figure 6 Effect of whole-cell catalyst addition, with and without additional substrate, on 15β-hydroxycyproterone acetate production. Reactions were performed in shake flasks with 1 mM cyproterone acetate and an initial catalyst concentration of 50 g/L WCW. After 4 h, additional 150 g/L WCW was added to the reaction represented with △, both catalyst and substrate (1 mM) were added to the reaction represented with □ and buffer was added to the control (○) to compensate for the change in volume.

In a further attempt to improve the biocatalyst yield, the reusability of the whole-cell system was investigated to decrease the cost contribution of the catalyst and increase the economic potential of a resting cell process. Removal of the product by solvent extraction between batches was explored. Washing with buffer did not have any effect on the product in the cell pellet fraction. Exposing the cells to the organic solvent ethyl acetate completely destroyed the activity of the cells. Furthermore, washing with decanol removed the product from the cells, but at the same time damaged the catalyst resulting in around 30 % relative conversion compared to the first batch (Figure 7).

Transport and cofactor dependence

The potential limitations of the whole-cell system in terms of substrate transport across the cell membrane and cofactor regeneration were ruled out as seen in Figure 8. The reactions were performed with resting whole-cells in shake flasks and NADPH was added in 1 mM (stoichiometric to substrate) and 2 mM final concentrations. The influence of cofactor addition and the cell permeabilization methods (sonication, acetone treatment or freeze-thawing) on the reaction rate was investigated. The initial rates measured in these experiments did not show any significant difference (data not shown). In addition, Figure 8 shows that no significant difference was observed in the final product concentration either, regardless of permeabilization treatment or external addition of cofactor. The cofactor is assumed to pass the cell membrane and enter the cell, similarily to observations in *E. coli* where this was monitored by a decreasing absorbance of the supernatant at 340 nm (unpublished work, results not shown). The results demonstrate that the cofactor regeneration of the host *B. megaterium* MS941 is sufficient to support the observed biocatalytic reaction rates and that the natural redox partners are sufficiently expressed to transport electrons from the cofactor to the active site of the overexpressed P450. The substrate transport that has been shown to limit a CYP106A2-catalyzed steroid transformation in *E. coli* [5] was not limiting the reaction studied here in *B. megaterium*, according to the tested permeabilization methods, emphasizing the suitability of this whole-cell catalyst.

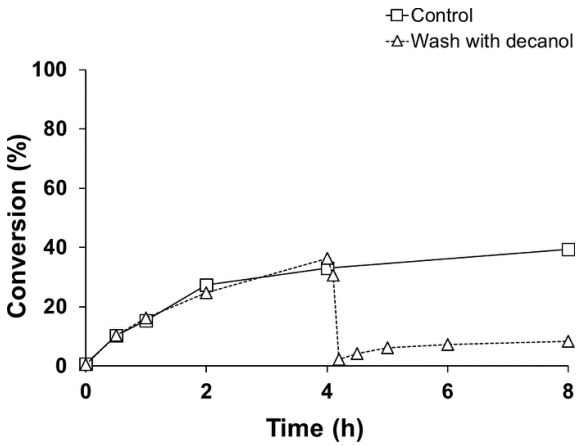

Figure 7 Cell recycling by product extraction using decanol. □ represents the control and △ the cells washed with decanol after 4 h. Reactions were performed with resting cells in shake flasks, using 1 mM cyproterone acetate and an initial catalyst concentration of 100 g/L WCW. 1 mM substrate was added when starting each reaction but only to the washed cells at 4 h.

In vivo substrate and product inhibition

The influence of increasing substrate and product concentrations on the reaction performance was also investigated *in vivo* with the recombinant *B. megaterium* MS941 strain overexpressing CYP106A2. The substrate inhibition studies were

performed within a concentration range of 50 µM to 1 mM. When using up to 200 µM substrate concentration, complete conversion of the substrate took place already within 2 h, while at higher substrate concentrations the conversion stopped at an approximate product concentration of 300 µM (70 % conversion in the case of 400 µM and 27 % in the case of 1000 µM CPA) (Figure 9), showing a similar trend as the *in vitro* experiments.

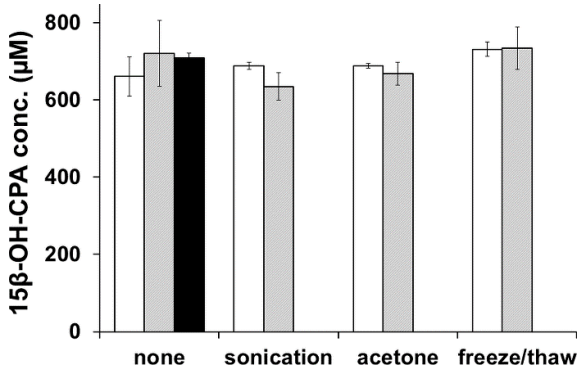

Figure 8 Effect of different cell permeabilization methods and cofactor addition on 15β-hydroxycyproterone acetate production. White bars represent the results without cofactor addition, grey bars have 1 mM NADPH and the black bar have 2 mM NADPH added. All reactions were run using 1 mM cyproterone acetate, 2 % DMSO and 100 g/L WCW cells from the same fermentation batch. Error bars are 1σ.

Product removal strategies

To remove the product and push the reaction equilibrium in the forward direction, thereby enhancing the reaction performance, the use of two water-immiscible solvents, diisononylphtalate ($C_{26}H_{42}O_4$) and hexadecane ($C_{16}H_{34}$) (selected to be compatible with the whole-cell catalyst and with oxygen requiring reactions) was investigated. However, solubilization of the substrate in these solvents, prior to addition to the aqueous phase containing the whole-cell catalyst, did not improve the reaction performance. The hydrophobicity of the substrate hinders the partitioning to the aqueous phase and thereby hampers the catalytic reaction (results not shown). The negative results could also be explained by analytical difficulties and problems with homogenous sampling in a solid–liquid 2-phase system.

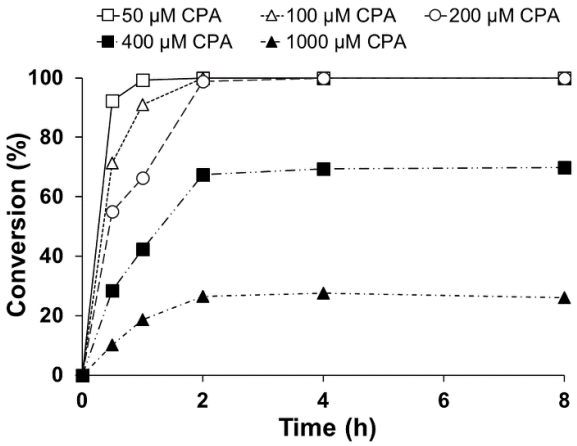

Figure 9 *In vivo* conversions performed in shake flasks with increasing substrate concentrations using resting cells. The reactions were performed in 100 mM potassium phosphate buffer (pH 7.4) at 30 °C, 150 rpm, with a substrate concentration ranging from 50 µM to 1 mM.

Another approach to maintain a low concentration of the dissolved product in the aqueous phase is to avoid the use of a miscible co-solvent and instead apply solid substrate. This approach requires that the rate of dissolution of the substrate into the aqueous phase is faster than the reaction rate so that it does not limit the observed reaction. However, this method was not successful either, most likely due to the low solubility and rate of dissolution of the substrate.

A third approach was to pre-solubilize the substrate in an aqueous solution of HP-β-CD ($(C_6H_9O_5)_7(C_3H_7O)_{4.5}$), in order to take advantage of its multiple effects. Cyclodextrin (CD), especially the derivatized forms, have been shown to be useful in enhancing steroid conversions by e.g. increasing the cell-wall permeability, stimulating cell growth and efficiently solubilizing hydrophobic substrates [2]. The complexation of β-CD with substrate and/or product also leads to lower amounts of free dissolved species and thereby lower inhibitory effects of either substrate or product on the catalyst, as suggested previously for steroid biotransformations [23,24]. Using CD-solubilized CPA, the transformations were performed first in shake flasks with 1 mM final concentration of the substrate. As a control, the conversion was also performed with the substrate dissolved in dimethyl sulfoxide (DMSO). The CPA was added from the 45 % CD solution, not exceeding 5 % of the reaction volume. During the

conversion, 250 µl reaction samples were taken at the indicated time points and the product/substrate ratio was analyzed by HPLC. Despite the slow initial rate, a higher conversion was reached within 4 h using CD as solubilizing agent, compared to the control. After 24 h, the conversion with CD showed 38 ± 0.05 % product formation, while the control could only reach 27 ± 4.6 % (Figure 10). Given the improved conversion, the same strategy was applied in the bioreactor (Figure 11). 98 % conversion of 1 mM substrate was achieved on a 400 mL scale compared to a final conversion of 55 % for the control without CD.

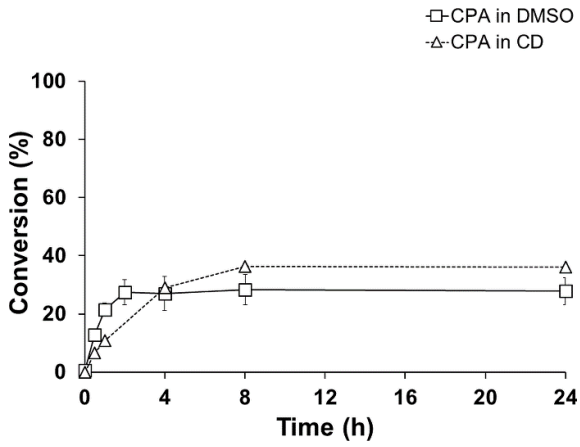

Figure 10 *In vivo* cyproterone acetate conversion in shake flasks, using 2-hydroxypropyl-β-cyclodextrin and DMSO for substrate solubilization. The reactions were carried out with resting cells, in 100 mM potassium phosphate buffer (pH 7.4) at 30 °C, 150 rpm. The substrate was pre-dissolved either in a 45 % CD solution mixed overnight (△) or in DMSO (□) with a final concentration of 1 mM.

Influence of reaction mixing

In this study, catalyst-dependent parameters, believed to be independent of the used scale, were investigated in shake flasks. Shake flask experiments are commonly used in research laboratories, providing a simple and fast tool to demonstrate the proof of concept. However, for process development and scale-up studies, a more controlled environment and a more easily scalable configuration is preferred. When comparing batch transformations between bioreactor and shake flasks under identical conditions, the former showed faster initial rates (Figure 12). This result indicates that increased mixing enhances the reaction rate, most likely due to increased mass transfer of poorly water-soluble substrate but also due to the increased aeration. These results also suggest that for processes targeting scale-up and industrial implementation, process development should be performed with the intended final reactor configuration, in this case a stirred tank reactor instead of shake flasks. This especially concerns reactions involving species with low water solubility and gaseous components (e.g. oxygen).

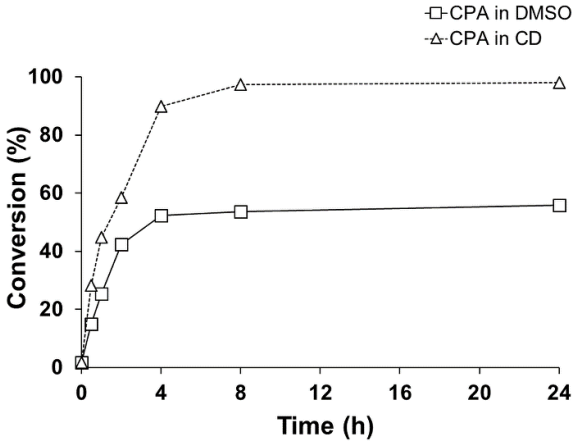

Figure 11 *In vivo* cyproterone acetate conversion in bioreactor, using 2-hydroxypropyl-β-cyclodextrin and DMSO for substrate solubilization. The reactions were carried out in 400 mL final volume with resting cells resuspended in 100 mM potassium phosphate buffer (pH 7.4) at 30 °C. The substrate was either pre-dissolved, in a 45 % CD solution mixed overnight (△) or in DMSO (□) with a final concentration of 1 mM.

Catalyst stability

The stability of a biocatalyst is crucial for the economic potential of a biocatalytic process. In this study we examined the storage stability, due to practical reasons, and more importantly, the stability under process conditions, under which the relevant information is collected. The dry cell weight and the correctly folded P450 were monitored during the process and it was found that the cells remained intact but the stability of the CYP106A2 was limited. One third of the correctly folded P450 is degraded after 4 h of the reaction and more than 50 % is lost after 24 h (Figure 13).

The storage stability of the catalyst was determined by running resting cell biotransformations with cells previously resuspended in buffer and stored gently shaken at 4 °C. No significant loss in reaction performance

was found over 7 days of storage (data not shown). The stability of the catalyst could potentially also be affected by the mode of operation. However, no significant difference was seen between growing and resting cells in terms of conversion, whole-cell stability or P450 stability.

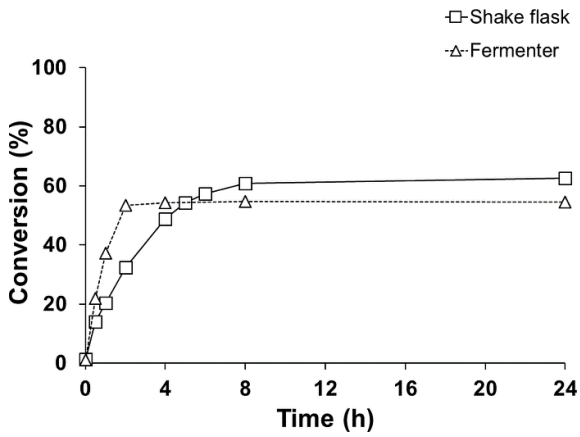

Figure 12 Comparison of 1 mM cyproterone acetate transformation in bioreactor and shake flask. The reactions were carried out using the same batch of cells, in a resting cell format (100 g/L WCW), and the substrate was added dissolved in DMSO. The initial rate of the reaction performed in the bioreactor (△) showed a higher initial rate compared to the reaction performed in shake flasks (□), although the reaction in the shake flask resulted in a higher final conversion.

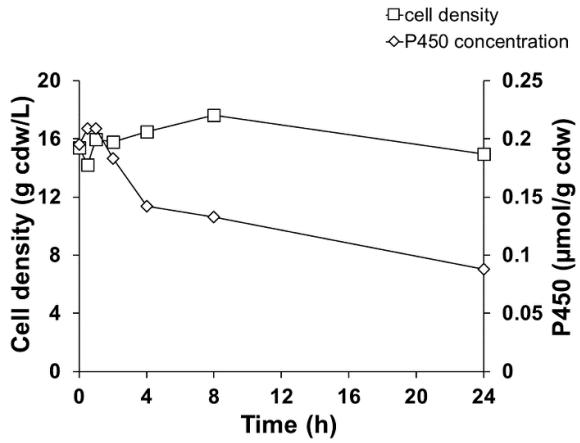

Figure 13 Stability of the whole-cell catalyst under process conditions. Reaction performed with resting cells in the bioreactor at 1 mM cyproterone acetate concentration and a cell density of 100 g/L WCW. Samples were collected at the indicated time points. The dry cell weight (□) and the P450 content (◇) were measured.

Discussion

Even though in the past decade significant progress was made to develop efficient biocatalysts for steroid transformations, there is still a great demand for greener and cost-efficient routes for valuable steroid production [2]. Microbial steroid transformations, using heterologously expressed cytochrome P450 enzymes are considered to be a promising approach, since the regio- and stereospecific hydroxylations are known to be challenging for synthetic steroid chemistry, suffering from low predictability and specificity [1,25]. However, in most cases the reactions performed at analytical scale are not directly applicable for industrial practice. For an industrial process, the economic feasibility needs to be considered. For guidance, at the current stage of process development, targets for economic metrics such as space-time yield (for a growing cell process), final product concentration and biocatalyst yield (for a resting cell process) can be used. For high-value products or pharmaceuticals, such as the 15β-OH-CPA, target values for product concentration of 20 g/L, a space-time yield of 2 g/L/h (for a growing cell process) and a biocatalyst yield of 10 g product/g dry cell weight (DCW) (for a resting-cell process) can be used as reference [21]. These targets can only be achieved using higher substrate concentrations, and problems associated with higher concentrations such as low solubility of the substrate, potential substrate or product inhibition and toxicity most likely will arise.

In a previous study, Hannemann and co-workers converted 11-deoxycorticosterone to 15β-hydroxy-11-deoxycorticosterone using CYP106A2, functionally expressed with bovine adrenal redox partners in a growing whole-cell *E. coli* host. According to our calculations, the molar substrate concentration applied in this study (0.5 mM) could result in a maximal final product concentration of 0.17 g/L. The space-time yield was reported to be 0.33 g/L/d, however, it has to be taken into account that the substrate was not fully converted after 24 h [13]. Nevertheless, the focus of the study was to design a whole-cell catalyst and demonstrate the applicability of a screening assay. The whole-cell system was then further improved by the coexpression of a cofactor regeneration system and was used for the 15β-hydroxylation of progesterone and

testosterone [5]. This system was shown to be limited by substrate transport across the cell membrane and solubility of the substrate was shown to be crucial for the reaction performance. The productivity concerning testosterone hydroxylation was reported to be 5.5 g/L/d using 0.5 mM initial substrate concentration and a lyophilized cell extract on a 20 mL scale, however, this value was extrapolated from a 30 min reaction. Taking into account the 0.5 mM initial substrate concentration the 96 % conversion could only lead to a final product concentration of 0.15 g/L. In the same study experiments with growing cells showed only 25 % selectivity towards the 15β position, considerably lower than resting cells (≥80 %). More recently, DHEA was regioselectively hydroxylated to 7β-OH-DHEA by CYP106A2 expressed in *B. megaterium* [12]. A benchmark 0.44 g/L total final product concentration was obtained upon addition of 1.5 mM substrate in a repeated batch mode, yielding 6 different products in 12 h, which is the highest reported concentration of the studies published so far. The selectivity towards the 7β-position was improved from 0.7 to 0.9 by changing the host from *B. megaterium* strain ATCC 13368 to MS941. The bottlenecks of the reaction were discussed but never investigated.

In our study a systematic approach was taken to identify catalyst- and reaction-related limitations to enable an efficient process with defined targets based on economic guidance. By addressing the identified limitations we managed to evaluate and improve the process performance. This is a novel approach compared to previous studies on steroid hydroxylation by CYP106A2. We investigated the regio- and stereoselective 15β-oxidation of CPA, in shake flasks and laboratory scale bioreactors. CYP106A2 was overexpressed in *B. megaterium* MS941 and proved to be a robust catalyst for the synthetic biotransformation of CPA. The *B. megaterium* host offers a protected environment for the enzyme, enhancing its stability, besides the cofactor regeneration provided by the cellular metabolism, which, according to our studies, was shown to be sufficient to not limit catalysis. The substrate transport across the membrane of the *B. megaterium* whole-cell catalyst turned out not to be a limiting factor either, as was described in the case of steroid hydroxylation by *E. coli* [5]. In contrast, the low overall solubility of the reactants, the limited stability of the P450, in combination with product inhibition, are suggested to be the main bottlenecks of this system.

The low solubility of substrate is a common challenge to many P450-catalyzed reactions. In the case of CPA the solubility is reported to be 0.64 mg/L [26] and 34 mg/L for the hydroxylated product [27]. However, this should be put in perspective to the aimed final product concentration of 20 g/L. Low steroid solubility is usually solved by the application of a water immiscible co-solvent but this approach has limitations at higher concentrations when the co-solvent can damage the biocatalyst [28]. This can partly be circumvented by the application of CDs. These cyclic oligosaccharides are used in e.g. drug delivery [29] and have also been applied in P450-catalyzed reactions, mainly as a solubilizing agent and to improve substrate transport across the cell membrane, however at limited substrate concentrations (50 mg/L) [23]. The effects of HP-β-CD on steroid dehydrogenation of the gram-positive bacteria *Arthrobacter simplex* was investigated by Shen and coworkers [30]. Cells pretreated with HP-β-CD showed double the initial rate and reached final conversion 1 h faster compared to the non-treated cells, although in the end both reached the same concentration. This was shown to be the result of the cell membrane permeabilization by altered lipid and protein profiles of the membrane. CDs have also been applied in other fermentation and biotransformation processes to avoid toxic and inhibitory effects of the substrate or product, as summarized by Singh *et al.* [31]. In this work, using HP-β-CD, we were able to achieve 98 % conversion of 1 mM CPA in a regio- and stereoselective manner within 8 h, resulting in 0.43 g/L product. This matches the literature benchmark for steroid conversion by CYP106A2 [12], yet the 8 h conversion time applied here improves the space-time yield by 31 %. This new approach of bottleneck identification, takes P450-catalyzed reactions one step further towards

higher product titers and economic viability. In our system, the time-dependent product inhibition was shown to limit final achievable product concentrations at higher substrate concentrations, thereby decreasing the reaction yield. By overcoming this problem, the main effect of CD was believed to be the complexation of the product in the lipophilic central cavity, thereby pulling it out of the hydrophilic environment present in the cell and pushing the equilibrium towards the product formation.

Conclusion

Ultimately, with the help of HP-β-CD, we could achieve a nearly complete conversion and a product formation of 0.43 g/L at a 400 mL scale, getting closer to industrial process requirements and a future large-scale application. However, in order to fully exploit the potential of the CD process, further optimization studies should be performed. Using CD to circumvent the identified bottlenecks of solubility and product inhibition, the stability of the P450 is still a challenge for an economically feasible process. Considering that the stability of the enzyme will make cell recycling difficult, and that no significant differences could be found between a growing and resting cell process, the preferred mode of operation for further process development would be growing cells. As stated above, the targets for an economically feasible growing cell process are a final product concentration of 20 g/L and a space-time yield of 2 g/L/h [21]. Although we could demonstrate a successful process development towards the suggested values by addressing the limitations, there is still room for improvement.

Materials and methods

Reagents and chemicals

All used chemicals were from standard sources and of highest grade available. Solvents of analytical grade were used for HPLC, while solvents used for large-scale extraction were of reagent grade. CPA was obtained from BIOTREND Chemikalien GmbH, Köln, Germany (≥98 % (HPLC)).

Bacterial strains and plasmids

The *in vivo* conversions were performed using a recombinant *B. megaterium* MS941 strain, a variant of DSM319, lacking the major extracellular protease gene *nprM* [32]. The host organism was transformed with the plasmid pSMF2.1C (CYP106A2 gene introduced within the SpeI/MluI sites) by a polyethylene glycol-mediated technique using protoplasts [9,16]. As control, the wild type *B. megaterium* MS941 strain was used (lacking the pSMF2.1 plasmid, but naturally containing cytochrome P450 genes) to confirm that the reaction is catalyzed by the CYP106A2 enzyme. The wild type strain did not display any activity towards the substrate (data not shown) and no P450 was detected using CO difference spectroscopy [33], indicating that the P450 expression and catalytic activity reported is assigned to the overexpressed CYP106A2.

Protein expression, purification and spectral characterization

The expression and purification of the CYP106A2 protein was performed as described previously [6,34]. For the reconstituted *in vitro* system, a truncated form of bovine adrenodoxin ($Adx_{4–108}$) was used in combination with bovine adrenodoxin-reductase (AdR), their expression and purification was completed as described elsewhere [35,36]. The characteristics of the purified CYP106A2 were analyzed by UV-visible absorbance spectroscopy. The spectrum was recorded in a range of 200 to 700 nm with a double beam spectrophotometer (UV-1800, UV-2101 PC, Shimadzu Corporation, Kyoto, Japan) and analyzed constantly during the purification process, to determine the Q value (A_{417}/A_{280}), which was in all cases above 1.5, suggesting a high amount of correctly folded, active P450s. The samples taken from the bacterial cultures during cultivation or conversion were spun down and the pellet kept frozen at -20 °C until measurement when the samples were resuspended in 100 mM potassium phosphate buffer, pH 7.4. The concentration of the purified protein and the protein expressed in the whole-cell system was determined by CO difference spectroscopy

according to the method of Omura and Sato [33], using an extinction coefficient of 91 mM^{-1} cm^{-1}.

Substrate binding assay

The substrate binding spectrum was investigated using a double-beam spectrophotometer (UV-2101PC, Shimadzu, Japan) and tandem quartz cuvettes. The analysis took place in 800 µL total volume. One chamber of each cuvette contained 10 µM solution of CYP106A2 in 50 mM potassium phosphate buffer pH 7.4, while the other chamber was filled with buffer. CPA was dissolved in DMSO at a stock concentration of 10 mM. The enzyme was titrated with the substrate in a concentration range of 5 to 150 µM. After each titration step the spectrum was recorded in a range of 350 to 500 nm.

***In vitro* conversions and enzyme kinetics**

The *in vitro* conversion of CPA was carried out with a reconstituted system in a final volume of 250 µL at 30 °C for 30 min in 50 mM potassium phosphate buffer (pH 7.4), containing 20 % (v/v) glycerol. The reconstituted system contained bovine AdR (1 µM), a truncated form of $Adx_{4–108}$ (10 µM), CYP106A2 (0.5 µM), a NADPH-regenerating system [MgCl2 (1 mM), glucose-6-phosphate (5 mM), glucose-6-phosphate dehydrogenase (1 U), and NADPH (0.1 µM)], and CPA (200 µM). The reaction was started by adding NADPH (1 mM) and incubated at 30 °C. The assay was stopped by the addition of 250 µL of ethyl acetate, mixed vigorously, and extracted twice. The combined organic phases were evaporated and the residues were dissolved in the HPLC mobile phase (60:40% ACN:H_2O) and subjected to analysis.

Reaction kinetics of CPA and CYP106A2 were performed for 2 min as described above, using bovine AdR (0.5 µM), bovine $Adx_{4–108}$ (5 µM) and CYP106A2 (0.25 µM). The substrate concentration varied from 20 to 250 µM. Product amounts were determined by plotting the amount of product formed (nmol product/nmol P450/min) against the substrate concentration (µM). Each reaction was performed six times, the data represents the mean of these independent results. Data were fitted by hyperbolic regression with the help of Origin (OriginLab Corporation, Massachusetts, USA).

The substrate inhibition studies were performed using a 20 mM CPA stock solution dissolved in DMSO and added in a final concentration of 200 to 1200 µM. Studying the product inhibition, the substrate was added in a final concentration of 400 µM, while the purified product concentration ranged from 0 to 1200 µM. The reactions took place for 60 min, then the samples were extracted and subjected to HPLC analysis as described before.

Heterologous expression in shake flasks

Pre-cultures were inoculated from a -80 °C glycerol stock, using 25 mL complex TB medium (24 g/L yeast extract, 12 g/L soytone, 2.31 g/L KH_2PO_4 and 12.5 g/L K_2HPO_4) supplemented with 10 mg/L tetracycline and incubated overnight, at 150 rpm, 30 °C. The main culture, containing 250 mL complex medium (supplemented with the corresponding amount of tetracycline) was inoculated with 1 % of the culture volume from the pre-culture. The main culture was incubated until an OD_{578} = 0.5, when 5 g/L xylose solution was added to induce expression. After 24 h expression, the cells were harvested (4500 x g, 4 °C, 15 min), the cell pellet was washed and resuspended in 100 mM potassium phosphate buffer (pH 7.4).

Heterologous expression at fermenter scale

The fermentation process was adapted from Korneli and coworkers [37]. A -80 °C glycerol stock was used to inoculate the first pre-culture with LB medium which was used to inoculate a second pre-culture with batch medium (3.52 g/L KH_2PO_4; 6.62 g/L Na_2HPO_4*$2H_2O$; 0.3 g/L $MgSO_4$*7 H_2O; 25 g/L $(NH_4)2SO_4$; 1 g/L yeast extract and trace elements as described [37]). The first pre-culture was incubated for 8 h in a 100 mL shake flask with 10 mL LB medium at 150 rpm, 37 °C. 100 mL batch medium supplemented with 5 g/L fructose was used for the cultivation of the second pre-culture in a 1 L flask, inoculated from the first pre-culture to an OD_{600} of 0.1. After 12 h of cultivation, it served as inoculum for the fermenter. The batch medium in the fermenter was

supplemented with 15 g/L fructose. The feed medium consisted of 150 g/L fructose; 5 g/L D-xylose; 9.9 g/L KH_2PO_4; 14.98 g/L Na_2HPO_4; 0.3 g/L $MgSO_4*7H_2O$, 25 g/L $(NH_4)_2SO_4$. All media preparations were supplemented with 10 mg/L tetracycline. The fed-batch fermentation process was carried out in a 1 L Infors Multifors fermentation vessel (Infors HT, Bottmingen, Switzerland). Initial conditions were set to 37 °C; pH 7.0; aeration 0.5 Lpm and pO_2 setpoint 20 % controlled by stirrer. The fermenter was inoculated to a final OD_{600} of 0.7 and induced at an OD_{600} of 10 with 5 g/L xylose. The induction at a higher OD_{600} in the fermenter, compared to shake flask, is due to the higher possible final cell density utilizing a fed-batch process. At the time of induction, the temperature was decreased to 30 °C, agitation was increased to 1 Lpm and a linear feed was initiated. The pH was controlled during the process with 5 M NaOH and 1 M H_3PO_4. Cells were harvested by centrifugation and washed by resuspension in 100 mM potassium phosphate buffer, pH 7.4. 20 mM fructose was added to the cells for direct use in biotransformation or stored at 4 °C, gently shaking, at a cell density of 200 g/L WCW.

Bioconversion in shake flasks

The small scale conversion of CPA was performed with resting cells in a 15 mL culture volume using 100 mL baffled shake flasks. The catalyst concentration was 100 g/L WCW, unless otherwise stated. To obtain sufficient amount of product (mg) for NMR structure characterization, the conversion was scaled up to 50 mL, using 300 mL baffled shake flasks. CPA was added in 200 µM final concentration from a 20 mM DMSO stock solution. The use of DMSO did not exceed 2 % of the culture volume. Every 4 h, 2 M fructose solution was added as carbon source in a final concentration of 20 mM. 250 µL samples were taken at indicated time points to monitor the conversion. The samples were extracted twice using 250 µL ethyl acetate, the organic phases collected and evaporated to dryness for the subsequent analysis by reverse-phase HPLC. In the case of product isolation, the reaction was stopped and the steroids were extracted twice by ethyl acetate. The organic phase was dried over anhydrous $MgSO_4$ and concentrated to dryness in a rotavapor (Büchi R-114). The yellowish residue was dissolved in the mobile phase of the HPLC and filtered through a sterile syringe filter (Rotilabo syringe filter, 0.22 µm, Carl Roth GmbH, Karlsruhe, Germany). The product purification was completed by preparative HPLC, according to its retention time. The collected fractions were evaporated to dryness and analyzed by NMR spectroscopy. The *in vivo* substrate and product inhibition was studied in shake flasks, using resting cells, as described for the *in vitro* studies.

HPLC analysis

The HPLC analysis was performed either on a Jasco system consisting of a Pu-980 HPLC pump, an AS-950 sampler, a UV-975 UV/Vis detector, and an LG-980–02 gradient unit (Jasco, Gross-Umstadt, Germany) or on a Dionex UltiMate 3000 HPLC equipped with a Photodiode Array Detector (Dionex, Thermo Scientific, Sunnyvale, CA, USA). A reversed-phase ec MN Nucleodor C_{18} (3 µM, 4.0x125 mm) column (Macherey-Nagel, Betlehem, PA, USA) was used and kept at an oven temperature of 40 °C. An isocratic gradient of acetonitrile:water in a ratio of 60:40 was applied using a flow rate of 0.8 mL/min. UV detection of the substrate and product was accomplished at 282 nm. Product isolation was performed using preparative reversed-phase HPLC (ec MN Nucleodur C18 VP (5 µM, 8x250 mm), Macherey-Nagel, Betlehem, PA, USA) with a flow rate of 2.5 mL/min. The results are presented as conversion %, calculated from the product area divided by the sum of substrate and product areas. Regarding the product inhibition experiments, when product was added initially to the system, the data is presented as relative conversion (subtracting the initially added product) or calculated back to concentrations from conversions.

NMR characterization of the main metabolite

The NMR spectrum was recorded in $CDCl_3$ with a Bruker DRX 500 NMR spectrometer at 300 K. The chemical shifts were relative to TMS using the

standard δ notation in parts per million. The 1D NMR (^{1}H and ^{13}C NMR, DEPT135) and the 2D NMR spectra (gs-HH-COSY, gs-NOESY, gs-HSQCED, and gs-HMBC) were recorded using the BRUKER pulse program library. All assignments were based on extensive NMR spectral evidence.

The product (P1) was identified as 15β-hydroxycyproterone acetate (15β-OH-CPA) (3.4 mg). In comparison to cyproterone acetate the NMR spectra of its conversion product showed signals for an additional secondary hydroxyl group (δ_H 4.50 ddd, J = 7.5, 6.0 and 2.0 Hz; δ_C 68.86). Its position at C-15 could be deduced by vicinal couplings of the methin proton with H-14 (δ_H 1.93 dd, J = 12.0 and 6.0 Hz), H-16α (δ_H 2.47 dd, J = 16.8 and 7.5 Hz) and H-16β (δ_H 3.03 dd, J = 16.8 and 2.0 Hz) in the HHCOSY and with C-13 (δ_C 47.00) and C-17 (δ_C 96.11) in HMBC. The β orientation of the hydroxyl was obvious by the NOESY effects of H-15 to H-16α and to H-9 (δ_H 1.53 m) and H-14, both in α position. In addition, the coupling constants found for H-15α resembled those for other closely related steroids, e.g. 15β-hydroxy-11-deoxycortisol [8]. Selected ^{1}H NMR data of 15β-hydroxycyproterone acetate could be found in the literature [38] and matched with our values. ^{1}H NMR ($CDCl_3$, 500 MHz): δ 0.89 dt (6.3 and 4.7 Hz, cPr-Ha), 1.01 s (3xH-18), 1.27 s (3xH-19), 1.29 ddd (9.0, 7.8 and 4.7 Hz, cPr-Hb), 1.53 m (H-9), 1.62 m (2H, H-11β and H-12β), 1.74 td (7.8 and 6.3 Hz, H-1), 1.93 dd (12.0 and 6.0 Hz, H-14), 1.98 m (H-11α), 2.03 m (H-2), 2.04 m (H-1 2α), 2.09 s (3x OCOC*H*$_3$), 2.10 s (3xH-21), 2.47 dd (16.8 and 7.5 Hz, H-16α), 2.73 td (12.0 and 2.3 Hz, H-8), 3.03 dd (16.8 and 2.0 Hz, H-16β), 4.50 ddd (7.5, 6.0 and 2.0 Hz, H-15), 6.20 brs (H-4), 6.44 d (2.3 Hz, H-7). ^{13}C NMR ($CDCl_3$, 125 MHz): δ 12.30 (CH_2, cPr), 16.95 (CH_3, C-18), 20.74 (CH_2, C-11), 21.11 (C, OCO*C*H_3), 22.86 (CH_3, C-19), 25.24 (CH, C-2), 26.12 (CH, C-1), 26.35 (CH_3, C-21), 31.96 (CH_2, C-12), 34.44 (CH, C-8), 38.84 (C, C-10), 43.13 (CH_2, C-16), 47.00 (C, C-13), 47.98 (CH, C-9), 52.80 (CH, C-14), 68.86 (CH, C-15), 96.11 (C, C-17), 120.47 (CH, C-4), 130.45 (C, C-6), 136.30 (CH, C-7), 152.32 (C, C-5), 170.51 (C, O*C*OCH$_3$), 197.98 (C, C-3), 202.84 (C, C-20).

Transport and cofactor dependence

Transport limitation was examined by different cell membrane permeabilization methods prior to the biocatalytic reaction. Both mechanical and chemical methods were applied (freeze-thawing, acetone treatment and ultra-sonication). Frozen cells were spun down and the pellet was kept at −20 °C overnight. Acetone-treated cells were incubated with 5 % acetone for 2 min while vortexing and mechanical disruption was performed by sonication for 2 min (amplitude 60 %, 0.5 s cycles) (UP400 S; Hielscher Ultrasonic GmbH, Teltow, Germany). Following the permeabilization treatment (acetone and sonication) cells were spun down and the pellet resuspended in 100 mM potassium phosphate buffer pH 7.4. Cofactor was added to the untreated control samples and to the permeabilized ones, once and twice stoichiometric amounts relative to substrate concentration.

Storage stability

To examine the storage stability of the whole-cell catalyst, the transformation was performed with resting cells after 1, 3 and 7 days of storage. The cells were stored at 4 °C, gently shaking at a cell density of 200 g/L WCW in 100 mM potassium phosphate buffer, pH 7.4. 20 mM fructose was added as carbon source at the time of harvest, after 1 and 3 days of storage and also at the start of the reactions.

Cyclodextrin

As an alternative substrate feeding strategy, the substrate was pre-dissolved in a 45 % (w/v) solution of HP-β-CD in sterile-filtered MilliQ water and stirred overnight using a magnetic stirrer.

Optical density and dry cell weight determination

To estimate the cell concentration, the optical density at 600 nm (OD_{600}) was monitored and the gravimetric dry cell weight (g/L DCW) was determined. Samples collected for dry cell weight

measurement were spun down, the supernatant was discarded and the pellet was kept at −20 °C until further analysis. Thereafter the pellets were thawed and resuspended in the original sample volume using 100 mM potassium phosphate buffer, pH 7.4. Dry cell weight was measured in triplicates by filtering the samples through a pre-weighed 0.22 µm PES membrane filter (Frisenette, Knebel, Denmark) applying vacuum. The filters were washed with buffer, dried in a microwave oven and weighed after equilibrating to room temperature in a desiccator.

Bioconversion in bioreactor

Biocatalysis in bioreactors was performed in the same vessels as the fermentation (Infors Multifors, Infors HT, Bottmingen, Switzerland) in a working volume of 400 mL. Set points applied were: 30 °C, aeration 1 Lpm, pO_2 30 % controlled by agitation, pH 7.2 controlled with 5 M NaOH and 1 M H_3PO_4. 2 M stock solution of fructose was added at time point 0, 4 and 8 h in a final concentration of 20 mM. CPA was dissolved in DMSO and added in a final concentration of 1 mM, the DMSO content not exceeding 2 % of the total volume. For an accurate comparison of growing and resting cells half of the fermentation volume was removed after 16 h and this fraction was harvested by centrifugation, washed and resuspended in 100 mM potassium phosphate buffer, pH 7.4. Resuspended cells were transferred to a bioreactor, parallel to the still growing cells. Fructose and xylose were continuously fed, for both resting and growing cells, at half the volumetric rate compared to the fermentation due to half the volume.

Abbreviations

AdR, Adrenodoxin reductase; Adx, Adrenodoxin; *B. megaterium*, *Bacillus megaterium*; CD, Cyclodextrin; CPA, Cyproterone acetate, 15β-OH-CPA, 15β-hydroxycyproterone acetate; DHEA, Dehydroepiandrosterone; DMSO, Dimethyl sulfoxide; DCW, Dry cell weight; HP-β-CD, 2-hydroxypropyl-β-cyclodextrin; HPLC, High-performance liquid chromatography; *E. coli*, *Escherichia coli*; NMR, Nuclear magnetic resonance; P450, Cytochrome P450 enzymes; WCW, Wet cell weight.

Competing interests

The authors declare that they have no competing interests.

Authors' contributions

FMK and MTL contributed equally to the biochemical and biotechnological experiments and both drafted the manuscript. JZ did the NMR measurement and the structure determination of the produced hydroxysteroid in this work. JMW and RB participated in the design of the project, interpretation of the results and assisted in the manuscript drafting. All authors read and approved the final manuscript.

Acknowledgements

This work was generously supported by the People Programme (Marie Curie Actions) of the European Union's 7th Framework Programme (FP7/2007-2013), P4FIFTY - FP7 PEOPLE ITN 2011–289217. The authors thank Dr. Daniela Schmitz for helpful discussions on the project, Wolfgang Reinle and Birgit Heider-Lips for the excellent expression and purification of AdR and $Adx_{4–108}$.

References

1. Bernhardt R, Urlacher VB. Cytochromes P450 as promising catalysts for biotechnological application: chances and limitations. Appl Microbiol Biotechnol. 2014;98(14):6185–203.
2. Donova MV, Egorova OV. Microbial steroid transformations: current state and prospects. Appl Microbiol Biotechnol. 2012;94(6):1423–47.
3. Bureik M, Bernhardt R. Steroid hydroxylation: microbial steroid biotransformations using cytochrome P450 enzymes. In: Schmid RD, Urlacher VB, editors. *Modern Biooxidation: Enzymes, Reactions and Applications*. KGaA, Weinheim: Wiley-VCH Verlag GmbH & Co; 2007. p. 155–76.
4. Tong W, Dong X. Microbial biotransformation: recent developments on steroid drugs. Recent Pat Biotechnol. 2009;3(2):141–53.
5. Zehentgruber D, Hannemann F, Bleif S, Bernhardt R, Lütz S. Towards preparative scale steroid hydroxylation with cytochrome P450 monooxygenase CYP106A2. ChemBioChem. 2010;11(5):713–21.
6. Lisurek M, Kang M, Hartmann RW, Bernhardt R. Identification of monohydroxy progesterones produced by CYP106A2 using comparative HPLC and electrospray ionisation collision-induced dissociation mass spectrometry. Biochem Biophys Res Commun. 2004;319(2):677–82.
7. Berg A, Gustafsson JA, Ingelman-Sundberg M. Characterization of a cytochrome P-450-dependent steroid hydroxylase system present in *Bacillus megaterium*. J Biol Chem. 1976;251(9):2831–8.
8. Kiss FM, Schmitz D, Zapp J, Bernhardt R: Comparison of CYP106A1 and CYP106A2 from *Bacillus megaterium* - identification of a novel 11-oxidase activity. Appl Microbiol Biotechnol 2015; In press.
9. Bleif S, Hannemann F, Zapp J, Hartmann D, Jauch J, Bernhardt R. A new *Bacillus megaterium* whole-cell catalyst for the hydroxylation of the pentacyclic triterpene 11-keto-β-boswellic acid (KBA) based on a recombinant cytochrome P450 system. Appl Microbiol Biotechnol. 2012;93(3):1135–46.
10. Bleif S, Hannemann F, Lisurek M, von Kries JP, Zapp J, Dietzen M, et al. Identification of CYP106A2 as a Regioselective Allylic Bacterial Diterpene Hydroxylase. ChemBioChem. 2011;12(4):576–82.
11. Schmitz D, Zapp J, Bernhardt R. Hydroxylation of the triterpenoid dipterocarpol with CYP106A2 from *Bacillus megaterium*. FEBS J. 2012;279(9):1663–74.
12. Schmitz D, Zapp J, Bernhardt R. Steroid conversion with CYP106A2 - production of pharmaceutically interesting DHEA metabolites. Microb Cell Fact. 2014;13:81.

13. Hannemann F, Virus C, Bernhardt R. Design of an *Escherichia coli* system for whole cell mediated steroid synthesis and molecular evolution of steroid hydroxylases. J Biotechnol. 2006;124(1):172–81.
14. Virus C, Lisurek M, Simgen B, Hannemann F, Bernhardt R. Function and engineering of the 15β-hydroxylase CYP106A2. Biochem Soc Trans. 2006;34(6):1215–8.
15. Meinhardt F, Stahl U, Ebeling W. Highly efficient expression of homologous and heterologous genes in *Bacillus megaterium*. Appl Microbiol Biotechnol. 1989;30(4):343–50.
16. Barg H, Malten M, Jahn M, Jahn D. Protein and vitamin production in *Bacillus megaterium*. Methods Biotechnol. 2005;18:205–23.
17. Vary PS, Biedendieck R, Fuerch T, Meinhardt F, Rohde M, Deckwer W, et al. *Bacillus megaterium* - from simple soil bacterium to industrial protein production host. Appl Microbiol Biotechnol. 2007;76(5):957–67.
18. Neumann F, Toepert M. Pharmacology of antiandrogens. J Steroid Biochem. 1986;25(5):885–95.
19. Frith RG, Phillipou G. 15-Hydroxycyproterone acetate and cyproterone acetate levels in plasma and urine. J Chromatogr, Biomed Appl. 1985;338(1):179–86.
20. Petzoldt K, Steinbeck H, Elger W. 15 Hydroxylation of 1α,2α-methylene steroids. U.S. Patent 4,337,311, June 29, 1982.
21. Lundemo MT, Woodley JM. Guidelines for development and implementation of biocatalytic P450 processes. Appl Microbiol Biotechnol 2015; In press.
22. Ewen KM, Ringle M, Bernhardt R. Adrenodoxin—a versatile ferredoxin. IUBMB Life. 2012;64(6):506–12.
23. Roglic U, Plazl I, Znidarsic-Plazl P. Batch and continuous transformation of progesterone by *Rhizopus nigricans* pellets in the presence of β-cyclodextrin. Biocatal Biotransform. 2007;25(1):16–23.
24. Singer Y, Shity H, Bar R. Microbial transformations in a cyclodextrin medium. Part 2. Reduction of androstenedione to testosterone by *Saccharomyces cerevisiae*. Appl Microbiol Biotechnol. 1991;35(6):731–7.
25. Pellissier H, Santelli M. Chemical and biochemical hydroxylations of steroids. A review. Org Prep Proced Int. 2001;33(1):1–58.
26. ChemSpider [http://www.chemspider.com/Chemical-Structure.9496.html]
27. ChemSpider [http://www.chemspider.com/Chemical-Structure.143151.html]
28. Laane C, Boeren S, Vos K, Veeger C. Rules for optimization of biocatalysis in organic solvents. Biotechnol Bioeng. 1987;30(1):81–7.
29. Davis ME, Brewster ME. Cyclodextrin-based pharmaceutics: past, present and future. Nat Rev Drug Discovery. 2004;3(12):1023–35.
30. Shen Y, Liang J, Li H, Wang M. Hydroxypropyl-β-cyclodextrin-mediated alterations in cell permeability, lipid and protein profiles of steroid-transforming *Arthrobacter simplex*. Appl Microbiol Biotechnol. 2014. doi:10.1007/s00253-014-6089-5.
31. Singh M, Sharma R, Banerjee UC. Biotechnological applications of cyclodextrins. Biotechnol Adv. 2002;20(5–6):341–59.
32. Wittchen K, Meinhardt F. Inactivation of the major extracellular protease from *Bacillus megaterium* DSM319 by gene replacement. Appl Microbiol Biotechnol. 1995;42(6):871–7.
33. Omura T, Sato R. The carbon monoxide-binding pigment of liver microsomes. I. Evidence for its hemoprotein nature. J Biol Chem. 1964;239(7):2370–8.
34. Simgen B, Contzen J, Schwarzer R, Bernhardt R, Jung C. Substrate Binding to 15β-Hydroxylase (CYP106A2) Probed by FT Infrared Spectroscopic Studies of the Iron Ligand CO Stretch Vibration. Biochem Biophys Res Commun. 2000;269(3):737–42.
35. Sagara Y, Wada A, Takata Y, Waterman MR, Sekimizu K, Horiuchi T. Direct expression of adrenodoxin reductase in *Escherichia coli* and the functional characterization. Biol Pharm Bull. 1993;16(7):627–30.
36. Uhlmann H, Beckert V, Schwarz D, Bernhardt R. Expression of bovine adrenodoxin in *E. coli* and site-directed mutagenesis of /2 Fe-2S/ cluster ligands. Biochem Biophys Res Commun. 1992;188(3):1131–8.
37. Korneli C, Bolten CJ, Godard T, Franco-Lara E, Wittmann C. Debottlenecking recombinant protein production in *Bacillus megaterium* under large-scale conditions-targeted precursor feeding designed from metabolomics. Biotechnol Bioeng. 2012;109(6):1538–50.
38. Bhargava AS, Seeger A, Guenzel P. Isolation and identification of 15-β-hydroxycyproterone acetate as a new metabolite of cyproterone acetate in dog, monkey and man. Steroids. 1977;30(3):407–18.

3. Discussion and outlook

Cytochrome P450 monooxygenases are considered as unique biocatalysts due to their ability to introduce atomic oxygen into non-activated hydrocarbons. They are amongst the most potent enzymes to exploit as industrial biocatalysts, capable of performing regio- and stereo-selective hydroxylations of complex molecules such as steroids [29]. Today, there are more than 300 approved steroid drugs, making them the second largest marketed medical product group after antibiotics [115, 116]. The pharmaceutical activity of steroidal drugs is strongly influenced by their functional groups, for instance a selectively introduced hydroxyl group could result in distinct physiological functions [107]. Selective regio-/stereochemistry is challenging to achieve by classical chemical approaches making P450s even more interesting for the pharmaceutical industry. Bacterial P450s are of particular interest, since, being soluble enzymes, they display higher expression levels, stability and often higher substrate specificity compared to their eukaryotic counterparts [13]. The biosynthesis of novel steroid drugs and drug precursors by bacterial species is a well-established tool in the pharmaceutical industry. Despite the fact that microorganisms are widely used for steroid modifications, the responsible enzyme catalyzing the reaction is usually not identified and/or characterized [106, 107]. The increasing number of sequenced bacterial genomes enables the continuous identification of novel P450s, providing a variety of uncharacterized catalysts with potential value for metabolite production, such as the CYP106A1 from the *B. megaterium* strain DSM 319 [81, 92]. The in depth analysis of the bacterial P450s described in this work contributes to the exploration of their so far unknown potentials, providing a detailed characterization of the CYP106A subfamily towards their future application as industrial biocatalysts for steroid hydroxylation.

Our approach started off with a comparison of the well-studied CYP106A2 enzyme and its subfamily member CYP106A1, sharing 63 % sequence identity (**Chapter 2.1**). Although CYP106A1 was recently identified by Brill *et al.* (2014) [81] and was shown to successfully convert steroids by Lee *et al.* (2014) [82], its potential value for steroid transformations was not thoroughly investigated. We focused on the differences between the subfamily members with respect to substrate binding, enzyme activity and product pattern, using a library of 23 steroids, from which 13 novel substrates were identified for CYP106A1 and 7 for CYP106A2. Difference spectroscopy was used to reveal the binding properties of all tested steroids towards the enzymes. Out of 23, only 4 (β-estradiol, estrone, pregnenolone and 17α-hydroxypregnenolone) did not display a type I shift, all with similar structural characteristics, an aromatic A-ring or a double bond between C5 and C6. However, due to the opposing results (type I shift) with another 3-hydroxy-Δ^5 steroid, dehydroepiandrostenedione, we could not draw an explicit conclusion about such structures. Despite the lack of spin shift induction, pregnenolone and 17α-hydroxypregnenolone were converted by both enzymes, coinciding with previous results and supporting that type I binding is an indication but not a necessity for conversion [100, 121-123]. The lack of spin-shift induction could be explained by the absence of a hydrogen bond acceptor in the case of the pregnenolone structure, which results in weaker binding to the heme iron and only partial displacement

of the water as sixth ligand. Regarding the aforementioned estrogens, neither type I shift nor a conversion were detected; most probably due to the lower flexibility of the aromatic A-ring interfering with the binding of the substrate [100]. 3-oxo-Δ^4-steroids were the first and for long the only known substrates described for CYP106A2. However, in our study we came across two exceptions, 19-hydroxyandrostenedione and adrenosterone, which despite the 3-oxo-Δ^4-moiety were not subjects for conversion. Since these steroids have a high structural similarity to the known substrate, androstenedione, the additional hydroxyl group at C19 or the keto-function at C11 may account for the unsuccessful conversion.

Subsequently, the substrates were narrowed down to those 6 (androstenedione, corticosterone, 11-deoxycorticosterone (DOC), 11-deoxycortisol (RSS), cortisol and cortisone) whose conversion revealed differences between the enzymes concerning the product pattern or activity. Binding studies demonstrated similar steroid affinities to both subfamily members as reflected by their dissociation constants (K_D). The strongest binding was observed for DOC (68 ± 2 µM with CYP106A1 and 50 ± 1 µM with CYP106A2) and androstenedione (77 ± 2 µM and 81 ± 10 µM, respectively) with both enzymes, while functionalized substrates at C11 or C17 showed fairly weak interactions.

Previously established whole-cell biocatalysts [81, 88] were applied for the biotransformations on a preparative scale, leading to a sufficient amount of products for structure elucidation by NMR. Concerning C21-steroids such as, DOC, RSS and cortisone, both subfamily members favored the 15β-hydroxylation. However, the CYP106A1 conversions were shown to be less selective in all cases producing additional mono- and dihydroxysteroids at 6β, 7β and 7β,15β positions. Such distinct behavior was also observed regarding androstenedione, where CYP106A2 formed the 15β-hydroxy compound as main product, while CYP106A1 produced only the 6β and 7β-hydroxy derivatives. In the literature, 6 and 7-substituted 1,4,6-androstatriene-3,17-diones have been described as suitable inhibitors of CYP19A1, the enzyme responsible for the development of post-menopausal breast cancer [124, 125]. The 6β and 7β-hydroxyandrostenediones produced by CYP106A1 could serve as precursors for further functionalization, the hydroxyl function being an easily accessible reaction site, thus, an important feature for drug design and development.

Even though most steroid hydroxylations took place at the B- and D-rings, the transformation of 11β-hydroxysteroids produced unexpected results: CYP106A1 performed the 11-dehydrogenation of both cortisol and corticosterone, whereas CYP106A2 demonstrated the same with corticosterone (yet still producing the 15β-hydroxy derivative as main metabolite). Besides the unprecedented CYP106A 11-oxidase activity, the transformation of cortisol to cortisone is also remarkable, since both steroid hormones have important roles as pharmaceutical agents: cortisone being widely used as a short-term pain killer and anti-inflammatory drug and cortisol applied as an immunosuppressive drug against severe allergic reactions. The production of cortisol at an industrial scale started in the 1940s, when it was proved to be an efficient treatment for symptoms of rheumatoid arthritis. Over the decades its production was reduced from a complex 31-step to an 11-step chemical synthesis in combination with microbial

bioconversion. Today, the industrial production of cortisone starts from stigmasterol through the 11α-hydroxylation of progesterone with *Rhizopus nigricans*, followed by the chemical modification to cortisol and then to cortisone. Another possibility is the chemical conversion of diosgenin to cortexolone, which is 11β-hydroxylated by *Curvularia lunata* to cortisol [35, 117]. However in each strategy the last reaction step leading to cortisone is still accomplished by synthetic chemistry. Even though microbial 11-oxidations were described from the 1950s, involving e.g. *Cunninghamella blakesleeana*, *Trichoteum roseum* and *Absidia regnieri*, none of these microbes were implemented for the last step of the industrial cortisone production [126]. We propose that the identified CYP106A 11-oxidase activity could serve as an alternative to the chemical reaction step. However, concerning the low selectivity of the reaction, additional protein engineering and strain optimization must be applied to enhance the 11-keto formation. To facilitate this, the homology model based on the CYP106A2 crystal structure [102] or the CYP106A1 crystal structure itself has to be attained. This could serve to define the substrate-interacting amino acids and provide a better understanding of the connection between high spin-shift induction and conversion of certain substrates. Additionally, based on our results, the steroid-hydroxylase and 11-oxidase function of the CYP106A subfamily could be further exploited by screening a steroid library including only high-value pharmaceuticals to target the efficient production of their hydroxy derivatives used as drugs or human drug metabolites.

In summary, the substrate array of the CYP106A subfamily was extended, revealing 13 new steroid substrates for CYP106A1 and 7 for CYP106A2. The latter was shown to be more selective towards the 15β-hydroxylation, whereas CYP106A1 produced hydroxy-metabolites at positions 6β, 7β, 9α and 15β. In addition, a previously unknown 11-oxidase activity of the CYP106A subfamily was observed during the conversion of 11β-hydroxysteroids. The selectively introduced hydroxyl groups in the steroid backbone makes these derivatives valuable as drug precursors or drug metabolites, stressing the advantage of the CYP106A subfamily over chemical approaches for the production of fine chemicals and pharmaceuticals.

The 11-oxidase activity observed for the CYP106A subfamily is uncommon for P450 catalysis. Such an 11-oxidation reaction was only suggested to occur for one other P450, CYP11B1, transforming cortisol to cortisone, yet, the mechanism was never investigated [127]. In **Chapter 2.2** we aimed to obtain a better understanding of the 11-dehydrogenation mechanism focusing on the CYP106A1 enzyme. Although CYP106A1 catalyzed the 11-oxidation of both corticosterone and cortisol, due to the multiple product formation observed in both transformations, none of these were considered suitable to study the kinetic solvent isotope effect (KSIE) on the reaction. Therefore, analogous substrates were probed with hydroxyl function at C-11 (prednisolone, dexamethasone and 11β-hydroxyandrostenedione (11-OH-AD)) to identify a suitable model reaction resulting in single product formation. The steroid conversions were carried out first *in vitro* then *in vivo* using resting whole-cells. Single product formation was only observed for 11-OH-AD, yet, all obtained product structures were elucidated in order to broaden

our understanding of the CYP106A1-mediated steroid transformations and to obtain functionalized glucocorticoids of potential pharmaceutical importance. The main products of dexamethasone and prednisolone were identified as the 15β-hydroxy compounds. Nevertheless, the 11-keto formation was also detected in both cases. Additionally, the formation of the main human metabolite, 6β-hydroxydexamethasone, was also observed, while in the case of prednisolone a 1(2)-double bond hydrogenation took place, speculated to be the outcome of an uncharacterized enzyme present in the *B. megaterium* MS941 strain.

The conversion of 11-OH-AD yielded a single 11-keto product, adrenosterone, hence this reaction was chosen to further investigate the mechanism using KSIE. The conversion was performed, first in protiated, then in deuterated buffer system, displaying a 2.25 times faster product formation upon H/D exchange. This corresponds to an inverse KSIE (k_H/k_D) of 0.44, suggesting the involvement of the ferric peroxoanion in the 11-oxidation. Since the P450-mediated 11-oxidation of steroids was studied here for the first time, similar alcohol-oxidations by P450s described in literature have been considered for possible equivalents. For this purpose, the microsomal cyclohex-2-en-1-ol oxidation [128], the CYP3A11-dependent hydroxy-Δ^8-tetrahydrocannabinol conversion [129] and the CYP2E1 mediated ethanol oxidation [130] were reviewed. In all these cases the gem-diol and the combination of gem-diol and double hydrogen abstraction pathways were suggested for the mechanism, propounding Cpd I as reactive intermediate. These propositions are analogous to standard P450-mediated hydroxylations, which are believed to proceed through the Cpd I-mediated H-rebound mechanism [131-133]. However, the involvement of Cpd I seems not to be reconcilable with our observations concerning the 11-oxidation, which suggests the involvement of the ferric peroxoanion.

To exclude the influence of the unproductive pathways and the potential H_2O_2-mediated substrate oxidation (reverse peroxide shunt), the *in vitro* conversions were performed with the addition of radical scavengers and in the presence of H_2O_2 or cumene hydroperoxide. The presence of radical scavengers did not alter the catalytic rate compared to the rate observed in the protiated system, while with H_2O_2 or cumene hydroperoxide no conversion was detected. These results exclude the influence of a slower uncoupling reaction rate in deuterated buffer on the KSIE, thus suggesting that the catalysis takes place with the help of the ferric peroxo intermediate via a nucleophilic attack at C11 hydroxyl function.

To sum up, in **Chapter 2.2**, we present three novel substrates (prednisolone, dexamethasone and 11-OH-AD) for the 11-oxidation by CYP106A1. Single 11-keto product formation was found for 11-OH-AD, while prednisolone and dexamethasone displayed 6β- and 15β-hydroxylated derivatives, besides the 11-keto product. Since hydroxysteroids are well-suited precursors for further steroid functionalization, the production of such derivatives using CYP106A1 is considered to be a promising approach for the pharmaceutical industry. The selective conversion of 11-OH-AD was chosen to further investigate the 11-oxidation mechanism. An inverse KSIE was observed in the catalytic activity, indicating for the first time the ferric peroxoanion as reactive intermediate in a P450-mediated oxidation.

The involvement of the ferric peroxo species was based on the experimental results obtained from the KSIE in this study. However, further evidence could be provided by spectroscopic characterization (e.g.: electron paramagnetic resonance, X-ray, raman resonance etc.) of the reactive intermediate, also serving as an interesting topic for future research [134, 135]. As for further follow-up experiments, a broader library of 11-hydroxysteroid analogues could be screened, targeting only substrates with known and valuable 11-keto metabolites. Besides, by obtaining the CYP106A1 homology model/crystal structure, computational substrate docking studies may help to define amino acids which potentially influence enzyme activity/specificity. Consequently, via the production of rationally designed mutants, the selectivity of the 11-oxidation could be improved. In lack of mechanistic and structural data, the mutants could be produced by directed evolution. To provide a rapid preliminary screening method of the forthcoming CYP106A1 mutants, suitable for the analysis of the cortisol-cortisone turnover, a fluorimetric assay developed by Appel *et al.* (2005) [136] has been established (**Appendix 5.1**).

Finally, with the aim of establishing a model for potential industrial scale P450-biocatalysis, the CYP106A2 based *B. megaterium* MS941 system was applied for the conversion of cyproterone acetate (CPA) in a collaborative project with the Technical University of Denmark (**Chapter 2.3**). CPA is a synthetic derivative of 17α-hydroxyprogesterone, an anti-androgen with additional progestogen and antigonadotropic properties. It has been long used in the treatment of prostate cancer to control severe hypersexuality in males, as well as for the treatment of hirsutism and acne in females and as a component of oral contraceptive pills (Diane 35 or Bella Hexal 35 in Germany) [137-140].

The synthetic antiandrogen was first transformed under *in vitro* conditions using purified CYP106A2 enzyme, followed by the *in vivo* conversion with a recombinant *B. megaterium* whole-cell system, in which CYP106A2 was overexpressed with the autologous redox partners present in the MS941 strain. The single conversion product was then purified using reverse phase HPLC and the subsequent NMR characterization confirmed the structure of 15β-hydroxycyproterone acetate (15β-OH-CPA), also known as the main human metabolite. The product retained anti-androgen activity but only 10 % progestogen potency of CPA, which makes it a potentially better option for the treatment of solely androgen-induced problems, particularly in males [141]. To evaluate the potentially altered pharmaceutical effect of 15β-OH-CPA, the cell growth and drug sensitivity of the human prostate carcinoma cell line, LNCaP, was investigated using an XTT cell proliferation assay (**Appendix 5.2**).

Besides its potential pharmaceutical value, another motivation for its alternative process development was the significant price difference between the substrate and the product, the latter being 375 fold more expensive (Santa Cruz Biotechnology, http://www.scbt.com/, 2015). This suggests a rather pricy process, however, detailed information about the production is not available. Considering the product's pharmaceutical importance and presumed costly current production, our goal was to perform a scale-up of the selective 15β-oxidation of CPA from shake flasks to laboratory scale bioreactors. To improve the process performance, working towards a future large-scale production of 15β-OH-CPA, we

identified and addressed the limitations associated with the catalyst and the reaction. To recognize the bottlenecks we reviewed and analyzed the already described difficulties associated with P450 whole-cell applications [29, 40]:

- Transcellular transport limitation
- Cofactor (NADP(H)) limitation
- Substrate/product inhibition and/or toxicity
- Poor substrate/product solubility

B. megaterium MS941 has proven to be a stable host organism providing a protective environment for the CYP106A2 enzyme. Following the conversion of CPA, both, substrate and product, were found to be in the cell pellet fraction, either inside or attached to the cell membrane. The increase of the biocatalyst concentration during the reaction time did not improve the yield, possibly due to the fast substrate uptake into the cells. The recycling of the catalyst was also examined, on one hand to improve the biocatalyst yield and on the other hand to decrease the cost contribution of the catalyst. The removal of the attached product was attempted by washing the cells either with buffer or organic solvents (ethyl acetate and decanol). Washing with buffer showed no effect on product elimination, while the organic solvents damaged the catalyst resulting in no or limited further activity.

The transport limitation across the cell membrane was probed using different membrane permeabilization methods (freeze-thawing, ultrasonication, acetone treatment) in combination with stoichiometric amounts of cofactor addition. Neither the permeabilization nor the cofactor addition had any influence on the conversion rates compared with the untreated control cells, which lead to the conclusion that the *B. megaterium* cells show no hindrance of transcellular transport and that the cellular cofactor regeneration is sufficient not to limit catalysis.

The inhibitory effects of substrate and product were investigated under *in vitro* and *in vivo* conditions. The increasing substrate concentration had no effect on the initial rate. However, the reactions seemed to stop, following an approximate 300 µM substrate consumption, consistent with the results of the product inhibition studies, indicating hindered catalytic activity above a product concentration of 200 µM. The stability of the biocatalyst, an important factor in assessing the economic feasibility of the bioprocess, was examined under process conditions as well as throughout the storage of the cells. Monitoring the cell dry weight and the P450 concentration during the transformation, a significant loss in the correctly folded P450 concentration was observed after 4 h of conversion, while the *Bacillus* cells seemed to remain undamaged. During 7 days of storage, no substantial loss in activity was found compared to conversion made with freshly harvested cells.

Concluding our preliminary studies, the main bottlenecks of the reaction were identified as:

- limited P450 stability (under process conditions)
- low overall solubility of the reactants
- product inhibition

To identify the best mode of operation for the process, we performed the biotransformation using both, resting and growing cells, keeping in mind that the instability of the CYP106A2 enzyme might be a limiting factor in the process. Interestingly, our results showed no significant difference between growing and resting cells in terms of conversion rate, whole-cell or P450 stability. The latter lead to the conclusion, that the preferred operation mode, being economically favorable, time- and labor-saving, is the use of growing cells.

The poor solubility of the reactants was addressed by alternative substrate feeding strategies, by adding the solid substrate to the system, dissolving the substrate in water-immiscible solvents (diisononylphtalate and hexadecane) or aqueous CD solution. The solid feeding of the substrate did not succeed, most likely due to the low dissolution rate of the substrate. The use of water-immiscible organic solvents did not improve the reaction performance either, owing to the strong hydrophobic character of the solvents hampering the substrate partitioning to the aqueous phase, thus limiting the catalytic reaction. Our ultimate approach was the application of the aqueous solution of a CD derivative, 2-HP-β-CD. Functionalized CD derivatives were already described in the literature to enhance steroid conversion by solubilizing hydrophobic substrates, increasing the cell-wall permeability, transcellular transport and supporting cell growth [106]. Besides resolving solubility issues, CDs were shown to have an effect on the potential substrate and/or product inhibition by forming a complex with the respective compound, thus lowering its local concentration [55, 142]. The 2-HP-β-CD derivative was selected due to its highly efficient steroid solubilizing capacity [143], its relatively low influence on cell growth, no denaturing effect on proteins, no enzyme inhibition and reasonable price [144, 145].

The transformation of CPA was performed first in shake flasks and subsequently in the bioreactor, applying CD as solubilizing agent, parallel to the organic solvent DMSO, used for the control reactions. The shake flask conversions using CD showed only a moderate (~10 %) improvement in the relative conversion compared to the DMSO control. Interestingly, applying the same strategy in the bioreactor resulted in an almost complete (~98 %) substrate conversion on a 400 mL scale, representing a 43 % improvement of the relative conversion compared to the control reaction. The undoubtable improvement achieved in the bioreactor also highlights the added value of the reactor configuration providing a controlled environment and easily scalable system. The increased mixing and aeration could contribute to the enhancement of the reaction rate resulting in improved mass transfer of the poorly soluble substrate. Based on these observations, we stress the advantage of process development in the final reactor configuration, in our case, using a small-scale stirred tank reactor instead of shake flasks.

To conclude, in **Chapter 2.3** we were able to present the successful process development of 15β-hydroxycyproterone acetate production based on a systematic strategy involving the identification and a step by step analysis of the reaction bottlenecks. As a result, we were able to attain an almost complete substrate conversion resulting in a 0.43 g/L product concentration at a 400 mL scale using 2-HP-β-CD as solubilizing agent. Although these results provide a stable basis for a possible industrial-scale application of CYP106A2, to achieve the recommended target values for an economically feasible

industrial production (final product concentration of 20 g/L and space-time yield of 2 g/L/h) there is still room for further optimization [40]. Future challenges could include the investigation of further, chemically modified CD derivatives such as methyl-CD, permethyl-β-CD or other hydroxypropyl-CDs which could increase the concentration of steroids in aqueous medium to 20 g/L or higher [146, 147]. Optimizing the transformation using the best possible CD candidate would allow us to reach higher substrate concentrations, resulting in enhanced reaction yields and ultimately to get closer to the above stated economic targets.

4. List of abbreviations

11-OH-AD	11β-hydroxyandrostenedione
15-OH-CPA	15β-hydroxycyproterone acetate
2-HP-β-CD	2-hydroxypropyl-β-cyclodextrin
B. megaterium	*Bacillus megaterium*
CD	Cyclodextrin
CPA	Cyproterone acetate
Cpd 0	Compound 0
Cpd I	Compound I
CPR	Cytochrome P450 reductase
CTS	Charcoal treated/stripped serum
DHT	Dihydrotestosterone
DMSO	Dimethyl sulfoxide
DOC	11-deoxycorticosterone
E. coli	*Escherichia coli*
EDTA	Ethylenediaminetetraacetic acid
FAD	Flavin adenine dinucleotide
FBS	Fetal bovine serum
FMN	Flavin mononucleotide
HPLC	High performance Liquid chromatography
K_D	Dissociation constant
KSIE	Kinetic solvent isotope effect
NAD(P)H	Nicotinamide adenine dinucleotide (phosphate)
NMR	Nuclear magnetic resonance
P450	Cytochrome P450
RSS	11-deoxycortisol/Reichstein's substance S
S. cerevisiae	*Saccharomyces cerevisiae*
SRS	Substrate recognition site

5. Appendix

5.1. Investigating the applicability of a fluorescence assay for the analysis of cortisol-cortisone turnover by CYP106A1

To provide a suitable analysis for the cortisol-cortisone turnover and a rapid preliminary screening method of the forthcoming CYP106A1 mutants with altered 11-oxidase activity, a fluorimetric assay developed by Appel *et al.* (2005) [136] has been implemented. The assay is based on the formation of a fluorescent charged resonance complex when cortisol is incubated with the mixture of sulfuric acid and acetic acid. The strong fluorescence of cortisol was attributed to the carbonium ion formation at C11 and the C3 keto group protonation upon sulfuric acid addition. In the case of 11-deoxycortisol, only a minor fluorescence was detected, resulting from the C3 keto group protonation, since the structure lacks a functional group at C11.

Based on these results, our intention was to find out, whether any difference could be detected in the fluorescence behavior of cortisol and cortisone, which could form the basis of the 11-oxidation analysis. The steroids were incubated in isobutyl methyl ketone in a black, acid-resistant 96-well microplate with an acid mixture (90:10 sulfuric / acetic acid) for fluorescence development. The excitation (300-520 nm) and emission spectra (510-700 nm) of the steroids were measured with constant emission (λ_{em} 530 nm) and excitation wavelengths (λ_{ex} 490 nm), respectively, to detect the different fluorescent behavior of cortisol and its CYP106A1-dependent product, cortisone.

Cortisone showed a significantly lower relative fluorescence intensity (R.F.U.) than cortisol (**Figure A1**). Such behavior can be explained by the presence of the 11-oxo-function of cortisone, which alters the intensity and characteristics of the resulting fluorescence spectra.

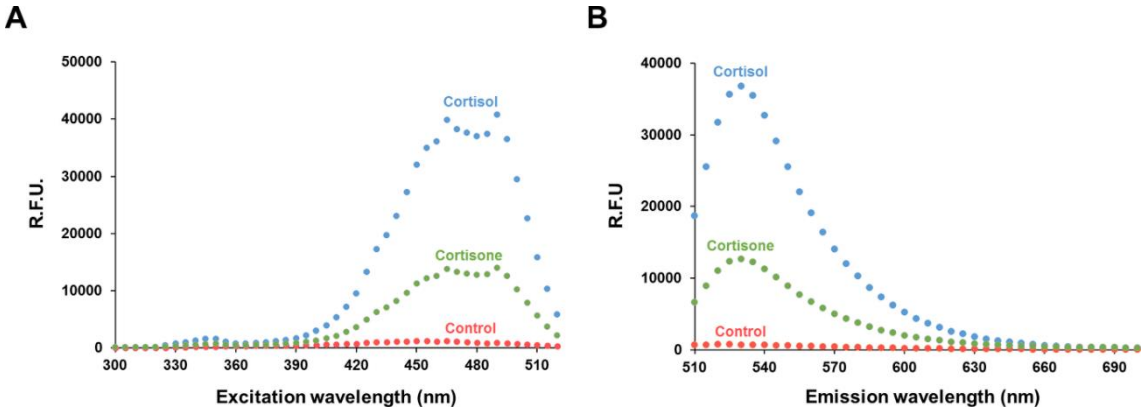

Figure A1 - Excitation (A) and emission (B) spectra of the fluorescent cortisol (blue) and cortisone (green) complexes formed in the acidic medium in comparison to the steroid-free control (red). The spectra were recorded with a constant emission wavelength of 530 nm and an excitation wavelength of 490 nm, respectively.

The differences between the substrate and product allow the detection of the changes in conversion efficiency. This makes this assay suitable for the screening of mutants with improved

11-oxidation activity reflected by their decreasing fluorescence. Although the assay does not diminish the potential selection of false positive mutants, it still serves as a fast and reliable first filter for the evaluation of mutants followed by a more precise HPLC analysis.

5.2. XTT-based cell proliferation assay using the LNCaP cell line, cyproterone acetate and its product

To get an insight into the possibly altered effect of the 15β-OH-CPA on tumor cells, the cell growth and drug sensitivity of the human prostate carcinoma cell line, LNCaP, were probed using an XTT cell proliferation assay kit (Sigma-Aldrich, Germany). The LNCaP cells have been isolated from a metastatic lesion of human prostate cancer and have been applied for long as an experimental model to assess new hormonal therapies [148]. The cell line has been considered to be androgen-dependent and shown to be inhibited by antiandrogens *in vitro* [149].

The effect of CPA, 15β-OH-CPA and dihydrotestosterone (DHT), an androgen hormone with high androgen receptor affinity found in the prostate, was tested on the LNCaP cells. The cell proliferation was investigated in 96-well tissue culture plates. Half of the cells were cultivated in RPMI 1640 medium containing 5 % fetal bovine serum (FBS), while the other half was fed with the same medium supplemented with 5 % charcoal-treated serum (CTS), depleted of steroid hormones. 48 h after seeding and attachment of the cells, the medium was replaced containing increasing concentrations (0.01 nM to 10 μM) of the corresponding steroid dissolved in DMSO. The untreated control was supplemented only with DMSO. The cells were incubated for 7 days prior to the XTT assay.

The DHT treatment correlated with the earlier results from Horoszewicz *et al*. [148], which have shown that DHT stimulates cell proliferation in CTS-containing media but shows a dose-dependent suppression of cell proliferation in media with FBS. Surprisingly, CPA and 15β-OH-CPA had no significant effect on the cell proliferation in either of the used media compared to the control. However, since the absorbance readings of the assay were too low in all the cases, a clear conclusion about the differences was not possible. Despite increasing the cell numbers per well and prolonging incubation time with the XTT reagent, no improvement was achieved. Therefore, further studies are necessary to evaluate possible differences in the action of CPA and its product, 15β-OH-CPA, which was proposed to have great potential as an alternative antiandrogen drug.

6. References

1. Nelson, D. R. (2013) A world of cytochrome P450s, *Philosophical Transactions of the Royal Society of London B: Biological Sciences.* **368**.
2. Urlacher, V. B. & Eiben, S. (2006) Cytochrome P450 monooxygenases: perspectives for synthetic application, *Trends in biotechnology.* **24**, 324-330.
3. Werck-Reichhart, D. & Feyereisen, R. (2000) Cytochromes P450: a success story, *Genome Biology.* **1**, reviews 3003.1–3003.9.
4. Bernhardt, R. (2006) Cytochromes P450 as versatile biocatalysts, *Journal of Biotechnology.* **124**, 128-145.
5. Brodie, B. B., Axelrod, J., Cooper, J. R., Gaudette, L., La Du, B. N., Mitoma, C. & Udenfriend, S. (1955) Detoxication of drugs and other foreign compounds by liver microsomes, *Science.* **121**, 603-604.
6. Axelrod, J. (1955) The enzymatic demethylation of ephedrine *Journal of Pharmacology and Experimental Therapeutics.* **114**, 430-438.
7. Klingenberg, M. (1958) Pigments of rat liver microsomes, *Archives of Biochemistry and Biophysics.* **75**, 376-386.
8. Garfinkel, D. (1958) Studies on pig liver microsomes. I. Enzymic and pigment composition of different microsomal fractions, *Archives of Biochemistry and Biophysics.* **77**, 493-509.
9. Omura, T. & Sato, R. (1962) A New Cytochrome in Liver Microsomes, *Journal of Biological Chemistry.* **237**, 1375-1376.
10. Ichikawa, Y., Hiwatashi, A. & Yamano, T. (1978) Behaviors on NAD(P)H-reduction and their magnetic absorptions of multiple molecular forms of cytochromes P-450 and P-448, *Medical journal of Osaka University.* **28**, 205-214.
11. Palmer, G. & Reedijk, J. (1991) Nomenclature Committee of the International Union of Biochemistry (NC-IUB). Nomenclature of electron-transfer proteins. Recommendations 1989, *Biochimica et Biophysica Acta.* **1060**, 599-611.
12. Nebert, D. W., Nelson, D. R., Adesnik, M., Coon, M. J., Estabrook, R. W., Gonzalez, F. J., Guengerich, F. P., Gunsalus, I. C., Johnson, E. F. & Kemper, B. (1989) The P450 superfamily: updated listing of all genes and recommended nomenclature for the chromosomal loci, *DNA.* **8**, 1-13.
13. Hannemann, F., Bichet, A., Ewen, K. M. & Bernhardt, R. (2007) Cytochrome P450 systems--biological variations of electron transport chains, *Biochimica et Biophysica Acta.* **1770**, 330-344.
14. Bernhardt, R. (1996) Cytochrome P450: structure, function, and generation of reactive oxygen species, *Reviews of Physiology, Biochemistry and Pharmacology.* **127**, 137-221.
15. Gunsalus, I. C. & Sligar, S. G. (1978) Oxygen reduction by the P450 monoxygenase systems, *Advances in Enzymology and Related Areas in Molecular Biology.* **47**, 1-44.
16. Lambeth, J. D., Geren, L. M. & Millett, F. (1984) Adrenodoxin interaction with adrenodoxin reductase and cytochrome P-450scc. Cross-linking of protein complexes and effects of adrenodoxin modification by 1-ethyl-3-(3-dimethylaminopropyl)carbodiimide, *Journal of Biological Chemistry.* **259**, 10025-10029.
17. Hanukoglu, I. (1996) Electron transfer proteins of cytochrome P450 systems, *Advances in Molecular and Cell Biology.* **14**, 29-55.
18. Graham, S. E. & Peterson, J. A. (1999) How Similar Are P450s and What Can Their Differences Teach Us?, *Archives of Biochemistry and Biophysics.* **369**, 24-29.
19. Presnell, S. R. & Cohen, F. E. (1989) Topological distribution of four-alpha-helix bundles, *Proceedings of the National Academy of Sciences of the United States of America.* **86**, 6592-6596.
20. Nelson, D. R., Koymans, L., Kamataki, T., Stegeman, J. J., Feyereisen, R., Waxman, D. J., Waterman, M. R., Gotoh, O., Coon, M. J., Estabrook, R. W., Gunsalus, I. C. & Nebert, D. W. (1996) P450

superfamily: update on new sequences, gene mapping, accession numbers and nomenclature, *Pharmacogenetics.* **6**, 1-42.

21. Denisov, I. G., Makris, T. M., Sligar, S. G. & Schlichting, I. (2005) Structure and Chemistry of Cytochrome P450, *Chemical Reviews.* **105**, 2253-2278.
22. Poulos, T. L., Finzel, B. C. & Howard, A. J. (1987) High-resolution crystal structure of cytochrome P450cam, *Journal of molecular biology.* **195**, 687-700.
23. Peterson, J. A. & Graham, S. E. (1998) A close family resemblance: the importance of structure in understanding cytochromes P450, *Structure.* **6**, 1079-1085.
24. Gotoh, O. (1992) Substrate recognition sites in cytochrome P450 family 2 (CYP2) proteins inferred from comparative analyses of amino acid and coding nucleotide sequences, *Journal of Biological Chemistry.* **267**, 83-90.
25. Pochapsky, T., Kazanis, S. & Dang, M. (2010) Conformational Plasticity and Structure/Function Relationships in Cytochromes P450, *Antioxidants and Redox Signaling.* **13**, 1273-1296.
26. Koshland, D. E. (1958) Application of a Theory of Enzyme Specificity to Protein Synthesis, *Proceedings of the National Academy of Sciences of the United States of America.* **44**, 98-104.
27. Makris, T. M., Davydov, R., Denisov, I. G., Hoffman, B. M. & Sligar, S. G. (2002) Mechanistic Enzymology of Oxygen Activation by the Cytochromes P450 *Drug Metabolism Reviews.* **34**, 691-708.
28. Matsunaga, I., Yamada, A., Lee, D.-S., Obayashi, E., Fujiwara, N., Kobayashi, K., Ogura, H. & Shiro, Y. (2002) Enzymatic Reaction of Hydrogen Peroxide-Dependent Peroxygenase Cytochrome P450s: Kinetic Deuterium Isotope Effects and Analyses by Resonance Raman Spectroscopy, *Biochemistry.* **41**, 1886-1892.
29. Bernhardt, R. & Urlacher, V. B. (2014) Cytochromes P450 as promising catalysts for biotechnological application: chances and limitations, *Applied microbiology and biotechnology.* **98**, 6185-6203.
30. Urlacher, V. B. & Girhard, M. (2012) Cytochrome P450 monooxygenases: an update on perspectives for synthetic application, *Trends in biotechnology.* **30**, 26-36.
31. Julsing, M., Cornelissen, S., Buhler, B. & Schmid, A. (2008) Heme-iron oxygenases: powerful industrial biocatalysts?, *Current Opinion in Chemical Biology.* **12**, 177-186.
32. Ortiz de Montellano, P. R. (2010) Hydrocarbon Hydroxylation by Cytochrome P450 Enzymes, *Chemical Reviews.* **110**, 932-948.
33. Schulz, S., Girhard, M. & Urlacher, V. B. (2012) Biocatalysis: Key to Selective Oxidations, *ChemCatChem.* **4**, 1889-1895.
34. Chefson, A. & Auclair, K. (2006) Progress towards the easier use of P450 enzymes, *Molecular BioSystems.* **2**, 462-469.
35. Urlacher, V. (2014) Catalysis with Cytochrome P450 monooxygenases in *Handbook of Green Chemistry* (Cabtree, R. & Anastas, P., eds), John Wiley & Sons.
36. Labinger, J. A. (2004) Selective alkane oxidation: Hot and cold approaches to a hot problem, *Journal of Molecular Catalysis.* **220**, 27-35.
37. Bornscheuer, U. T. & Buchholz, K. (2005) Highlights in Biocatalysis – Historical Landmarks and Current Trends, *Engineering in Life Sciences.* **5**, 309-323.
38. Grogan, G. (2011) Cytochromes P450: exploiting diversity and enabling application as biocatalysts, *Current Opinion in Chemical Biology.* **15**, 241-248.
39. O'Reilly, E., Kohler, V., Flitsch, S. L. & Turner, N. J. (2011) Cytochromes P450 as useful biocatalysts: addressing the limitations, *Chemical Communications.* **47**, 2490-2501.
40. Lundemo, M. T. & Woodley, J. M. (2015) Guidelines for development and implementation of biocatalytic P450 processes, *Applied microbiology and biotechnology.* **99**, 2465-2483.
41. Kelly, S. L. & Kelly, D. E. (2013) Microbial cytochromes P450: biodiversity and biotechnology. Where do cytochromes P450 come from, what do they do and what can they do for us?, *Philosophical Transactions of the Royal Society B: Biological Sciences.* **368**, 20120476.

42. Sakaki, T. (2012) Practical Application of Cytochrome P450, *Biological and Pharmaceutical Bulletin.* **35**, 844-849.

43. van Beilen, J. B., Duetz, W. A., Schmid, A. & Witholt, B. (2003) Practical issues in the application of oxygenases, *Trends in biotechnology.* **21**, 170-177.

44. Cornelissen, S., Julsing, M. K., Volmer, J., Riechert, O., Schmid, A. & Bühler, B. (2013) Whole-cell-based CYP153A6-catalyzed (S)-limonene hydroxylation efficiency depends on host background and profits from monoterpene uptake via AlkL, *Biotechnology and Bioengineering.* **110**, 1282-1292.

45. Chen, R. R. (2007) Permeability issues in whole-cell bioprocesses and cellular membrane engineering, *Applied microbiology and biotechnology.* **74**, 730-738.

46. Grant, C., Woodley, J. M. & Baganz, F. (2011) Whole-cell bio-oxidation of n-dodecane using the alkane hydroxylase system of *P. putida* GPo1 expressed in *E. coli*, *Enzyme and Microbial Technology.* **48**, 480-486.

47. Julsing, M. K., Schrewe, M., Cornelissen, S., Hermann, I., Schmid, A. & Bühler, B. (2012) Outer Membrane Protein AlkL Boosts Biocatalytic Oxyfunctionalization of Hydrophobic Substrates in *Escherichia coli*, *Applied and Environmental Microbiology.* **78**, 5724-5733.

48. Zehentgruber, D., Hannemann, F., Bleif, S., Bernhardt, R. & Lütz, S. (2010) Towards preparative scale steroid hydroxylation with cytochrome P450 monooxygenase CYP106A2, *Chembiochem.* **11**, 713-721.

49. Schewe, H., Kaup, B.-A. & Schrader, J. (2008) Improvement of P450BM-3 whole-cell biocatalysis by integrating heterologous cofactor regeneration combining glucose facilitator and dehydrogenase in *E. coli*, *Applied microbiology and biotechnology.* **78**, 55-65.

50. Cornelissen, S., Liu, S., Deshmukh, A., Schmid, A. & Bühler, B. (2011) Cell physiology rather than enzyme kinetics can determine the efficiency of cytochrome P450-catalyzed C–H-oxyfunctionalization, *Journal of Industrial Microbiology & Biotechnology.* **38**, 1359-1370.

51. Eastburn, S. D. & Tao, B. Y. (1994) Applications of modified cyclodextrins, *Biotechnology Advances.* **12**, 325-339.

52. Shen, Y., Liang, J., Li, H. & Wang, M. (2015) Hydroxypropyl-β-cyclodextrin-mediated alterations in cell permeability, lipid and protein profiles of steroid-transforming *Arthrobacter simplex*, *Applied microbiology and biotechnology.* **99**, 387-397.

53. Brewster, M. E. & Loftsson, T. (2007) Cyclodextrins as pharmaceutical solubilizers, *Advanced Drug Delivery Reviews.* **59**, 645-666.

54. Fokina, V. V., Karpov, A. V., Sidorov, I. A., Andrjushina, V. A. & Arinbasarova, A. Y. (1997) The influence of β-cyclodextrin on the kinetics of 1-en-dehydrogenation of 6α-methylhydrocortisone by *Arthrobacter globiformis* cells, *Applied microbiology and biotechnology.* **47**, 645-649.

55. Roglič, U., Plazl, I. & Žnidaršič-Plazl, P. (2007) Batch and continuous transformation of progesterone by *Rhizopus nigricans* pellets in the presence of β-cyclodextrin, *Biocatalysis and Biotransformation.* **25**, 16-23.

56. Jadoun, J. & Bar, R. (1993) Microbial transformations in a cyclodextrin medium. Part 4. Enzyme vs microbial oxidation of cholesterol, *Applied microbiology and biotechnology.* **40**, 477-482.

57. Jadoun, J. & Bar, R. (1993) Microbial transformations in a cyclodextrin medium. Part 3. Cholesterol oxidation by *Rhodococcus erythropolis*, *Applied microbiology and biotechnology.* **40**, 230-240.

58. Singh, M., Sharma, R. & Banerjee, U. C. (2002) Biotechnological applications of cyclodextrins, *Biotechnology Advances.* **20**, 341-359.

59. Ro, D.-K., Paradise, E. M., Ouellet, M., Fisher, K. J., Newman, K. L., Ndungu, J. M., Ho, K. A., Eachus, R. A., Ham, T. S., Kirby, J., Chang, M. C. Y., Withers, S. T., Shiba, Y., Sarpong, R. & Keasling, J. D. (2006) Production of the antimalarial drug precursor artemisinic acid in engineered yeast, *Nature.* **440**, 940-943.

60. Ajikumar, P. K., Xiao, W.-H., Tyo, K. E. J., Wang, Y., Simeon, F., Leonard, E., Mucha, O., Phon, T. H., Pfeifer, B. & Stephanopoulos, G. (2010) Isoprenoid Pathway Optimization for Taxol Precursor Overproduction in *Escherichia coli*. *Science.1191652*.**330**, 70-74.

61. Duport, C., Spagnoli, R., Degryse, E. & Pompon, D. (1998) Self-sufficient biosynthesis of pregnenolone and progesterone in engineered yeast, *Nature Biotechnology*. **16**, 186-189.

62. Szczebara, F. M., Chandelier, C., Villeret, C., Masurel, A., Bourot, S., Duport, C., Blanchard, S., Groisillier, A., Testet, E., Costaglioli, P., Cauet, G., Degryse, E., Balbuena, D., Winter, J., Achstetter, T., Spagnoli, R., Pompon, D. & Dumas, B. (2003) Total biosynthesis of hydrocortisone from a simple carbon source in yeast, *Nature Biotechnology*. **21**, 143-149.

63. Petzoldt, K., Annen, K., Laurent, H. & Wiechert, R. (1982) Process for the preparation of 11-beta-hydroxy steroids in *Schering Aktiengesellschaft* (Patent, U., ed) Germany.

64. Serizawa, N. & Matsuoka, T. (1991) A two component-type cytochrome P-450 monooxygenase system in a prokaryote that catalyzes hydroxylation of ML-236B to pravastatin, a tissue-selective inhibitor of 3-hydroxy-3-methylglutaryl coenzyme A reductase, *Biochimica et Biophysica Acta.* **1084**, 35-40.

65. Watanabe, I., Nara, F. & Serizawa, N. (1995) Cloning, characterization and expression of the gene encoding cytochrome P-450sca-in2 from *Streptomyces carbophilus* involved in production of pravastatin, a specific HMG-CoA reductase inhibitor, *Gene*. **163**, 81-85.

66. Sawada, N., Sakaki, T., Yoneda, S., Kusudo, T., Shinkyo, R., Ohta, M. & Inouye, K. (2004) Conversion of vitamin D3 to 1α,25-dihydroxyvitamin D3 by *Streptomyces griseolus* cytochrome P450SU-1, *Biochemical and biophysical research communications.* **320**, 156-164.

67. Hayashi, K., Sugimoto, H., Shinkyo, R., Yamada, M., Ikeda, S., Ikushiro, S., Kamakura, M., Shiro, Y. & Sakaki, T. (2008) Structure-Based Design of a Highly Active Vitamin D Hydroxylase from *Streptomyces griseolus* CYP105A1, *Biochemistry*. **47**, 11964-11972.

68. Katsumoto, Y., Fukuchi-Mizutani, M., Fukui, Y., Brugliera, F., Holton, T. A., Karan, M., Nakamura, N., Yonekura-Sakakibara, K., Togami, J., Pigeaire, A., Tao, G.-Q., Nehra, N. S., Lu, C.-Y., Dyson, B. K., Tsuda, S., Ashikari, T., Kusumi, T., Mason, J. G. & Tanaka, Y. (2007) Engineering of the Rose Flavonoid Biosynthetic Pathway Successfully Generated Blue-Hued Flowers Accumulating Delphinidin, *Plant and Cell Physiology*. **48**, 1589-1600.

69. Holton, T. A., Brugliera, F., Lester, D. R., Tanaka, Y., Hyland, C. D., Menting, J. G. T., Lu, C.-Y., Farcy, E., Stevenson, T. W. & Cornish, E. C. (1993) Cloning and expression of cytochrome P450 genes controlling flower colour, *Nature*. **366**, 276-279.

70. Schroer, K., Kittelmann, M. & Lütz, S. (2010) Recombinant human cytochrome P450 monooxygenases for drug metabolite synthesis, *Biotechnology and Bioengineering.* **106**, 699-706.

71. Vary, P., Biedendieck, R., Fuerch, T., Meinhardt, F., Rohde, M., Deckwer, W.-D. & Jahn, D. (2007) *Bacillus megaterium* - from simple soil bacterium to industrial protein production host, *Applied microbiology and biotechnology*. **76**, 957-967.

72. David, F., Westphal, R., Bunk, B., Jahn, D. & Franco-Lara, E. (2010) Optimization of antibody fragment production in Bacillus megaterium: The role of metal ions on protein secretion, *Journal of Biotechnology*. **150**, 115-124.

73. Korneli, C., David, F., Biedendieck, R., Jahn, D. & Wittmann, C. (2013) Getting the big beast to work—Systems biotechnology of *Bacillus megaterium* for novel high-value proteins, *Journal of Biotechnology*. **163**, 87-96.

74. Biedendieck, R., Borgmeier, C., Bunk, B., Stammen, S., Scherling, C., Meinhardt, F., Wittmann, C. & Jahn, D. (2011) Chapter ten - Systems Biology of Recombinant Protein Production Using *Bacillus megaterium* in *Methods in Enzymology* (Daniel Jameson, M. V. & Hans, V. W., eds) pp. 165-195, Academic Press.

75. Jordan, E., Hust, M., Roth, A., Biedendieck, R., Schirrmann, T., Jahn, D. & Dubel, S. (2007) Production of recombinant antibody fragments in *Bacillus megaterium*, *Microbial Cell Factories.* **6**, 2.

76. Stammen, S., Müller, B. K., Korneli, C., Biedendieck, R., Gamer, M., Franco-Lara, E. & Jahn, D. (2010) High-Yield Intra- and Extracellular Protein Production Using *Bacillus megaterium*, *Applied and Environmental Microbiology*. **76**, 4037-4046.

77. Korneli, C., Bolten, C. J., Godard, T., Franco-Lara, E. & Wittmann, C. (2012) Debottlenecking recombinant protein production in *Bacillus megaterium* under large-scale conditions—targeted precursor feeding designed from metabolomics, *Biotechnology and Bioengineering.* **109**, 1538-1550.

78. He, J. S. & Fulco, A. J. (1991) A barbiturate-regulated protein binding to a common sequence in the cytochrome P450 genes of rodents and bacteria, *Journal of Biological Chemistry*. **266**, 7864-7869.

79. Whitehouse, C. J. C., Bell, S. G. & Wong, L.-L. (2012) P450BM3 (CYP102A1): connecting the dots, *Chemical Society Reviews.* **41**, 1218-1260.

80. He, J., Ruettinger, R., Liu, H. & Fulco, A. (1989) Molecular cloning, coding nucleotides and the deduced amino acid sequence of P-450BM-1 from *Bacillus megaterium*., *Biochimica et Biophysica Acta.* **1009**, 301-303.

81. Brill, E., Hannemann, F., Zapp, J., Bruning, G., Jauch, J. & Bernhardt, R. (2014) A new cytochrome P450 system from *Bacillus megaterium* DSM319 for the hydroxylation of 11-keto-beta-boswellic acid (KBA), *Applied microbiology and biotechnology.* **98**, 1701-1717.

82. Lee, G.-Y., Kim, D.-H., Kim, D., Ahn, T. & Yun, C.-H. (2014) Functional characterization of steroid hydroxylase CYP106A1 derived from *Bacillus megaterium*, *Archives of Pharmacal Research.* 1-10.

83. Berg, A., Gustafsson, J. & Ingelman-Sundberg, M. (1976) Characterization of a cytochrome P-450-dependent steroid hydroxylase system present in *Bacillus megaterium*, *The Journal of biological chemistry.* **251**, 2831-2838.

84. Berg, A., Ingelman-Sundberg, M. & Gustafsson, J. (1979) Isolation and characterization of cytochrome P-450meg, *Acta Biologica et Medica Germanica*. **38**, 333-344.

85. Nguyen, K., Virus, C., Gunnewich, N., Hannemann, F. & Bernhardt, R. (2012) Changing the regioselectivity of a P450 from C15 to C11 hydroxylation of progesterone, *Chembiochem.* **13**, 1161-1166.

86. Virus, C. & Bernhardt, R. (2008) Molecular evolution of a steroid hydroxylating cytochrome P450 using a versatile steroid detection system for screening, *Lipids.* **43**, 1133-1141.

87. Bleif, S., Hannemann, F., Lisurek, M., Kries, J., Zapp, J., Dietzen, M., Antes, I. & Bernhardt, R. (2011) Identification of CYP106A2 as a regioselective allylic bacterial diterpene hydroxylase, *Chembiochem.* **12**, 576-582.

88. Bleif, S., Hannemann, F., Zapp, J., Hartmann, D., Jauch, J. & Bernhardt, R. (2012) A new *Bacillus megaterium* whole-cell catalyst for the hydroxylation of the pentacyclic triterpene 11-keto-beta-boswellic acid (KBA) based on a recombinant cytochrome P450 system, *Applied microbiology and biotechnology.* **93**, 1135-1146.

89. Schmitz, D., Zapp, J. & Bernhardt, R. (2012) Hydroxylation of the triterpenoid dipterocarpol with CYP106A2 from *Bacillus megaterium*, *The FEBS journal.* **279**, 1663-1674.

90. He, J., Liang, Q. & Fulco, A. (1995) The molecular cloning and characterization of BM1P1 and BM1P2 proteins, putative positive transcription factors involved in barbiturate-mediated induction of the genes encoding cytochrome P450BM-1 of *Bacillus megaterium*., *Journal of Biological Chemistry.* **270**, 18615-18625.

91. Shaw, G. C., Hsueh, Y. H. & Kao, H. S. (2000) The basal-level expression of the cytochrome P450(BM-1) gene is negatively affected by the bm1P1 gene of *Bacillus megaterium*, *Current Microbiology.* **40**, 47-50.

92. Eppinger, M., Bunk, B., Johns, M. A., Edirisinghe, J. N., Kutumbaka, K. K., Koenig, S. S. K., Huot Creasy, H., Rosovitz, M. J., Riley, D. R., Daugherty, S., Martin, M., Elbourne, L. D. H., Paulsen, I., Biedendieck, R., Braun, C., Grayburn, S., Dhingra, S., Lukyanchuk, V., Ball, B., Ul-Qamar, R., Seibel, J., Bremer, E., Jahn, D., Ravel, J. & Vary, P. S. (2011) Genome Sequences of the Biotechnologically Important *Bacillus megaterium* Strains QM B1551 and DSM319, *Journal of Bacteriology.* **193**, 4199-4213.

93. McAleer, W. J., Jacob, T. A., Turnbull, L. B., Schoenewaldt, E. F. & Stoudt, T. H. (1958) Hydroxylation of progesterone by *Bacillus cereus* and *Bacillus megaterium*, *Archives of Biochemistry and Biophysics.* **73**, 127-130.

94. Berg, A., Ingelman-Sundberg, M. & Gustafsson, J. A. (1979) Purification and characterization of cytochrome P-450meg, *Journal of Biological Chemistry.* **254**, 5264-5271.

95. Berg, A. & Rafter, J. J. (1981) Studies on the substrate specificity and inducibility of cytochrome P-450meg, *Biochemical Journal.* **196**, 781-786.

96. Rauschenbach, R., Isernhagen, M., Noeske-Jungblut, C., Boidol, W. & Siewert, G. (1993) Cloning sequencing and expression of the gene for cytochrome P450meg, the steroid-15β-monooxygenase from *Bacillus megaterium* ATCC 13368, *Molecular and General Genetics.* **241**, 170-176.

97. Virus, C., Lisurek, M., Simgen, B., Hannemann, F. & Bernhardt, R. (2006) Function and engineering of the 15beta-hydroxylase CYP106A2, *Biochemical Society Transactions.* **34**, 1215-1218.

98. Hannemann, F., Virus, C. & Bernhardt, R. (2006) Design of an *Escherichia coli* system for whole cell mediated steroid synthesis and molecular evolution of steroid hydroxylases, *Journal of Biotechnology.* **124**, 172-181.

99. Agematu, H., Matsumoto, N., Fujii, Y., Kabumoto, H., Doi, S., Machida, K., Ishikawa, J. & Arisawa, A. (2006) Hydroxylation of Testosterone by Bacterial Cytochromes P450 Using the *Escherichia coli* Expression System, *Bioscience, Biotechnology, and Biochemistry.* **70**, 307-311.

100. Schmitz, D., Zapp, J. & Bernhardt, R. (2014) Steroid conversion with CYP106A2 - production of pharmaceutically interesting DHEA metabolites, *Microbial Cell Factories.* **13**, 81.

101. Janocha, S. & Bernhardt, R. (2013) Design and characterization of an efficient CYP105A1-based whole-cell biocatalyst for the conversion of resin acid diterpenoids in permeabilized *Escherichia coli*, *Applied microbiology and biotechnology.* **97**, 7639-7649.

102. Janocha, S. (2013) Umsatz von Harzsäuren durch die bakteriellen Cytochrome CYP105A1 und CYP106A2 - Strukturelle Grundlagen und potentielle Anwendungen. Universität des Saarlandes, Saarbrücken.

103. Lisurek, M., Kang, M., Hartmann, R. & Bernhardt, R. (2004) Identification of monohydroxy progesterones produced by CYP106A2 using comparative HPLC and electrospray ionisation collision-induced dissociation mass spectrometry, *Biochemical and biophysical research communications.* **319**, 677-682.

104. Lisurek, M., Simgen, B., Antes, I. & Bernhardt, R. (2008) Theoretical and experimental evaluation of a CYP106A2 low homology model and production of mutants with changed activity and selectivity of hydroxylation, *Chembiochem.* **9**, 1439-1449.

105. Souness, G. W. & Morris, D. J. (1996) 11α- and 11β-Hydroxyprogesterone, Potent Inhibitors of 11β-Hydroxysteroid Dehydrogenase, Possess Hypertensinogenic Activity in the Rat, *Hypertension.* **27**, 421-425.

106. Donova, M. & Egorova, O. (2012) Microbial steroid transformations: current state and prospects, *Applied microbiology and biotechnology.* **94**, 1423-1447.

107. Fernandes, P., Cruz, A., Angelova, B., Pinheiro, H. M. & Cabral, J. M. S. (2003) Microbial conversion of steroid compounds: recent developments, *Enzyme and Microbial Technology.* **32**, 688-705.

108. Lednicer, D. (2010) Introduction in *Steroid Chemistry at a Glance* pp. 2-9, John Wiley & Sons, Ltd.

109. Callewaert, F., Boonen, S. & Vanderschueren, D. (2010) Sex steroids and the male skeleton: a tale of two hormones, *Trends in Endocrinology & Metabolism.* **21**, 89-95.

110. Rubtsov, A. V., Rubtsova, K., Kappler, J. W. & Marrack, P. (2010) Genetic and hormonal factors in female-biased autoimmunity, *Autoimmunity Reviews.* **9**, 494-498.

111. Garcia-Segura, L. M. & Balthazart, J. (2009) Steroids and neuroprotection: New advances, *Frontiers in Neuroendocrinology.* **30**, 5-9.

112. Waters, C. M. & Bassler, B. L. (2005) QUORUM SENSING: Cell-to-Cell Communication in Bacteria, *Annual Review of Cell and Developmental Biology*. **21**, 319-346.

113. Rupprecht, R. (2003) Neuroactive steroids: mechanisms of action and neuropsychopharmacological properties, *Psychoneuroendocrinology*. **28**, 139-168.

114. Baker, M. E. (2011) Origin and diversification of steroids: Co-evolution of enzymes and nuclear receptors, *Molecular and cellular endocrinology*. **334**, 14-20.

115. Bureik, M. & Bernhardt, R. (2007) Steroid Hydroxylation: Microbial Steroid Biotransformations Using Cytochrome P450 Enzymes in *Modern Biooxidation* pp. 155-176, Wiley-VCH Verlag GmbH & Co. KGaA.

116. Tong, W. Y. & Dong, X. (2009) Microbial biotransformation: recent developments on steroid drugs, *Recent Patents on Biotechnology* **3**, 141-153.

117. Carballeira, J. D., Quezada, M. A., Hoyos, P., Simeó, Y., Hernaiz, M. J., Alcantara, A. R. & Sinisterra, J. V. (2009) Microbial cells as catalysts for stereoselective red–ox reactions, *Biotechnology Advances*. **27**, 686-714.

118. Choudhary, M. I., Erum, S., Atif, M., Malik, R., Khan, N. T. & Atta ur, R. (2011) Biotransformation of (20S)-20-hydroxymethylpregna-1,4-dien-3-one by four filamentous fungi, *Steroids*. **76**, 1288-1296.

119. Choudhary, M. I., Sultan, S., Khan, M. T. H. & Rahman, A.-u. (2005) Microbial transformation of 17α-ethynyl- and 17α-ethylsteroids, and tyrosinase inhibitory activity of transformed products, *Steroids*. **70**, 798-802.

120. Janeczko, T., Dmochowska-Gładysz, J., Kostrzewa-Susłow, E., Białońska, A. & Ciunik, Z. (2009) Biotransformations of steroid compounds by *Chaetomium sp.* KCH 6651, *Steroids*. **74**, 657-661.

121. Ferrero, V. E. V., Di Nardo, G., Catucci, G., Sadeghi, S. J. & Gilardi, G. (2012) Fluorescence detection of ligand binding to labeled cytochrome P450 BM3, *Dalton Transactions*. **41**, 2018-2025.

122. Girhard, M., Klaus, T., Khatri, Y., Bernhardt, R. & Urlacher, V. (2010) Characterization of the versatile monooxygenase CYP109B1 from *Bacillus subtilis*, *Applied microbiology and biotechnology*. **87**, 595-607.

123. Simgen, B., Contzen, J., Schwarzer, R., Bernhardt, R. & Jung, C. (2000) Substrate binding to 15beta-hydroxylase (CYP106A2) probed by FT infrared spectroscopic studies of the iron ligand CO stretch vibration, *Biochemical and Biophysical Research Communications*. **269**, 737-742.

124. Li, P. K. & Brueggemeier, R. W. (1990) 7-Substituted 1,4,6-androstatriene-3,17-diones as enzyme-activated irreversible inhibitors of aromatase, *Journal of steroid biochemistry*. **36**, 533-539.

125. Numazawa, M., Kamiyama, T., Tachibana, M. & Oshibe, M. (1996) Synthesis and Structure−Activity Relationships of 6-Substituted Androst-4-ene Analogs as Aromatase Inhibitors, *Journal of medicinal chemistry*. **39**, 2245-2252.

126. Shirasaka, M., Takasaki, R. & Tsurutan, M. (1960) Microbiological 11β-Hydroxy Dehydrogenation of Corticosterone, *Nature*. **186**, 390-391.

127. Suhara, K., Takeda, K. & Katagiri, M. (1986) P-45011β-dependent conversion of cortisol to cortisone, and 19-hydroxyandrostenedione to 19-oxoandrostenedione, *Biochemical and biophysical research communications*. **136**, 369-375.

128. Bellucci, G., Chiappe, C., Pucci, L. & Gervasi, P. G. (1996) The Mechanism of Oxidation of Allylic Alcohols to α,β-Unsaturated Ketones by Cytochrome P450, *Chemical Research in Toxicology*. **9**, 871-874.

129. Matsunaga, T., Tanaka, H., Higuchi, S., Shibayama, K., Kishi, N., Watanabe, K. & Yamamoto, I. (2001) Oxidation Mechanism of 7-Hydroxy-Δ8-tetrahydrocannabinol and 8-Hydroxy-Δ9-tetrahydrocannabinol to the Corresponding Ketones by CYP3A11, *Drug Metabolism and Disposition*. **29**, 1485-1491.

130. Wang, Y., Yang , C., Wang, H., Han , K. & Shaik, S. (2007) A New Mechanism for Ethanol Oxidation Mediated by Cytochrome P450 2E1: Bulk Polarity of the Active Site Makes a Difference, *Chembiochem*. **8**, 277-281.

131. Groves, J. T. (2006) High-valent iron in chemical and biological oxidations, *Journal of Inorganic Biochemistry.* **100**, 434-447.

132. Liu, Y. & Ortiz de Montellano, P. R. (2000) Reaction Intermediates and Single Turnover Rate Constants for the Oxidation of Heme by Human Heme Oxygenase-1, *Journal of Biological Chemistry.* **275**, 5297-5307.

133. Vidakovic, M., Sligar, S. G., Li, H. & Poulos, T. L. (1998) Understanding the Role of the Essential Asp251 in Cytochrome P450cam Using Site-Directed Mutagenesis, Crystallography, and Kinetic Solvent Isotope Effect, *Biochemistry.* **37**, 9211-9219.

134. Krest, C. M., Onderko, E. L., Yosca, T. H., Calixto, J. C., Karp, R. F., Livada, J., Rittle, J. & Green, M. T. (2013) Reactive Intermediates in Cytochrome P450 Catalysis, *Journal of Biological Chemistry.* **288**, 17074-17081.

135. Luthra, A., Denisov, I. G. & Sligar, S. G. (2011) Spectroscopic features of cytochrome P450 reaction intermediates, *Archives of Biochemistry and Biophysics.* **507**, 26-35.

136. Appel, D., Schmid, R., Dragan, C.-A., Bureik, M. & Urlacher, V. (2005) A fluorimetric assay for cortisol, *Analytical and Bioanalytical Chemistry.* **383**, 182-186.

137. Neumann, F. & Töpert, M. (1986) Pharmacology of antiandrogens, *Journal of steroid biochemistry.* **25**, 885-895.

138. Sciarra, F., Toscano, V., Concolino, G. & Di Silverio, F. (1990) Antiandrogens: Clinical applications, *The Journal of steroid biochemistry and molecular biology.* **37**, 349-362.

139. Wooltorton, E. (2003) Diane-35 (cyproterone acetate): safety concerns, *CMAJ: Canadian Medical Association Journal.* **168**, 455-456.

140. Pasquali, R. & Gambineri, A. (2014) Therapy Of Endocrine Disease: Treatment of hirsutism in the polycystic ovary syndrome, *European Journal of Endocrinology.* **170**, 75-90.

141. Frith, R. & Phillipou, G. (1985) 15-Hydroxycyproterone acetate and cyproterone acetate levels in plasma and urine., *Journal of Chromatography* **338**, 179-186.

142. Singer, Y., Shity, H. & Bar, R. (1991) Microbial transformations in a cyclodextrin medium. Part 2. Reduction of androstenedione to testosterone by *Saccharomyces cerevisiae*, *Applied microbiology and biotechnology.* **35**, 731-737.

143. Lahiani-Skiba, M., Barbot, C., Bounoure, F., Joudieh, S. & Skiba, M. (2006) Solubility and Dissolution Rate of Progesterone-Cyclodextrin-Polymer Systems, *Drug Development and Industrial Pharmacy.* **32**, 1043-1058.

144. Manosroi, A., Saowakhon, S. & Manosroi, J. (2008) Enhancement of androstadienedione production from progesterone by biotransformation using the hydroxypropyl-β-cyclodextrin complexation technique, *The Journal of steroid biochemistry and molecular biology.* **108**, 132-136.

145. Ma, Y.-H., Wang, M., Fan, Z., Shen, Y.-B. & Zhang, L.-T. (2009) The influence of host–guest inclusion complex formation on the biotransformation of cortisone acetate Δ1-dehydrogenation, *The Journal of steroid biochemistry and molecular biology.* **117**, 146-151.

146. Andrushina, V. A., Druzhinina, A. V., Yaderets, V. V., Stitsenko, T. S. & Voishvillo, N. E. (2011) Hydroxylation of steroids by *Curvularia lunata* mycelium in the presence of methyl-β-cyclodextrine, *Applied Biochemistry and Microbiology.* **47**, 42-48.

147. Wang, M., Zhang, L., Shen, Y., Ma, Y., Zheng, Y. & Luo, J. (2009) Effects of hydroxypropyl-β-cyclodextrin on steroids 1-en-dehydrogenation biotransformation by *Arthrobacter simplex* TCCC 11037, *Journal of Molecular Catalysis B: Enzymatic.* **59**, 58-63.

148. Horoszewicz, J. S., Leong, S. S., Kawinski, E., Karr, J. P., Rosenthal, H., Chu, T. M., Mirand, E. A. & Murphy, G. P. (1983) LNCaP Model of Human Prostatic Carcinoma, *Cancer Research.* **43**, 1809-1818.

149. Bologna, M., Muzi, P., Biordi, L., Festuccia, C. & Vicentini, C. (1995) Finasteride dose-dependently reduces the proliferation rate of the LnCap human prostatic cancer cell line in vitro, *Urology.* **45**, 282-290.